

Preparation and characterization of nanometer-sized mechano-responsive liposomes for physically-triggered drug delivery

Inauguraldissertation

zur

Erlangung der Würde eines Doktors der Philosophie
vorgelegt der

Philosophisch-Naturwissenschaftlichen Fakultät
der Universität Basel

von

Sofiya Matviykiv

Basel, 2019

Genehmigt von der Philosophisch-Naturwissenschaftlichen Fakultät

auf Antrag von:

Prof. Dr. Bert Müller, Erstbetreuer
Prof. Dr. Jörg Huwyler, Zweitbetreuer
Prof. Dr. Regine Willumeit-Römer, externe Expertin

Basel, den 11. Dezember 2018

Prof. Dr. Martin Spiess, Dekan

Contents

Summary	v
Zusammenfassung	vii
List of Publications	ix
1 Introduction	1
Contributions	7
2 Results	9
2.1 Liposomes — bio-inspired nano-containers for physically triggered targeted drug delivery	9
2.2 Immunocompatibility of Rad-PC-Rad liposomes <i>in vitro</i> , based on human complement activation and cytokine release	24
2.3 Small-angle neutron scattering study of temperature-induced struc- tural changes in liposomes	57
3 Conclusions and Outlook	65
Bibliography	67
Acknowledgments	71
Curriculum Vitae	73

Summary

Cardiovascular diseases remain the leading causes of death worldwide, accounting for 17.7 million deaths every year — 31% of all global deaths. Atherosclerosis is an underlying disease process in blood vessels that leads to the accumulation of cholesterol plaques and a narrowing of the arterial lumen. If the plaque bursts, the components are flushed into the bloodstream, triggering intravascular thrombosis and leading to vascular occlusions. Heart attack or stroke are the most dangerous medical consequences of this. In such an event, time is of utmost importance because the infarcted organ suffers from necrosis without re-establishment of blood perfusion within a few minutes. Currently, emergency treatment provided in the ambulance involves intravenous injection of vasodilators that act systemically to dilate blood vessels and re-establish blood supply. However, this works systemically and even at a low dose lead to peripheral resistance decrease of the vessels and thereby hypotension. This generally inhibits the blood perfusion and thus the drug cannot work optimally at the location of the constricted vessel. Therefore, the development of a smart and effective drug delivery system, capable of releasing the drug locally, is desired. Critically constricted arteries give rise to increased wall shear stress that can be used as a physical trigger to release the therapeutics. Liposomes belong to the most attractive carriers for drug targeting in medical fields. Recently, mechano-responsive liposomes prepared from artificial phospholipids were suggested as nanocontainers for delivery and release of vasodilators at constrictions of arteries. This thesis project gives insight into the physicochemical properties of the mechano-responsive liposomes, determines their thermal stability at physiologically relevant body temperatures, and demonstrates their *in vitro* immunocompatibility.

The preliminary characterization of nanometer-size liposomes is essential for the development of clinically relevant drug delivery systems. The mechano-sensitive liposomes Pad-PC-Pad and Rad-PC-Rad were studied by means of dynamic light scattering and transmission electron microscopy at cryogenic temperatures to determine size distribution and shape. In both cases, the liposomes were found to be around 100 nm in size with a variety of shapes. To prevent liposome aggregation as a consequence of the low zeta potential, a steric stabilization using polyethylene-glycol-grafted phospholipids was applied.

To ensure mechano-responsive behavior at body temperature, the liposomes' structure should be stable at physiological and elevated body temperatures. Therefore, the structural changes of liposomes were evaluated in a temperature range from 22 to 42 °C. Small-angle neutron scattering was used to measure the radius, eccentricity, and bilayer thickness of liposomes. Pad-PC-Pad liposomes already undergo structural changes at 35 °C. Further heating to 42 °C and subsequent cooling to room temperature resulted in a decreased eccentricity by an order of magnitude and a 20% increase of bilayer thickness, indicating the loss of membrane interdigitation. Rad-PC-Rad liposomes, however, show thermal stability up to 42 °C. Thus, Rad-PC-Rad liposomes possess sufficient thermal stability for drug delivery to atherosclerotic hu-

man blood vessels.

To advance this technology towards clinical applications, the *in vitro* immunocompatibility of liposomes was investigated. The systemic administration of liposomes may trigger an immediate activation of the immune system, resulting in a hypersensitivity reaction. This reaction is driven by the activation of the complement system, which can stimulate the production of pro-inflammatory cytokines. Experiments demonstrated that both the Pad-PC-Pad and Rad-PC-Rad liposomal formulations exhibited low-to-moderate levels of complement proteins compared to the Food-and-Drug-Administration-approved liposomal drugs such as Doxil[®] and AmBisome[®]. Within the restricted number of individuals, one outlier was detected, suggesting that a substantially higher number of donors should be incorporated into future studies.

Zusammenfassung

Herz-Kreislauf-Erkrankungen sind weltweit die häufigste Todesursache. 17,7 Millionen Menschen sterben jährlich. Das sind 31% aller Todesfälle. Atherosklerose führt in Blutgefässen zu Plaque und einer Verengung des Querschnitts. Platzt eine Plaque, so werden die Bestandteile in die Blutbahn geschwemmt, lösen eine intravaskuläre Thrombose aus und führen zu Gefäßverschlüssen. Herzinfarkt oder Schlaganfall sind die gefährlichsten medizinischen Konsequenzen davon. In derartigen Fällen spielt die Zeit eine zentrale Rolle. Da in wenigen Minuten der infarzierte Organteil ohne rasche Retablierung der Blutperfusion, langsam nekrotisiert. Bereits im Krankenwagen wird dem Patienten ein gefässerweiterndes Medikament gespritzt, um das lokale Gefäss zu erweitern und die Blutversorgung zu retablieren. Nur wirkt das systemisch und führt bei schon geringer Dosis zur peripheren Resistenzabnahme der Gefässe und dabei zu einer Hypotonie. Diese Hypotonie hemmt allgemein die organische Blutperfusion und somit kann das Medikament lokal nicht optimal wirken. Deshalb ist die Entwicklung von einer pfiffigen und wirksamen Medikamentenfreisetzung an den Verengungen der Gefässe äusserst wünschenswert. Bedenklich verengte Blutgefässe führen zu einer erhöhten Scherspannung, die man als Steuerimpuls für die Wirkstofffreisetzung nutzen kann. Liposomen gehören zu den attraktivsten Trägersystemen in der Medizin. Unlängst wurde vorgeschlagen, dass man mechanisch reaktive Liposome auf Basis von künstlichen Phospholipiden als Nano-Container für die Zuführung und Freisetzung von gefässerweiternden Medikamenten an die krankhaften Gefässverengungen nutzen kann.

Das Dissertationsprojekt führt zu Erkenntnissen über die physikalisch-chemischen Eigenschaften der mechanisch reaktiven Liposome, ihre thermische Stabilität bei physiologisch relevanten Körpertemperaturen und zeigt ihre Immunverträglichkeit. Die mechanisch reaktiven Liposome Pad-PC-Pad und Rad-PC-Rad wurden mittels dynamischer Lichtstreuung und Tieftemperatur-Transmissionselektronenmikroskopie untersucht, um deren Grösse und Form zu bestimmen. In beiden Fällen hatten die vielfältig geformten Liposome eine Grösse von etwa 100 nm. Um die Zusammenlagerung der Liposome als Folge des geringen Zeta-Potentials zu verhindern, wurde als räumlicher Stabilisator Polyglykol auf die Phospholipide aufgepfropft.

Um die mechanische Reaktionsfähigkeit bei Körpertemperatur zu garantieren, sollten die Struktur der Liposome auch bei erhöhter Körpertemperatur stabil sein. Deshalb wurden die strukturellen Änderungen im Temperaturbereich zwischen 22 und 42 °C ausgewertet. Kleinwinkel-Neutronen-Streuung wurde verwendet, um den Radius und die Exzentrizität der Liposome sowie die Dicke der zugehörigen Phospholipid-Doppelschicht zu vermessen. Pad-PC-Pad Liposome zeigen bereits bei 35 °C strukturelle Veränderungen. Das weitere Heizen auf 42 °C und anschliessende Abkühlen auf Raumtemperatur führt zu einer um eine Grössenordnung verringerten Exzentrizität und einem 20%igen Anstieg der Doppellagendicke. Diese Beobachtung deutet auf den Verlust der wechselseitigen Verzahnung der Lipide hin. Demgegenüber sind Rad-PC-Rad Liposome bis 42 °C thermisch stabil. Folglich sind Rad-PC-Rad Lipo-

some für die Wirkstofffreisetzung in atherosklerotischen Blutgefäßen des Menschen thermisch genügend stabil.

Um diese Technologie in Richtung klinischer Anwendungen voranzutreiben, wurde die Immunverträglichkeit der Liposome *in vitro* untersucht. Die systemische Gabe der Liposome könnte eine sofortige Aktivierung des Immunsystems auslösen und zu überempfindlichkeitsreaktionen führen. Eine derartige Reaktion wird durch die Aktivierung des Komplementsystems getrieben, die die Produktion von proinflammatorischen Cytokinen anregen kann. Die Experimente haben gezeigt, dass sowohl Pad-PC-Pad als auch Rad-PC-Rad Liposome im Vergleich zu von der FDA anerkannten Liposomen-basierten Medikamenten wie Doxil[®] and AmBisome[®] nur einen geringen Gehalt an Komplementärproteinen aufweisen. Innerhalb der eingeschränkten Anzahl an Spendern wurde ein Ausreisser gefunden. Deshalb sollte die Zahl der Spender für zukünftige Studien substantiell erhöht werden.

List of Publications

Journal Publications

S. Matviykov, H. Deyhle, J. Kohlbrecher, F. Neuhaus, A. Zumbuehl, B. Müller, “Small-angle neutron scattering study of temperature-induced structural changes in liposomes”, *Langmuir*, in press (2019) (doi:10.1021/acs.langmuir.9b01603)

S. Matviykov, M. Buscema, G. Gerganova, T. Mészáros, G.T. Kozma, U. Mettal, F. Neuhaus, T. Ishikawa, J. Szebeni, A. Zumbuehl, B. Müller, “Immunocompatibility of Rad-PC-Rad liposomes *in vitro*, based on human complement activation and cytokine release”, *Precision Nanomedicine* **1**, 45–67, (2018) (doi:10.29016/180410.1)

M. Buscema, **S. Matviykov**, T. Mészáros, G. Gerganova, A. Weinberger, U. Mettal, D. Mueller, F. Neuhaus, E. Stalder, T. Ishikawa, R. Urbanics, T. Saxer, T. Pfohl, J. Szebeni, A. Zumbuehl, B. Müller, “Immunological response to nitroglycerin-loaded shear-responsive liposomes *in vitro* and *in vivo*”, *Journal of Controlled Release* **264**, 14–23, (2017) (doi:10.1016/j.jconrel.2017.08.010)

S. Bugna, M. Buscema, **S. Matviykov**, R. Urbanics, A. Weinberger, T. Meszaros, J. Szebeni, A. Zumbuehl, T. Saxer, B. Müller, “Surprising lack of liposome-induced complement activation by artificial 1,3-diamidophospholipids *in vitro*”, *Nanomedicine: Nanotechnology, Biology, and Medicine* **12**, 845–849, (2016) (doi:10.1016/j.nano.2015.12.364)

Peer-Reviewed Conference Proceedings

S. Matviykov, M. Buscema, T. Mészáros, G. Gerganova, T. Pfohl, A. Zumbuehl, J. Szebeni, B. Müller, “Liposomes - bio-inspired nano-containers for physically triggered targeted drug delivery”, *Proceedings of SPIE* **10162**, 101620A (2017) (doi:10.1117/12.2258378)

S. Matviykov, M. Buscema, H. Deyhle, T. Pfohl, A. Zumbuehl, T. Saxer, B. Müller, “X-ray micro computed tomography for the visualization of an atherosclerotic human coronary artery”, *Journal of Physics: Conference Series* **849**, 012002 (2017) (doi:10.1088/1742-6596/849/1/012002)

M. Buscema, G. Schulz, H. Deyhle, A. Khimchenko, **S. Matviykov**, M. N. Holme, A. Hipp, F. Beckmann, T. Saxer, K. Michaud, B. Müller, “Histology-validated X-ray tomography for imaging human coronary arteries”, *Proceedings of SPIE* **9967**, 99670O (2016) (doi:10.1117/12.2238702)

Peer-Reviewed Conference Abstracts

S. Matviyiv, M. Buscema, S. Bugna, T. Mészáros, J. Szebeni, A. Zumbuehl, B. Müller, “Complement activation of artificial liposomes about 100 nm in diameter”, *European Cells and Materials* **32**, 2, 48 (2016)

M. Buscema, H. Deyhle, T. Pfohl, S. E. Hieber, **S. Matviyiv**, A. Zumbuehl, B. Müller, “Studying shear-stress sensitive liposomes using microfluidics”, *European Cells and Materials* **32**, 2, 31 (2016)

1 Introduction

According to the World Health Organization, cardiovascular diseases (CVDs) remain the major cause of morbidity and mortality worldwide, resulting in 17.7 million deaths per year [1]. 80% of all CVD-related deaths are due to heart attacks and strokes, with atherosclerosis the main contributor. Atherosclerosis is a complex inflammatory disease related to the damage and inflammation of endothelium as well as the accumulation of lipids and white blood cells, the proliferation of intimal-smooth-muscle cells, and finally tissue calcification that leads to a fibro-fatty plaque formation. Major risk factors for atherosclerosis include high cholesterol levels and high blood pressure. Fatty deposits (plaques) accumulate over years along the inside of artery walls, narrowing the lumen of the artery and obstructing the blood flow. Further growth of atherosclerotic plaque or its rupture triggers the formation of a blood clot, preventing oxygen supply to the heart and brain.

After a myocardial infarction or stroke, time is the most important factor in the treatment procedure. Treatments are mainly based on restoring the oxygenation and improving arterial hemodynamics. The established therapeutic option for the first line treatment of heart attack in ambulances involves systemic administration of vasodilators such as nitroglycerin (NTG) [2, 3]. However, their use is limited by the risk of hypotension and subsequent end-organ hypoperfusion. Inappropriate vasodilatation may induce a steep reduction in blood pressure, resulting in hemodynamic instability, ischemia, or renal failure, all of which leads to increased mortality [4]. Thrombolytic agents, such as tissue plasminogen activator (tPA) have been developed for dissolving blood clots with the aim of restoring and improving the blood flow [5]. However, indications of using free tPA are limited as its systemic administration carries a risk of hemorrhage that may be fatal [6].

The risk of systemic side effects from vasodilators or thrombolytic agents can be reduced through the development of a controlled, local drug delivery platform for the cardiovascular system. To this end, there has been a great focus on engineered biomaterials such as liposomes, polymeric, magnetic, and gold nanoparticles [7–9]. Liposomes are composed of phospholipids that self-assemble into closed bilayer structures in aqueous systems due to their amphiphilic nature. Nowadays, liposomes are the most common and well-investigated nanocarriers for drug delivery [10]. Their ability to encapsulate both hydrophilic and hydrophobic drugs in combination with their biocompatibility, biodegradability, and the possibility of controllable release kinetics, make liposomes an attractive pharmaceutical carrier. The release of the liposomes' cargo can be achieved upon various physical or biochemical stimuli, *i.e.* changes in shear stress, temperature, ultrasound, light, pH, enzymatic or redox reactions [11]. This thesis focuses on mechano-responsive liposomes that can be triggered by shear stress.

The mean physiologic wall shear stress in the human arterial system varies between 0.1 – 1.2 Pa [12]. Critically constricted arteries are characterized by substantially increased wall shear stress, at least one order of magnitude higher than the healthy

case (14.2 Pa at 80% of stenosis [13]). This increased shear stress can be used as a physical trigger to disrupt the liposome membrane, enabling drug release. The concept of shear stress responsive drug delivery has been previously proposed by two research groups. One approach is based on the delivery of microscale aggregates of nanoparticles coated with tPA to the obstructed blood vessels [14]. When exposed to abnormally high fluid shear stress, these aggregates break up into nanoscale components and induce rapid clot dissolution and restore normal flow [14]. Another approach was proposed by members of our research project based on delivery of mechano-responsive liposomes loaded with a vasodilator to the constricted arteries [15, 16].

In order to tailor the chemical composition and subsequent physical properties of mechano-responsive liposomes, the shear stress parameters of healthy and stenosed arteries need to be determined. Arterial wall shear stress can be computed using flow simulations, which in turn require information about the radius of the arterial lumen. Arterial morphology is often studied by means of histology, which can only offer two-dimensional information, significantly limiting its application to blood flow simulations. Additionally, tissue morphology can be altered due to preparation artefacts, which can originate from decalcification, cutting, and embedding, leading to tissue shrinkage or deformation. X-ray tomography can overcome this challenge, providing a non-destructive, quantitative 3D visualization of plaque-containing blood vessels at micrometer level [17–19]. Moreover, X-ray tomography allows for lumen segmentation — a crucial step for subsequent flow simulation analysis.

As part of this thesis, tomography datasets of a diseased human coronary artery were acquired using advanced laboratory X-ray micro computed tomography (μ CT) system in absorption contrast mode, which is well suited for discriminating anatomical structures with significant differences in X-ray absorption, including the determination of plaque morphology within artery and determination of the extent of stenosis resulting in lumen segmentation [20].

The human artery containing calcified atherosclerotic plaque was embedded in a paraffin and measured before and after decalcification to determine the cross-section of the lumen, the non-constricted area of the artery, and the changes in cross-section due to decalcification procedure.

Figure 1.1 compares virtual slices through the tomography dataset of the plaque-containing artery (A: top view, C: lateral view) and the same artery after decalcification process (B: top view, D: lateral view). In Figure 1.1A, the artery walls and plaque are clearly visible; however, the contrast in the surrounding fatty tissue is low. On the other hand, in Figure 1.1B, the artery wall is clearly visible thanks to better contrast. However, hard tissue residuals from the plaque decalcification are still present in the surrounding tissue (shown by yellow arrows). The presence of preparation artefacts including air bubble in the left lumen of calcified artery (Figure 1.1A) and small paraffin cracks inside the lumens of the decalcified artery (Figure 1.1B) are visible in the tomography datasets. Streak artefacts (whitish color on red background) around the highly X-ray absorbing calcified plaque were observed in the calcified sample (Figure 1.1A). These artefacts overlap with the morphology of the lumen and make segmentation more challenging.

The cross-sectional area of both the calcified and decalcified artery samples was extracted using the region-growing segmentation tool of VG Studio Max 2.1, which is a fast and convenient method to obtain the morphology of the lumen. The cross-

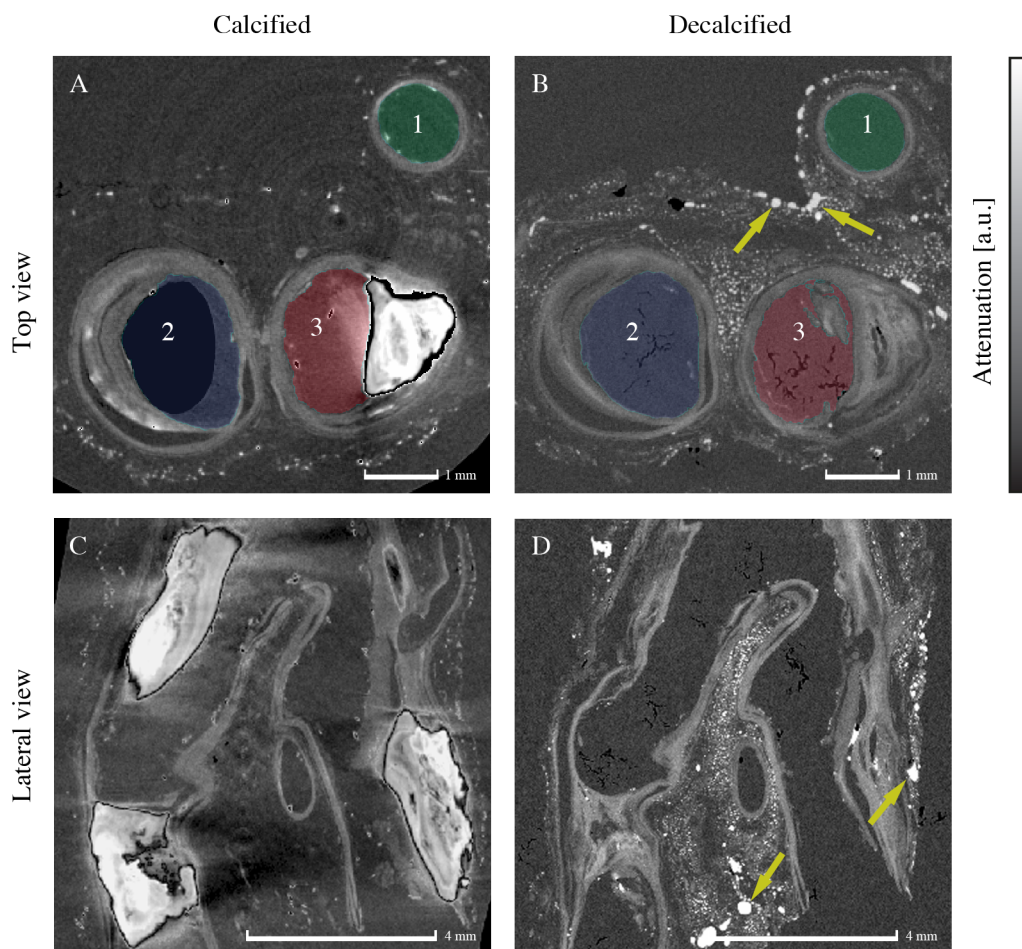


Figure 1.1: Axial slices of a calcified (A: top view, C: lateral view) and decalcified (B: top view, D: lateral view) human coronary artery embedded in paraffin, measured with absorption contrast μ CT. Region 1 (colored in green), region 2 (blue) and region 3 (red) in images A and B correspond to the cross-sectional area of three lumens. Region 3 of image A shows the calcified plaque, depicted in bright white — indicating high X-ray absorption.

sectional area was calculated and the results are presented in Table 1.1.

Numbers and related color indicate each region of the artery. The cross-sectional area of the segmented slice between the two samples before and after decalcification process decreased from 0.84 to 0.80 mm^2 (Region 1), from 2.42 to 2.40 mm^2 (Region 2), and from 1.86 to 1.82 mm^2 (Region 3), although the decrease was around the size of the measurement uncertainty. The artery shrinkage and the resulting decrease in lumen area may be caused by the chemical treatment during the decalcification process. Despite the removal of the atherosclerotic plaque in the Region 3, the area did not notably decrease, because the soft tissue was still present. The area of the calcified plaque was 1.07 mm^2 , whereas the area of the soft tissue residuals after decalcification was 1.02 mm^2 . Comparing these two slices from calcified and decalcified datasets, the decalcification process does not significantly change the cross section of the lumen. The datasets of unstained soft tissue showed surprisingly high contrast. One can reasonably assume that dehydration is the key factor, as it leads to increased tissue density, and thus, different attenuation values. A recent study

Table 1.1: The cross-sectional area of the artery lumen.

	Calcified artery area, mm ²	Decalcified artery area, mm ²
Region 1 (green)	0.84 ± 0.02	0.80 ± 0.02
Region 2 (blue)	2.42 ± 0.02	2.40 ± 0.02
Region 3 (red)	1.86 ± 0.02	1.82 ± 0.02

with high-resolution hard X-ray tomography demonstrated that paraffin embedding gives rise to an anisotropic shrinkage up to 65% with respect to formalin fixed tissues, suggesting that the artery lumen should be extracted before decalcification and paraffin embedding [19].

The lumen area calculated in this study is a starting point for the complete segmentation of the lumen, which is a prerequisite for quantitative blood flow simulations. These results demonstrate that μ CT is a valuable tool to study the morphology of diseased atherosclerotic artery.

Liposomes have demonstrated significant therapeutic advantages, but their clinical translation remains limited by the immunological barrier. Investigation of liposomes' interactions with the patient's immune system *in vitro* can help to prevent serious and potentially lethal reactions during clinical evaluation. When intravenously administered, liposomes immediately interact with blood components such as serum proteins, which function is to assist the innate immunity in rapid clearance of pathogens and other foreign dangerous materials. It is therefore expected that liposomes will be recognized by the immune system. The development of immunogenic reactions towards liposomes may lead to the prevention of targeted delivery, an altered pharmacokinetics, a loss of therapeutic effect, and the rise of potentially serious toxicities [21,22]. Through 2017, ten liposomal formulations have been approved by Food and Drug Administration (FDA) [23,24]. However, lipid-based nanoparticles are one of the most frequent nanomedicines to induce activation of immune system [25]. A very recent study reported that out of 15 nanotechnology-based drug products that are known to induce infusion reactions, 7 are liposomes [26]. An example of an acute adverse immune reaction caused by liposomes is complement activation-related pseudoallergy (CARPA) [22,27,28]. CARPA is non-IgE-mediated hypersensitivity reaction that can cause symptoms involving many organ systems (*e.g.* anaphylaxis, hypo- and hypertension, fever, headache, cardiopulmonary distress, *etc.*) with high reaction rate (up to 45%) [27]. The mechanisms and biological consequences of liposomes triggering the activation of the complement system are not completely understood. However, there is clear evidence that liposomes' physicochemical properties, including size, size distribution, composition, surface characteristics, and stability affect activation of immune system [25]. Therefore, the modulation of these characteristics can prolong the *in vivo* circulation of liposomes and their subsequent efficacy. Recently, a preclinical strategy for evaluation of potential adverse effects induced by nanomedicines was proposed [29]. This strategy is based on a three-tiered approach, combining physicochemical characterization of engineered nanomedicines, nanoparticles interaction and a hazard assessment featuring the detection of complement activation [29]. More importantly, *in vitro* and *in vivo* assessments of complement reactions are recommended by the European Medicines Agency as a preclinical assay in the development of liposomal drugs [30]. The level of complement activation can be verified by identifying the complement

split products in human sera, using enzyme-linked immunosorbent assay (ELISA). In Section 2.1, an *in vitro* study on the immunological response towards Pad-PC-Pad liposomes is reported. Bare and NTG-loaded Pad-PC-Pad liposomes, with and without PEG, at two concentrations were incubated with human sera. The concentration of complement proteins C4d, Bb and SC5b-9 was determined. Elevated level of C4d or Bb protein is evidence for the involvement of classical and lectin or alternative complement pathways, respectively. The level of complement activation induced by Pad-PC-Pad liposomes was compared to that one triggered by FDA-approved drugs (*e.g.* Doxil[®], Abelcet[®]).

In Section 2.2, an *in vitro* study on the immunocompatibility of Rad-PC-Rad liposomes was conducted. In this work the activation of the complement system was expanded to the detection of C3a and C5a anaphylatoxins and release of pro-inflammatory cytokines (*e.g.* IL-1 β , IL-6, IL-8, IL-12, TNF- α). The dependency between complement-induced anaphylatoxins production and secretion of cytokines was demonstrated [31]. Uncontrolled release of cytokines can induce potentially life-threatening conditions, including anaphylaxis and cytokine storm. Complement activation and cytokine release was suggested within a tiered approach for *in vitro* assessment of nanoparticle immunocompatibility [32]. Therefore, questions arose of whether Rad-PC-Rad liposomes carry a risk of potential *in vivo* hypersensitivity and if it can cause increased production of pro-inflammatory cytokines. Four Rad-PC-Rad liposomal formulations, bare and NTG-loaded, with and without PEG, at two phospholipid concentrations were incubated with human sera. For the detection of complement proteins concentration, samples were analyzed using ELISA. The level of complement activation induced by Rad-PC-Rad liposomes was compared to that one triggered by FDA-approved liposomal drugs (*e.g.* Doxil[®], AmBisome[®]). The cytokine immunoassay was performed by incubation of Rad-PC-Rad liposomes with isolated leukocytes and with human whole blood. Samples were analyzed using a flow cytometry assay.

Liposome stability is a major requirement for drug delivery. The drug encapsulated by the liposome should stay confined inside until the certain release stimuli being applied. To ensure an appropriate mechanism for action, liposome structural parameters have to be known and controlled. Shear-stress sensitive liposomes are intended for intravenous injection to the human body, therefore, they have to maintain structural stability over a physiologically relevant temperature range. The normal human body temperature range is typically stated as 36.5 – 37.5 °C. However, therapeutic hypothermia (< 35 °C) is routinely induced during cardiac surgery, and is recommended as a treatment strategy for cardiac arrest in international resuscitation guidelines [33]. The results of clinical trials demonstrated that mild therapeutic hypothermia (32 – 34 °C) showed an improvement of patients' survival [34,35]. At the other extreme, hyperthermia (37.5 – 38.5 °C) and hyperpyrexia (40 – 41 °C) of the human body have prevalent occasion and were investigated in detail [36]. Even higher temperatures (41.6 – 42 °C), known as critical thermal maximum of human body, might occur in life threatening conditions [37,38]. Therefore, in order to cover the potentially relevant physiological temperature range, liposomes were investigated over the 22 – 42 °C. Then samples were cooled down back to 22 °C to determine the reversibility of observed structural changes.

Pad-PC-Pad and Rad-PC-Rad liposomes, previously identified as potential candidates for targeted drug delivery to the atherosclerotic arteries, were extensively

studied [15, 39–43]. These liposomes along with a library of specifically modified 1,3-substituted lipids with 16:0-18:0 cis-double bonds and ester, amide and urea linkers were synthesized and studied in order to understand the unique behavior of mechanoresponsive liposomes [44]. Dynamic light scattering (DLS) was used to measure overall size of the liposomes. Liposome shape was investigated using transmission electron microscopy at cryogenic temperatures (cryo-TEM). However, cryo-TEM is limited by the number of liposomes observed, therefore a technique involving statistical averaging is desirable to provide a measurement of entire sample. Small-angle neutron scattering (SANS) was applied, allowing for higher resolution and statistical averaging. Previous studies have employed SANS to provide quantitative information about the liposomes' organization at the nanoscale and to investigate their structure-function relationship [45]. In our study, liposome size and shape as determined by DLS and cryo-TEM were used as starting values for SANS data fitting.

The results presented in the Section 2.3 provide quantitative information on the change in liposomes structural parameters (*e.g.* bilayer thickness, radius, eccentricity) across the whole range of physiologically relevant temperatures, as determined from the analysis of SANS data.

Contributions

The content of the *Results* chapter was achieved thanks to the support and strong collaboration between multi-disciplinary teams, including physicists, chemists, biologists and immunologists. Although the main work was done by the author of the present thesis (S.M.), it was supported by the valuable contributions of experienced scientists, namely, Prof. Dr. Bert Müller (B.M.), Dr. Andreas Zumbuehl (A.Z.), Prof. Dr. János Szebeni (J.S.), Dr. Hans Deyhle (H.D.), Dr. Joachim Kohlbrecher (J.K.), Dr. Thomas Pfohl (T.P.), Dr. Marzia Buscema (M.B.), Dr. Frederik Neuhaus (F.N.), Gabriela Gerganova (G.G.), Tamás Mészáros (T.M.), Dr. Gergely Tibor Kozma (G.T.K.), Dr. Ute Mettal (U.M.), Dr. Takashi Ishikawa (T.I.).

S.M. made substantial contributions in the following phases of the work: the study design and implementation, conduction of the experiments, data analysis, figure preparation and writing of the manuscripts.

The contributions of the co-authors are listed for each section of the Results chapter. All co-authors actively participated in discussion of the results, and provided critical feedback on the related manuscripts. The co-authors' order is equivalent to the order in the published or submitted manuscripts.

Section 2.1:

M.B.: Contributed to the study design, sample preparation and conduction of the *in vitro* experiment. Taught liposome preparation.

T.M.: Contributed during the *in vitro* experiment and data analysis. Taught the carrying out of immune assay.

G.G.: Contributed during the sample preparation, and the *in vitro* experiment.

T.P.: Contributed to the critical reviewing of the manuscript.

A.Z.: Provided the lipids for sample preparation. Transferred the knowledge about liposomes preparation and characterization. Contributed to the critical reviewing of the manuscript.

J.S.: Contributed to the study design and data interpretation. Transferred the knowledge about adverse immune reactions and complement system.

B.M.: Initiated the study. Contributed to the study design. Gave suggestions for the graphical representation of the figures. Contributed to the writing and critical reviewing of the manuscript.

Section 2.2:

M.B.: Contributed to the study design and sample preparation.

G.G.: Contributed to the study design, sample preparation and conduction of the *in vitro* experiment.

T.M.: Contributed during the *in vitro* experiment, data analysis and interpretation.

G.T.K.: Contributed to the study design, conduction of the *in vitro* experiment, data analysis and interpretation.

U.M.: Worked on the lipid synthesis. Contributed to the sample characterization for the encapsulation efficiency.

F.N.: Worked on the lipid synthesis. Contributed to the sample characterization for the release test.

T.I.: Performed cryo-TEM imaging of sample.

J.S.: Contributed to the study design and data interpretation.

A.Z.: Provided the lipids for sample preparation. Contributed to the critical reviewing of the manuscript.

B.M.: Initiated the study. Contributed to the study design. Gave suggestions for the graphical representation of the figures. Contributed to the writing and critical reviewing of the manuscript.

Section 2.3:

H.D.: Contributed to the data analysis and interpretation. Contributed to the writing and critical reviewing of the manuscript.

J.K.: Contributed during the data acquisition, analysis and interpretation. Transferred the knowledge about small-angle neutron scattering technique.

F.N.: Designed the study. Worked on the lipid synthesis and prepared samples. Contributed during the data acquisition.

A.Z.: Initiated and designed the study. Contributed during the data acquisition and interpretation. Contributed to the writing and critical reviewing of the manuscript.

B.M.: Gave suggestions for the graphical representation of the figures. Contributed to the writing and critical reviewing of the manuscript. Transferred the knowledge about writing scientific publications.

2 Results

2.1 Liposomes — bio-inspired nano-containers for physically triggered targeted drug delivery

Published in Proceedings of SPIE

Liposomes – bio-inspired nano-containers for physically triggered targeted drug delivery

Sofiya Matviyukiv^a, Marzia Buscema^a, Tamás Mészáros^{b,c}, Gabriela Gerganova^a, Thomas Pfohl^a,
Andreas Zumbühl^d, János Szebeni^{b,c} and Bert Müller^a

^aBiomaterials Science Center, University of Basel, Gewerbestrasse 14, 4123 Allschwil, Switzerland;

^bNanomedicine Research and Education Center, Semmelweis University, Nagyvárad tér 4, 1089
Budapest, Hungary; ^cSeroScience Ltd., Nagyvárad tér 4, 1089 Budapest, Hungary;

^dDepartment of Chemistry, University of Fribourg, Chemin du Musée 9, 1700 Fribourg, Switzerland

ABSTRACT

For natural scientists and engineers, learning from nature has tradition and is often driven by bio-inspired processes and materials. For example, engineers have designed multifunctional materials with hierarchical structures. Lipid bilayers, the principal components of cell membranes, can form vesicles, termed liposomes. Such liposomes are usually recognized as foreign by the immune system of a patient, which makes it challenging to use liposomes as containers for targeted drug delivery. There are, however, promising non-spherical, mechano-sensitive, artificial liposomes about 100 nm in diameter, which were recently identified. These bio-inspired containers offer a wide range of applications. In particular, the targeted release at critically stenosed arteries formed as a result of atherosclerosis significantly reduces the undesired side effects such as a drop of blood pressure. It is well known that FDA-approved liposomal drugs, currently on the market, often induce adverse immune responses. Therefore, to exclude the hypersensitivity of the recently discovered mechano-sensitive liposomes, we have performed *in vitro* complement activation experiments and related animal studies with pigs. Recently, it has been shown that the drug-free Pad-PC-Pad liposomes surprisingly lack any complement activation. In this study, we demonstrate that nitroglycerin-loaded liposomes with relevant human therapeutic dosage exhibit low complement activation compared to the FDA-approved phospholipid drugs, including Abelcet. Furthermore, the liposomal suspensions applied are stable for a period of more than two months. Consequently, the non-spherical liposomes of nanometer size we have developed are promising containers for physically triggered, targeted drug delivery.

Keywords: Nanotechnology, targeted drug delivery, atherosclerosis, biomimetic, liposome, shear stress, hypersensitivity, complement activation.

1. INTRODUCTION

Nanomedicine is at the frontline of nowadays therapy for targeted drug delivery and the global nanomedicine market continues to grow. It is expected to reach \$528 billion by 2019 [1]. The goal of such transporting system is to safely assist the delivery of a pharmaceutical compound to a specific targeted within the body, increasing the therapeutic index of the drug and decreasing acute side effects.

Nature has inspired most of the successfully introduced technologies, that are used in biomedical applications. Biomimetic systems were developed, based on the way how the natural systems are constructed. For instance, biological membranes, representing highly complex and dynamic structures, are mimicked in lipid self-assembly liposomes, closed, spherical vesicles, trapping an aqueous solution into inner environment (see Figure 1).

The spontaneous liposome formation is initiated when phospholipids, with two hydrophobic chains and a hydrophilic polar head group, are exposed to an aqueous environment. This configuration is energetically favored. Liposomes were firstly described by Bangham and Horne in 1964 [2]. Inspired by this architecture, liposomes appeared as a suitable concept for the development of drug delivery systems [3-5].

*bert.mueller@unibas.ch; phone +41 61 207 54 30; fax +41 61 207 54 99; www.bmc.unibas.ch

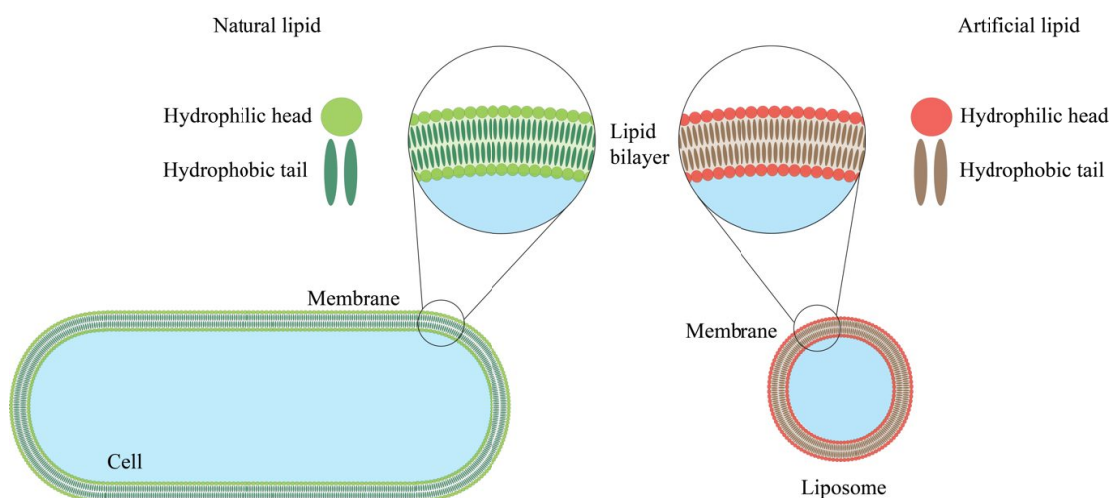


Figure 1. Schematic representation of cell and liposomal lipid bilayer structures. The size of a cell is roughly 100 times larger than the diameter of a liposome. However, in both cases the membrane thickness is the same, about 4-5 nm.

The types of phospholipids used in the fabrication of liposomes are crucial in determining the liposomal properties. Expanding into the non-natural chemical space, we have synthesized artificial 1,3-diamidophospholipids that form liposomes with a faceted morphology [6]. These nanometer-sized, lentil-shaped liposomes are sensitive to the mechanical stress, and have the unique property to release their cargo upon shaking [7]. It makes them a favorable candidate for delivery of vasodilators to constricted arteries, where the liposomes are exposed to an increased average wall shear stress, similar to shaking. Significant changes in the increase of shear stresses between healthy and constricted regions of arteries, are the result of the narrowing of the arterial blood vessels due to plaque formation related to the well-known disease atherosclerosis [8]. 17.5 million people die each year from cardiovascular diseases (CVDs), that is around 31% of all deaths worldwide [9]. These numbers obviously support the need of further studies, especially for the first line treatment of CVDs. Pre-hospital treatment of acute myocardial ischemia comprises bolus administration of nitroglycerin to dilate blood vessels [10]. When applied intravenously it may cause rapid systemic drop down of the blood pressure and, as a result, reduced blood perfusion, which can be lethal in severe cases. Therefore, its combination with nanostructured liposomes may improve the local efficacy of the encapsulated nitroglycerin and mitigate negative side effects.

Despite the successful clinical application of nanomedicines as a controlled drug delivery systems [11], the intravenously injected liposomal drugs are generally recognized by components of the innate immune system as foreign particles. This leads to the activation of a biochemical cascade of the innate immune system, termed complement activation (see Figure 2), resulting in severe hypersensitivity reactions (HSRs) [12]. There are three pathways that initiates complement activation and results in the formation of the membrane attack complex (MAC): the classical, lectin and alternative pathways. The classical pathway leads to complement activation via the binding of antibodies to pathogen surface antigens. This involves the recruitment of C1 complex, which subsequently activates its natural substrate C2 and C4. Mannose-binding lectin (MBL) protein binds to carbohydrate ligands on the pathogen surface, and together with MASP (Mannose-binding lectin-Associated Serine Proteases) they form a complex that proceeds to the cleavage of C2 and C4. The classical and lectin pathways converge at an early stage of the cascade. They trigger the formation of C3-convertase that continuously hydrolyzes C3, and results in amplification of the complement cascade signal. The possibility to study the role of classical and lectin pathways in complement activation, relies on the detection of the C4d protein. C4d is a split product of C4 activation, and is mainly interpreted as a trace of classical pathway activation, however, it is also derived from the lectin pathway [13]. An alternative pathway initiates when a cleaved C3b protein directly binds to the antigen, such as endotoxin, which is found in the outer membrane of bacteria, and elicit strong immune responses. Along the activation cascade, the factor B becomes cleaved, resulting in the formation of the split product Bb, which can be used as a marker for detection of the alternative pathway. The classical and lectin complement activation pathways converge with the alternative at the level of C3 convertase and proceeds into further cleavage of C5 with the subsequent

formation of the C5b-9 membrane attack complex on complement-activating surfaces as represented in Figure 2. It causes direct cell injury by the formation of transmembrane channels, which disrupt the cell membrane, leading to cell lysis and death. If the target membrane is absent, the C5b-9 complex binds to vitronectin (a regulatory S protein). Therefore, liposome-mediated complement activation in human serum was first monitored by measuring the generation of SC5b-9 complex, also termed Terminal Complement Complex (TCC), as a marker for the activation of the whole complement cascade [14].

We hypothesize that artificial liposomes of nanometer size exist that do not show any complement activation for the human therapeutic dose of encapsulated drug. In case of an at least partial approval, a wide variety of therapeutic applications can be envisioned.

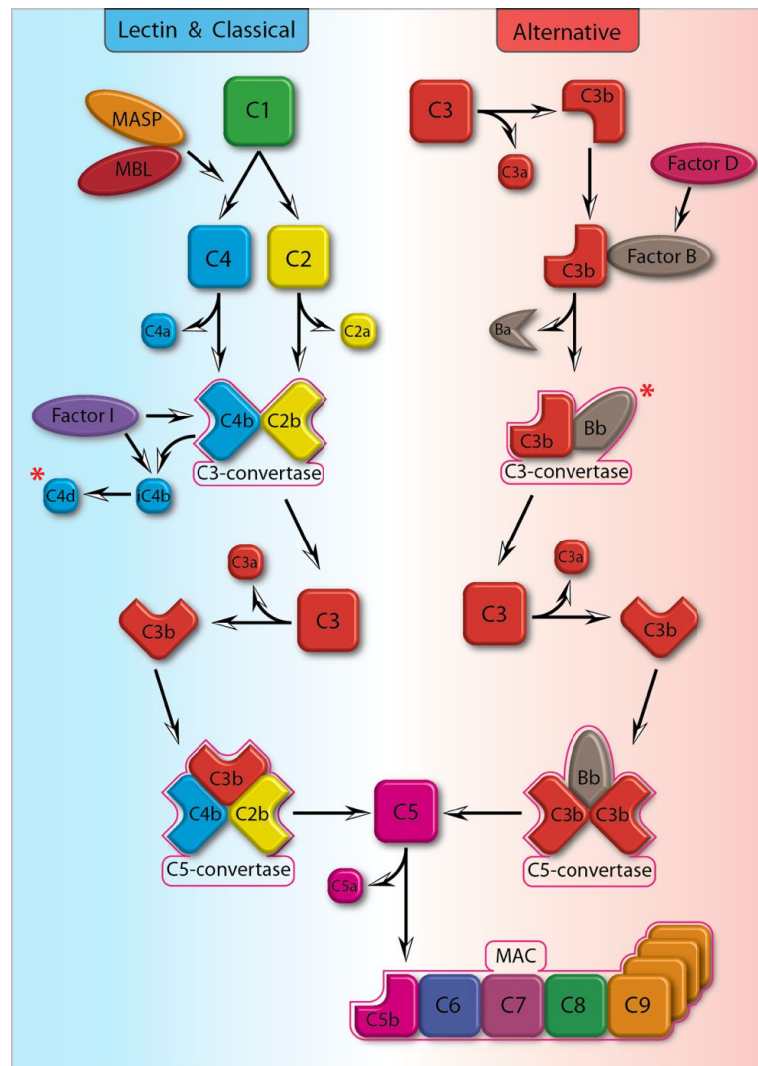


Figure 2. Schematic representation of the complement system cascade classified according to the classical, lectin, and alternative pathways.

2. MATERIALS AND METHODS

2.1 Materials for *in vitro* ELISA assay

Pad-PC-Pad (1,3-palmitoylamido-1,3-deoxy-*sn*-glycero-2-phosphatidylcholine) has been synthesized following the previously reported protocol [6, 7]. DSPE-PEG₂₀₀₀ (1,2-distearoyl-*sn*-glycero-3-phosphoethanolamine-N-[amino(polyethylene glycol)-2000]) was a generous gift from Lipoid GmbH (Germany). Commercial nitroglycerin (NTG) solution “Perlinganit” was purchased from UCB-Pharma AG (Switzerland), Zymosan - from Sigma-Aldrich Ltd. (Hungary) and saline solution (0.9 %, 308 mOsm/L) - from Teva Pharmaceuticals Zrt (Hungary). Doxil and Abelcet were used as purchased by the Nanomedicine Research and Education Center, Semmelweis University (Hungary). Human serum and pig plasma samples were obtained from healthy donors at the Semmelweis University, according to an approved phlebotomy protocol. Until usage, the samples were stored at a temperature of -80 °C. For the determination of classical, alternative pathways and terminal complement complex the following ELISA kits were used: MicroVue C4d, Bb and SC5b-9 Plus. ELISA kits were purchased from Quidel Corp. (San Diego, CA, USA).

2.2 Preparation of shear stress sensitive Pad-PC-Pad liposomes

Three liposomal formulations were prepared, namely A (Pad-PC-Pad/DSPE-PEG₂₀₀₀), B (Pad-PC-Pad/DSPE-PEG₂₀₀₀) and C (Pad-PC-Pad). Liposomes were prepared from Pad-PC-Pad and DSPE-PEG₂₀₀₀ phospholipids in compliance with a previously reported protocol [7], using the thin film method [15, 16]. Briefly, the lyophilized phospholipids were dissolved in chloroform, in appropriate molar ratios: A – 95:5, B – 95:5, C – 100 mol%. The initial phospholipid concentration was 10 mg/mL. Then, the solvent was removed by rotatory evaporation under reduced pressure, followed by high-vacuum drying overnight. Three lipid films were then hydrated for a period of 30 minutes each at the temperature of 60 °C, with the corresponding buffer: A - 0.1 vol % NTG, B - 0.9 vol % saline, C - 0.1 vol % NTG. Afterwards, the liposomal suspensions were subjected to ten freeze-thaw cycles: frozen in liquid nitrogen and thawed in a 60 °C water bath. The liposomes were sized by multiple extrusions through Nuclepore™ track-etched polycarbonate membrane filters (Whatman, GE Healthcare Life Sciences, UK) of pore sizes of 400, 200, and 100 nm diameter pore sizes, until their diameter distribution became almost monodisperse. Multiple extrusions were performed using a barrel extruder Liposfast LF-50 (Avestin Inc., Canada) at 50 bar N₂ pressure and a temperature of 65 °C. The samples loaded with Perlinganit were purified from excess of external NTG by buffer exchange using PD-10 desalting columns (GE Healthcare Bio-Sciences AB, Sweden), with an exclusion limit of 5,000 Da, following the manufacturer’s gravity protocol. The samples were stored at room temperature until use. To reach the human therapeutic dose (HTD) of encapsulated nitroglycerin each liposomal formulation (A, B, C) was diluted ten times (A*, B*, C*) before *in vitro* testing (*cf. section 3.2*).

2.3 Characterization of lentil-shaped Pad-PC-Pad liposomes

Measurement of size and size distribution

The size and size distribution (polydispersity index, PDI) of the obtained liposomes was determined by triplicate measurements of each sample with the dynamic light scattering (DLS) technique using a DelsaNano C instrument (Beckman Coulter, USA) at a temperature of 25 °C. Measurements were performed on freshly prepared samples. The average diameter of the liposomes within each sample and standard deviations were calculated using the Smoluchowski model (see Table 1 below). The liposome stability over time was tested after 10, 30 and 60 days subsequent to preparation (see Figure 4 below).

Measurement of zeta potential

The zeta (ζ) potential of the samples was measured using the laser Doppler electrophoresis technique on a Zetasizer Nano-ZS (Malvern Instruments Ltd., UK). Liposomes samples were freshly prepared and measured with the following specifications: 60 s sampling time; 0.8872 cP medium viscosity; 1.33 refractive index; 173° scattering angle, using non-invasive backscatter optics; 25 °C temperature (see Table 1 below). Data were analyzed using the Zetasizer software supplemented with the device. The zeta potential values were calculated using the Helmholtz–Smoluchowski’s equation.

Measurement of size and morphology

Liposomes size and morphology were analyzed using transmission electron microscopy (TEM), using CM-100 electron microscope (Philips, Eindhoven, Netherlands), operating at an accelerating voltage of 80 kV. Samples were prepared by liposome deposition onto a 400-mesh carbon/palladium-coated copper grid (Polysciences Inc., Eppelheim, Germany),

which was exposed for 10 s to plasma treatment prior to exploitation. Liposomal samples were negatively stained using a 2 % uranylacetate solution (Sigma-Aldrich, Buchs, Switzerland), and left to dry overnight at room temperature.

Determination of phospholipid concentration

The phospholipid content of the samples was determined by three independent measurements of each sample with the phosphate test 2.0 [17]. Briefly, 20 μL of a liposomal suspension was diluted 1:10 with ultrapure water (18.2 M Ωcm) in a 0.5 – 2 mL microwave vial (Biotage, Sweden). Then 500 μL of a mixture of nitric acid and sulfuric acid (3:1 v/v) were added. The vial was sealed and heated for a period of 20 minutes in a microwave (Biotage Initiator, Sweden) to a temperature of 180 $^{\circ}\text{C}$. After the vial was cooled down, the following solutions were added in sequence: water (2.3 mL), ammonium metavanadate and ammonium heptamolybdate coloring agent (1 mL), and sodium hydroxide solution (1 mL, 10 M). After a duration of 10 minutes the solution was pipetted into a 96-well plate (Nunc-Immuno plate F96 Polysorb, Denmark). Three repeated measurements with eight replicates were performed. The dilution factor specific to the 96-well plate was 33.3. The absorbance was measured at a wavelength of 405 nm using a MultiskanFC 96 plate reader (Thermo Scientific, USA).

2.4 *In vitro* complement ELISA assays for human serum samples

Six human sera were thawed to a temperature of 4 $^{\circ}\text{C}$ and mixed with the following samples: three liposomal suspensions (A, B, C) and their 10-times diluted versions (A*, B*, C*), negative controls (saline and nitroglycerin), FDA-approved liposomal suspension (Doxil) and lipid complex (Abelcet), and the positive control (Zymosan). Eleven samples were incubated with a serum from each of the six donors at a temperature of 37.1 $^{\circ}\text{C}$, in a ratio 3:1. A stock solution of each sample was prepared. After incubation period of 40 minutes the reaction was terminated by adding 10 mM ethylenediaminetetraacetic acid (EDTA), as stop solution. 0.5 M EDTA was diluted with specimen diluent provided by the kit to obtain a concentration of 10 mM. This 20-times sample dilution, is needed as a minimum dilution required to detect the optical density (OD). In order to obtain appropriate OD detection range for each of the samples, we prepared additional dilutions of some liposomal suspensions and positive control: SC5b-9 kit: A - 12x, B - 10x, Doxil - 1.5x, Abelcet - 10x, Zymosan - 25x; C4d kit: Zymosan - 2x; Bb kit: Abelcet - 4x; Zymosan - 6x. The negative control stayed undiluted. During the whole experiment the sera were kept in an ice bath to avoid any spontaneous complement activation. Figure 3 schematically represents the sample preparation steps for the ELISA assay.

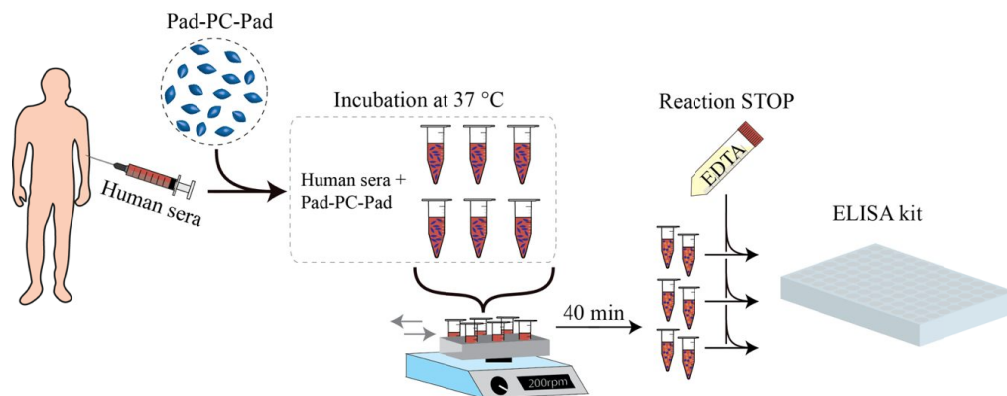


Figure 3. Schematic representation of sample preparation for *in vitro* complement assays of human sera.

Classical and alternative pathways of complement activation

To detect the activation of classical and alternative pathways, the levels of the C4d and Bb proteins were tested by MicroVue C4d and Bb Plus ELISA kits, according to manufacturer's instructions. Briefly, the assay wells were incubated with wash solution for a duration of one to two minutes at a temperature between 15 and 20 $^{\circ}\text{C}$ for two to three times. The samples' aliquot of 100 μL and standards, in the concentration range from 0 to 237 ng/mL (C4d) and from 0 to 660 ng/mL (Bb) were incubated in hydrated micro-assay plates for a period of 30 minutes at room temperature. Afterwards, the wells were washed five times with buffer and 50 μL of the appropriate horseradish peroxidase (HRP)-conjugated antibodies were added to each test well. The wells were washed with buffer for five times, and 100 μL of

substrate solution was added to each test well. Then, another incubation followed with a duration of 30 minutes (C4d) and 15 minutes (Bb), respectively, was done. After the incubation, the enzyme reaction was stopped chemically by adding 100 μ L of EDTA stop solution. The optical density of the wells in each kit was measured spectrophotometrically with a plate reader at wavelengths of 405 (C4d) and 450 nm (Bb).

Terminal complement complex (TCC)

The level of the SC5b-9 complex was evaluated by MicroVue SC5b-9 Plus ELISA kit. The ELISA assay was carried out according to manufacturer's instructions. Briefly, the assay wells were incubated with wash solution for a period of one to two minutes at a temperature between 15 and 20 °C. The samples' aliquot of 100 μ L and standards, in the concentration range from 0 to 185 ng/mL, were incubated in hydrated micro-assay plates for a duration of 60 minutes at room temperature. After incubation, the wells were washed with buffer for five times and 50 μ L of HRP-conjugate was added to each test well. After incubation for 30 minutes at room temperature, the wells were washed with buffer for five times, and 100 μ L of substrate solution was added to each test well. Afterwards, another incubation for a period of 15 minutes took place. Then the enzyme reaction was stopped chemically by adding 100 μ L of stop solution. The optical density of the wells in each kit was measured spectrophotometrically with a 96-well-plate plate reader (FLUOstar Omega, BMG Labtech, Germany) at wavelength of 450 nm.

2.5 Statistical analysis

The levels of SC5b-9, C4d and Bb in serum are expressed as mean \pm S.D. For data analysis, all samples were compared to saline, except Zymosan. Significance of differences between the groups was determined by ordinary one-way analysis of variance (ANOVA), followed by Dunnett's multiple comparison test. Differences between groups were considered statistically significant at $P \leq 0.05$. Statistical analysis was carried out using GraphPad Prism 6 (GraphPad Software Inc., CA, USA).

3. RESULTS

3.1 Characteristics of shear-stress-sensitive Pad-PC-Pad liposomes

Analysis of size and size distribution

The DLS results indicate the mean diameter of the liposomes containing 5 mol% DSPE-PEG₂₀₀₀ corresponded to 115 nm (B) and 130 nm (A), while the average size of formulation composed of Pad-PC-Pad only – was above 2.5 μ m (see Table 1). The liposome stability was tested over 60 days after sample preparation. The related results are shown in Figure 4. Figure 4 A-B demonstrate the presence of only one peak in A and B samples after 60 days, while C shows the presence of three peaks. The two peaks at around 3 and 30 μ m as well as the broad size distribution reveal the formation of liposomal aggregates. This was reflected in the PDI value, confirming that the sample was poly-disperse.

Analysis of zeta potential

The zeta potential was in the range from -0.4 to +3.1 mV (see Table 1). These values indicate that Pad-PC-Pad phospholipids are neutral and should exhibit a relatively low aggregation stability.

Table 1. Properties of liposomal formulations tested in this study. Lipid concentrations of each suspension were determined by the phosphate test 2.0 and shown as the mean of three repeated measurements \pm the relative error. DLS, PDI and ζ -potential values were given as the mean \pm standard deviation of a triplicate measurement.

Name	Lipid composition	Lipid content (mg/mL)	Average size (nm)	PDI	ζ -potential (mV)
A	Pad-PC-Pad/DSPE-PEG ₂₀₀₀	8.19 \pm 0.95	130.8 \pm 3.7	0.10 \pm 0.01	-0.42 \pm 0.4
B	Pad-PC-Pad/DSPE-PEG ₂₀₀₀	9.18 \pm 1.15	115.7 \pm 0.7	0.08 \pm 0.01	+1.26 \pm 0.45
C	Pad-PC-Pad	10.28 \pm 0.40	2659.3 \pm 247.4	0.91 \pm 0.11	+3.10 \pm 0.16

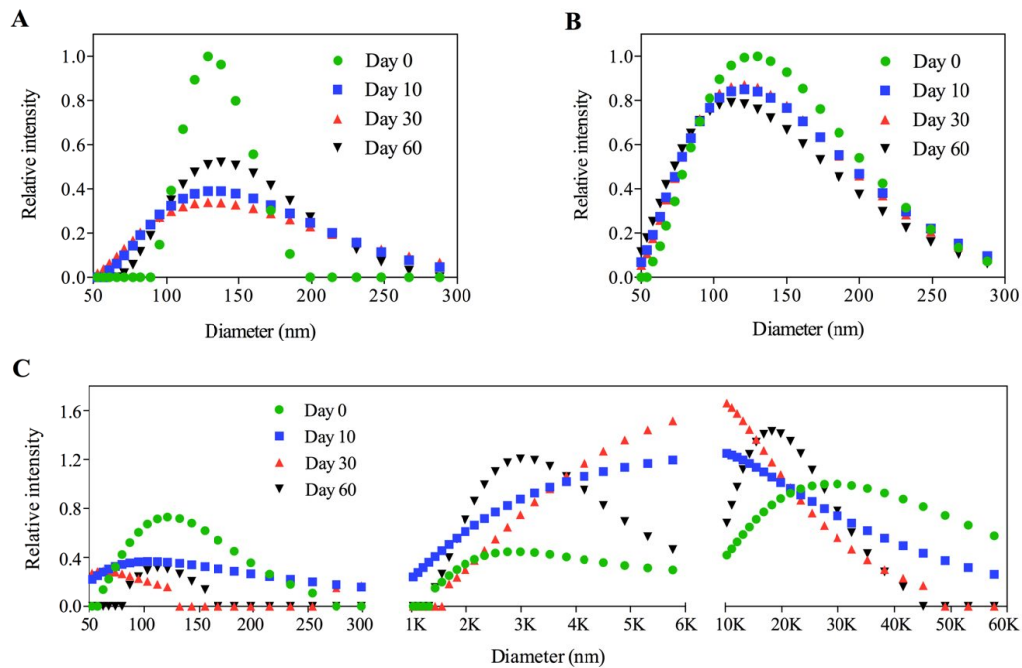


Figure 4. Size distribution of liposome samples A (A), B (B), C (C) measured 0, 10, 30, and 60 days after preparation.

Analysis of size and morphology

TEM analysis of all three Pad-PC-Pad liposomal formulation was performed. Figure 5 represents the characteristic micrographs of the A, B, and C samples. The images show a population of heterogeneous liposomes, with mean diameter of 111 ± 21.1 nm (A), 106 ± 23.5 nm (B) and 102 ± 17.7 nm (C). These data corroborate to the results of the DLS analysis (cf. Table 1).

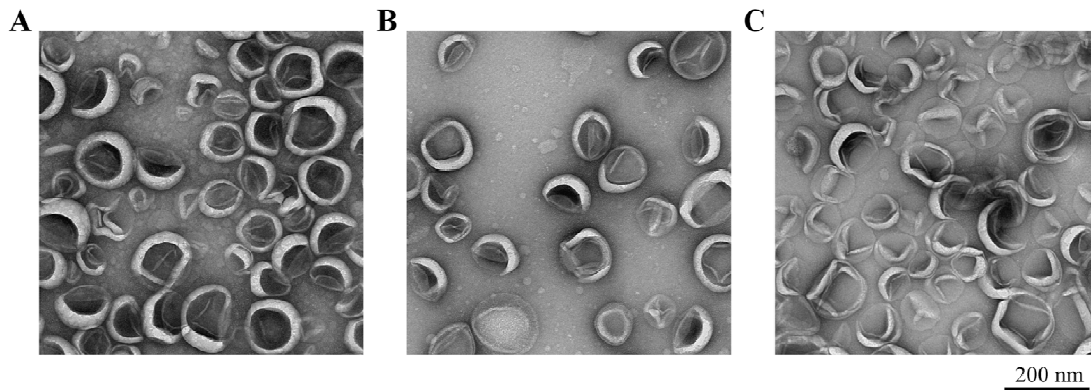


Figure 5. TEM image of liposomal suspensions A (A), B (B), C (C).

Analysis of phospholipid concentration

The total lipid concentration after extrusion was obtained from the phosphate test 2.0 and found to be in the range between 8.19 and 10.28 mg/mL (see Table 1). These values were expected, since samples were prepared with an initial

phospholipid concentration of 10 mg/mL. Both samples A and B contain lower amounts of phospholipids, possibly due to some loss of solution during the preparation steps. When PEG is coupled to hydrophobic molecules (such as phospholipids head groups), it essentially represents non-ionic surfactants. This makes PEGylated samples more difficult to extrude at high pressure without a loss of sample volume. On the contrary, sample C without PEG has shown a final concentration equivalent within the error to the initial one. This can also happen during the extrusion step. As Pad-PC-Pad liposomes were extruded at a temperature of 60 °C, after ~ 25 extrusion cycles, some volume of loading buffer could evaporate, thus increasing the phospholipid concentration.

3.2 Encapsulation volume of NTG

For the liposomal solution with a concentration of 10 mg/mL and known molecular weight of Pad-PC-Pad ($M_w = 734$ g/mol), we calculated the molecular concentration as 0.01 g of Pad-PC-Pad multiplied by its molecular weight 734 g/mol to 1.37×10^{-5} mol. Considering the Avogadro number 6.022×10^{23} mol⁻¹ we calculated the number of Pad-PC-Pad molecules in 10 mg/mL solution to 8.23×10^{18} molecules. We estimated an average liposome with 100 nm diameter would contain approximately 10^4 Pad-PC-Pad molecules. Therefore, we calculate number of liposomes as number of Pad-PC-Pad molecules 8.23×10^{18} divided by 10^4 molecules is equal to 8.23×10^{14} liposomes. Based on our previous studies, Pad-PC-Pad liposomes form the lenticular shape. Thus, the volume of one vesicle is calculated to be 4.75×10^{-13} μ L [7]. Taking this value in consideration, we can estimate the total volume of encapsulated buffer as 8.23×10^{14} liposomes times 4.75×10^{-13} μ L, which equals to 391 μ L. The calculated total encapsulation volume for one liposome is therefore 320 μ L (A), 359 μ L (B), and 402 μ L (C), respectively.

3.3 *In vitro* complement activation for human sera

Detection of classical and alternative pathways of complement activation

Figure 6A displays the results of the classical and lectin pathway tests. Formulation B elicited a two-fold elevation in the level of C4d versus saline, with a value comparable to Doxil. The level of C4d measured in the rest of the samples has not shown any significant difference in comparison to the negative control. Figure 6B provides the results of the alternative pathway test. None of the Pad-PC-Pad liposomes, regardless the concentration, showed any significant increase of the Bb level with respect to saline. Bb values of the Doxil samples were in the same range as for Pad-PC-Pad liposomes. Abelcet showed more than three-fold increase in Bb concentration versus saline, and up to eight-fold increase was elicited by Zymosan.

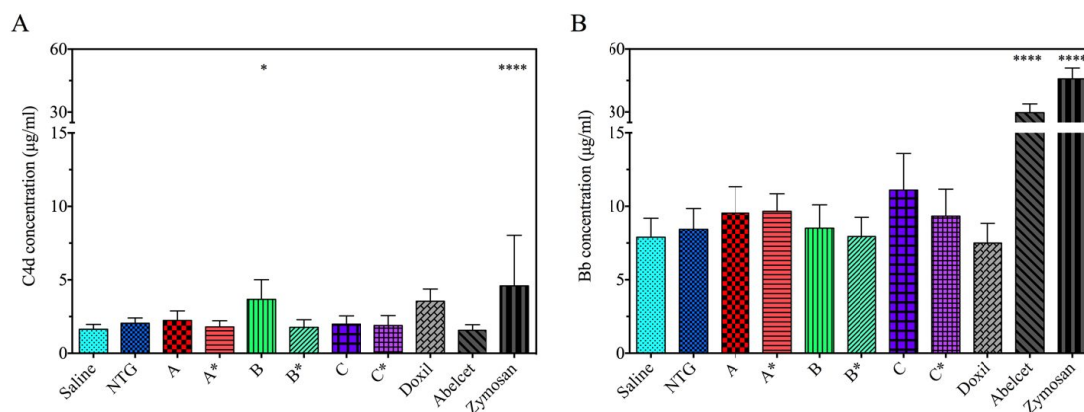


Figure 6. Detection of complement activation via classical, lectin and alternative pathways, using C4d (A) and Bb (B) ELISA kits. Human sera were incubated for a period of 40 minutes at body temperature with the following samples: saline, nitroglycerin, Pad-PC-Pad liposomes (A, A*, B, B*, C, C*), Doxil, Abelcet and Zymosan. Data are shown as the mean of six sera from donors and error bars as the standard deviation among the individuals. The values were normalized to the liposome concentration of 10 mg/mL (A, B, C samples) and 1 mg/mL (A*, B*, C* samples). Significance of differences among the groups was determined by an ordinary one-way ANOVA, followed by Dunnett's multiple comparison test ($P < 0.05$).

Detection of terminal complement complex

Figure 7 demonstrate the results of TCC activation. Formation of SC5b-9 complex was determined and to some extent, all liposomal formulations induced the formation of an SC5b-9 complex. Among the three Pad-PC-Pad liposomal formulations (A, B, C), the sample A, containing Pad-PC-Pad/DSPE-PEG₂₀₀₀ and loaded with nitroglycerin showed the highest SC5b-9 concentration in all tested individuals, 25-fold higher compared to the negative control. Sample C, containing Pad-PC-Pad and loaded with NTG, demonstrated lower, but still elevated level of TCC, that was twelve-fold higher in comparison to saline and NTG. B sample demonstrated the lowest SC5b-9 level that was comparable to Doxil and negative control. Two of the Pad-PC-Pad liposomal formulations, with ten times lower phospholipid concentration (B*, C*) have shown values similar to the negative controls. Within the standard deviation, the results were comparable to Doxil, indicating a mild, biologically non-significant reaction. A* sample displayed four times increased level of SC5b-9 complex, compared to saline and NTG. SC5b-9 concentrations of all three diluted samples were not considered statistically significant ($p > 0.05$), in comparison to saline. The level of SC5b-9 in Abelcet sample was ten-fold higher than in Doxil, and four- to eight-fold higher compared to diluted Pad-PC-Pad samples. Abelcet revealed high complement activation, statistically comparable to that of Zymosan.

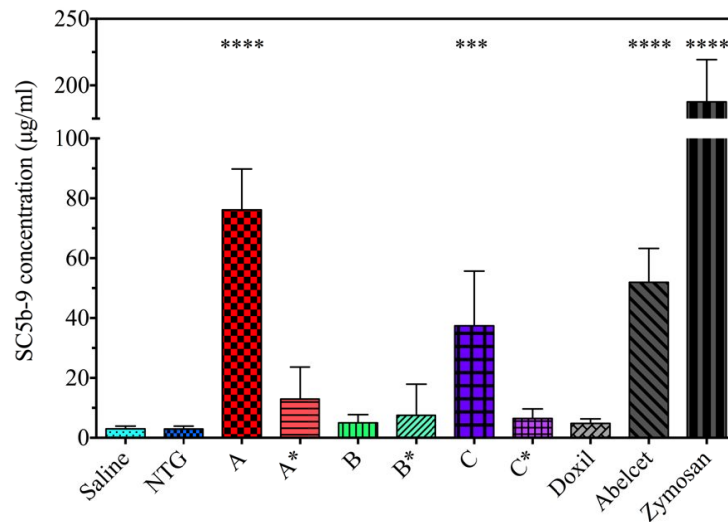


Figure 7. Level of activated SC5b-9 complex, after 40 minutes of incubation at body temperature with human sera. Sera were incubated with saline, nitroglycerin, Pad-PC-Pad liposomes (A, A*, B, B*, C, C*), Doxil, Abelcet and Zymosan. Data are shown as the mean of sera from six donors and error bars as the standard deviation among the individuals. The values were normalized to the liposome concentration of 10 mg/mL (A, B, C samples) and 1 mg/mL (A*, B*, C* samples). Significance of differences among the groups was determined by an ordinary one-way ANOVA, followed by Dunnett's multiple comparison test ($P < 0.05$).

3.4 Validation of results

The standard curve of the target protein for each kit is generated using the blank subtracted OD values for each standard and the assigned concentration for each standard (cf. Figure 8). The obtained standard curve must meet the validation requirements. The validation of the ELISA tests results has been verified by the determination of the slope (m), y-intercept, and correlation coefficient (r) of the derived best-fit for all standards. The results of Bb kits were analyzed using the second-order polynomial model, where instead of slope value, the calibration curve was characterized using the B0, B1 and B2 coefficients. All of the experimental values were within the specified reference ranges according to the kit's manufacturing instructions. Therefore, we can state that obtained results are well reliable and reproducible.

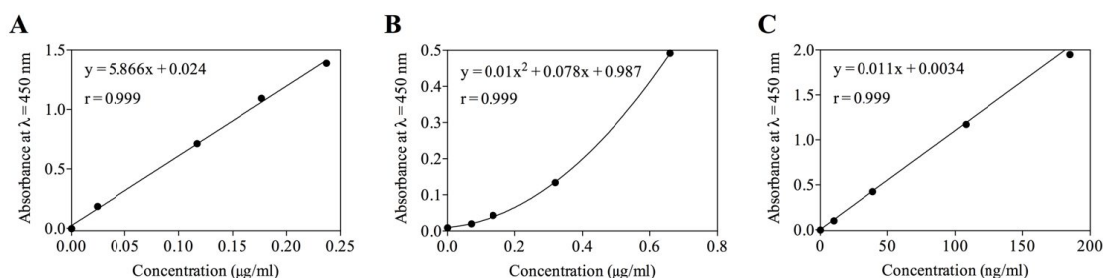


Figure 8. Calibration curves of C4d (A), Bb (B), SC5b-9 (C) ELISA tests.

4. DISCUSSION

Pad-PC-Pad liposomal characteristics

The A and B samples, both containing DSPE-PEG₂₀₀₀ demonstrate average diameter in the range of 115 – 130 nm, while the C sample, composed of Pad-PC-Pad only, has shown a 20 times higher diameter. This indicates the presence of liposomal aggregations within the solution. This observation was confirmed by the analysis of size distribution of the samples on the first day of preparation and after two months (cf. Figure 4C). The sample C revealed the presence of aggregates immediately after the preparation, and after the rest period of two months. As opposed to C, samples A and B were both stable, showed no aggregation and displayed a comparably low PDI value. Low stability of the Pad-PC-Pad sample was predicted by zeta potential measurements: the zeta potential is a key indicator of the stability of the colloidal systems, such as liposomes. It is directly related to the net charge of a particle and affects its mobility in the medium. Zeta potential indicates the degree of electrostatic repulsion between similarly charged particles in the solution. For nanometer-sized particles high zeta potential ensures the stability, meaning the solution will resist aggregation. On the contrary, if the zeta potential is small, attractive forces may dominate, leading to flocculation. The major part of most biological membranes is composed of phospholipids which are zwitterions and therefore neutrally charged. Pad-PC-Pad belongs to this group as well. The polar head group of Pad-PC-Pad molecule contains anionic phosphate and cationic ammonium groups, hence making it a zwitterionic molecule. Carrying both positive and negative electrical charges this molecule reveals a charge, close to neutral. A priori it can be assumed that liposomes with close to zero net charge will possess little or no electrophoretic mobility, therefore, low zeta potentials. This indication was confirmed by zeta potential measurements, where all of the three Pad-PC-Pad samples showed zeta potential close to zero. Colloids with zeta potential + 3 mV are considered as unstable with maximum agglomeration and precipitation [18]. Additionally, the formation of faceted Pad-PC-Pad liposomes hints at very stiff membranes, lacking the undulation forces that lead to vesicle repulsion in standard liposomal formulations [19]. Stable liposome suspensions require repulsive interactions to overcome the attractive forces. Another way to influence liposomes stability is to use steric stabilization, which can be achieved by covering the surface by incorporation of long, bulky molecules into the lipid bilayer. This would prevent aggregation due to increasing the steric distance between liposomes. Polyethylene glycol (PEG) is the most widely used stabilizer in pharmaceutical applications [20] and has been used for liposomes stabilization [21]. Therefore, due to the low stability of pure Pad-PC-Pad sample, we prepared samples containing PEG. Indeed, adding PEGylated lipids into the Pad-PC-Pad vesicles increased the stability of the liposomes and no aggregation was observed, as seen from the DLS results (Figure 4 A, B).

TEM is a powerful high-resolution technique, which may be also applied to characterize the size and morphology of nanoparticles. It allows to produce individual two-dimensional grayscale images, which can be later used to create the three-dimensional structure, using reconstruction software. From the images in Figure 5 it is seen that shape of all three Pad-PC-Pad liposomal samples appeared distorted, showing circular form, and not lentil-shaped, as reported previously [22]. The reason for this lies in the sample preparation where the drying step leads to vesicle rupture. All of the three samples analyzed by TEM revealed lower size when compared, to DLS results. This is related to the liposome shrinkage, caused by sample drying. According to DLS results, sample C formed aggregates. Nevertheless, according to results of TEM image (Figure 5C), the average size of separated liposomes was 102 ± 17.7 nm. It is also visible that the liposome distribution on the image is denser in comparison to A and B samples, meaning that pure Pad-PC-Pad liposomes tend to form aggregates. Minor differences in size values between DLS and TEM analysis are present also due to comparatively

lower count of vesicles analyzed via TEM. It should be noted that TEM analysis is a suboptimal tool to visualize liposomal formulations. In order to preserve initial morphology, and visualize liposomes in their native fully hydrated state, further imaging with a cryo-TEM is desirable.

Human therapeutic dose of NTG

The dosage of NTG should be adapted to the individual needs of the patient and to the response of controlled parameters, and the respective situation. The clinical dosage range is from 33 to 133 μg per minute [23]. Higher doses of 166 μg per minute are possible in rare cases [23]. In general, the results of treating acute hypertensive heart failure with intravenous bolus injection of 1 mg/mL of nitroglycerin were reported [24], as well as patients with severe decompensated heart failure with a bolus injection of 2 mg nitroglycerin [25] has been reported. Based on values obtained with the phosphate test for lipid concentration (Table 1), the encapsulated volume of NTG was calculated (*cf. section 3.2*). The quantity of nitroglycerin encapsulated in 10 mg/mL is about 391 μg , which is three times higher than the maximum dose. Therefore, a ten-fold dilution of each liposomal formulation was prepared and labeled as A*, B* and C*. Phospholipid content and encapsulated volume of NTG for these samples was calculated as ten times lower than initial one. However, the loading procedure of NTG into the liposomes was not optimized and the loading efficiency here certainly lies significantly lower than 100 %.

In vitro determination of complement activation

Overall, the level of C4d measured in all samples has shown low concentration of the protein, providing an evidence that complement activation of liposomes does not involve neither classical nor lectin pathways, at least to a major extent. Therefore, as the next step, the complement activation via alternative pathway was studied. We observed elevated levels of Bb concentration, caused by all the samples. This might be an indication that mainly the alternative pathway is involved in complement activation, caused by liposomal formulation. It was reported that increased Bb concentration in Doxil-sensitive sera, provides an evidence of its role in alternative pathway activation [26]. Abelcet has shown high activation of Bb protein, indicating a significant statistical difference. Abelcet is formulated from 1,2-dimyristoyl-*sn*-glycero-3-phosphorylcholine (DMPC) and 1,2-dimyristoyl-*sn*-glycero-3-phosphorylglycerol sodium salt (DMPG), containing amphotericin B, as active drug. A major difference between Abelcet and the rest of the samples is the shape and size of the particles, which could serve as a recognition factor for initiation of the complement activation. It consists of ribbon-like complexes, with size of 1.6 to 11.0 μm . We expected also high values of protein activation by Zymosan in the Bb kit, since it is an activator of the alternative pathway. The amount of Zymosan-activated protein increased and multiplied along the activation cascade.

Activation of TCC was represented by the concentration of the soluble C5b-9 protein complex, formed in human sera, after incubation with defined samples. The obtained values were normalized to the liposome concentration of 10 mg/mL (A, B, C) and 1 mg/mL (A*, B*, C*). This step was applied in order to improve data integrity and better differentiate the impact of the liposomal formulation upon the complement activation. Also, this helps to avoid misinterpretation of results due to higher or lower amounts of phospholipids within the sample.

The results of Figure 7 indicate that formulations A and C induce relatively strong complement activation. However, some studies suggest that if the complement activation was detected *in vitro*, does not necessarily mean that a patient will also develop HSRs *in vivo*. Only those with more than five- to ten-fold increased protein level may carry a risk of complement activation and related HSRs [27]. Such alignment of the results of A and C samples may be caused by the presence of NTG within the vesicles, particularly, by combination of Pad-PC-Pad loaded with NTG. Additionally, under the conditions used, the Pad-PC-Pad vesicles were incubated above their main transition temperature, which should lead to a full release of the entrapped NTG. However, when alone, NTG does not cause detectable immune reaction. Similar situation results were obtained for Doxil, that in the presence of doxorubicin influences the activation of the complement system [26]. Van den Hoven reported that prednisolone sodium phosphate encapsulated within the liposomal aqueous interior also causes increased chance of complement activation [28]. Besides, our recent study demonstrates that drug-free Pad-PC-Pad do not show any significant complement activation [22], as compared to their NTD-loaded liposomal counterparts. As follows, incorporation of certain drugs can cause physicochemical changes to the liposomal formulation, carrying a risk of elevated SC5b-9 concentration. Increased levels of complement activation by C sample can also be correlated with the presence of aggregates, that was confirmed by the DLS measurements. As can be seen from the results in Figure 7, no significant changes in complement activation were seen in the sample B, which contains PEG₂₀₀₀ coupled to DSPE. Sample B showed the lowest value of SC5b-9 concentration among three concentrated samples, and its value was comparable to the negative control. This result was compared with our previously reported

data, where Pad-PC-Pad liposomes loaded with PBS did not reveal complement activation after a period of 60 minutes of incubation [22]. Van den Hoven also suggests that PEGylated liposomal formulations carry a low risk for causing hypersensitivity reactions [28]. Besides, neither reduction of PEG chain length, nor decrease of PEG density at the liposome surface, significantly changes activation of complement system. However, Chanan-Khan and Szebeni both reported that PEGylated liposomal products, such as Doxil, can induce complement activation-related hypersensitivity reactions [26, 27]. However, not all the patients with complement activation displayed HSRs. As explained by Chanan-Khan, it may be related due to the involvement of certain factors, which can limit adverse consequences of activated complement peptides, released during complement activation [27]. The TCC activator Zymosan induces complement activation immediately and after 40 minutes of incubation and has reached up to 62-fold higher SC5b-9 concentration as compared to saline. It shall be mentioned that for this experiment one donor was found to be consistently more sensitive than the others. This individual could be prone to complement activation and contributes to significantly larger values towards the average (e.g. by factor of two for the A*, B*, C*). It is known that all types of liposomes can cause complement activation, which can be even enhanced due to variety of factors, such as positive or negative surface charge, increasing the size of liposomes, PEGylation of liposomes, presence of aggregates, presence of drugs in the extra-liposomal medium, high percentage (> 50 %) of cholesterol in the membrane, etc. [29]. It has been shown that PEGylated liposomes with 120 nm in diameter, composed of cholesterol, have shown significant increase in activation of Bb, indicating that size and presence of PEG molecules might be important for complement activation by triggering the alternative pathway [28]. Nevertheless, in our study we did not observe the effect of PEGylation on the complement cascade, neither in the pathway, nor in TCC tests. It is important to notice, that the type of molecule used for anchoring the PEG plays a certain role. In our case, we used DSPE, and not cholesterol. However, the liposomal aggregation in the C sample had its impact on the increased level of TCC formation. Similar statements about direct impact of the liposomal size, charge, and presence of PEG molecules on the complement activation, can be very subjective, as the type of formulation and phospholipid concentration can vary significantly from one liposomal formulation to another. To our knowledge, the complement system reactivity to the synthetic non-natural Pad-PC-Pad liposomes, loaded with nitroglycerin were reported for the first time, therefore a direct comparison with other researcher's reports is complicated.

5. CONCLUSIONS

Liposomes can trigger initiation of both classical and alternative complement pathways. Based on the absence of significant changes in C4d level, involvement of the classical and lectin pathways can be excluded in the complement activation by Pad-PC-Pad liposomes. Instead, we observed increased levels of Bb protein, among all the samples that is an indicator of potential involvement of the alternative pathway. However, no statistical significance between our liposomal formulations and the negative control was found. Current preliminary results demonstrate C-activation after 40 minutes of samples' incubation. Further studies will incorporate detailed analysis of complement activation over time, at the various time points. Besides, determination of the SC5b-9 complex formation of NTG-loaded Pad-PC-Pad liposomes in porcine sera would provide additional meaningful information for future *in vivo* studies.

In summary, our results indicate that nitroglycerin-loaded Pad-PC-Pad liposomes prepared of approximately 10 mg/mL phospholipids can carry an increased risk on hypersensitivity reaction. Nevertheless, their diluted counterparts demonstrate weak, biologically non-significant, complement activation only in some sensitive donors. Sensitivity for complement activation by liposomes is exhibited on an individual basis, suggesting that sensitive individuals could experience a hypersensitivity reaction. This warns about certain risk for infusion reactions of concentrated Pad-PC-Pad liposomes, loaded with nitroglycerin. However, as mentioned above, diluted liposomal formulations already contain sufficient HTD of the encapsulated drug. Therefore, the application of diluted Pad-PC-Pad liposomes is a promising formulation that deserves to be further investigated.

ACKNOWLEDGMENTS

This work was primarily funded by the Swiss National Science Foundation (SNSF) in the National Research Program (NRP) 62 'Smart Materials' and supported by the Swiss Government Excellence Scholarships for Foreign Scholars and Artists 2016-2017. The travel award provided by Swiss Society of Biomaterials and Regenerative Medicine is kindly acknowledged.

REFERENCES

- [1] Evers, P., "Nanotechnology in medical applications: the global market," BCC Research, (2015).
- [2] Bangham, A. D., and Horne, R., "Negative staining of phospholipids and their structural modification by surface-active agents as observed in the electron microscope," *Journal of molecular biology*, 8(5), 660IN2-668IN10 (1964).
- [3] Felnerova, D., Viret, J.-F., Glück, R., and Moser, C., "Liposomes and virosomes as delivery systems for antigens, nucleic acids and drugs," *Current Opinion in Biotechnology*, 15(6), 518-529 (2004).
- [4] Torchilin, V. P., "Recent advances with liposomes as pharmaceutical carriers," *Nature reviews Drug discovery*, 4(2), 145-160 (2005).
- [5] Gregoriadis, G., "Engineering liposomes for drug delivery: progress and problems," *Trends in biotechnology*, 13(12), 527-537 (1995).
- [6] Fedotenko, I. A., Zaffalon, P.-L., Favarger, F., and Zumbuehl, A., "The synthesis of 1, 3-diamidophospholipids," *Tetrahedron Letters*, 51(41), 5382-5384 (2010).
- [7] Holme, M. N., Fedotenko, I. A., Abegg, D., Althaus, J., Babel, L., Favarger, F., Reiter, R., Tanasescu, R., Zaffalon, P.-L., Ziegler, A., Müller, B., Saxer, T., and Zumbuehl, A., "Shear-stress sensitive lenticular vesicles for targeted drug delivery," *Nature nanotechnology*, 7(8), 536-543 (2012).
- [8] Holme, M. N., Schulz, G., Deyhle, H., Weitkamp, T., Beckmann, F., Lobrinus, J. A., Rikhtegar, F., Kurtcuoglu, V., Zanette, I., Saxer, T., and Müller, B., "Complementary X-ray tomography techniques for histology-validated 3D imaging of soft and hard tissues using plaque-containing blood vessels as examples," *Nature Protocols*, 9(6), 1401-1415 (2014).
- [9] WHO, "Cardiovascular disease: heart disease and stroke," *Global status report on noncommunicable diseases*, 95-103 (2014).
- [10] Nossaman, V. E., Nossaman, B. D., and Kadowitz, P. J., "Nitrates and nitrites in the treatment of ischemic cardiac disease," *Cardiology in review*, 18(4), 190 (2010).
- [11] Dawidczyk, C. M., Kim, C., Park, J. H., Russell, L. M., Lee, K. H., Pomper, M. G., and Searson, P. C. "State-of-the-art in design rules for drug delivery platforms: lessons learned from FDA-approved nanomedicines," *Journal of Controlled Release*, 187, 133-144 (2014).
- [12] Szebeni, J., Muggia, F., Gabizon, A., and Barenholz, Y., "Activation of complement by therapeutic liposomes and other lipid excipient-based therapeutic products: prediction and prevention," *Advanced drug delivery reviews*, 63(12), 1020-1030 (2011).
- [13] Cohen, D., Colvin, R. B., Daha, M. R., Drachenberg, C. B., Haas, M., Nickeleit, V., Salmon, J. E., Sis, B. Zhao, M.-H., "Pros and cons for C4d as a biomarker," *Kidney international*, 81(7), 628-639 (2012).
- [14] Hamad, I., Hunter, A. C., Szebeni, J., Moghimi, S. M., "Poly (ethylene glycol) s generate complement activation products in human serum through increased alternative pathway turnover and a MASP-2-dependent process," *Molecular immunology*, 46(2), 225-232 (2008).
- [15] Walde, P., "Preparation of vesicles (liposomes)," *Encyclopedia of nanoscience and nanotechnology*, American Scientific Publishers, 8(79), 43-79 (2004).
- [16] Olson, F., Hunt, C. A., Szoka, F. C., Vail, W. J., Papahadjopoulos, D., "Preparation of liposomes of defined size distribution by extrusion through polycarbonate membranes," *Biochimica et Biophysica Acta (BBA)-Biomembranes*, 557(1), 9-23 (1979).
- [17] Stalder, E., and Zumbuehl, A. "Phosphate Test 2.0," *CHIMIA International Journal for Chemistry*, 67(11), 819-821 (2013).
- [18] Riddick, T. M., "Control of colloid stability through zeta potential," *Blood*, 10(1), (1968).
- [19] Sackmann, E. "Membrane bending energy concept of vesicle-and cell-shapes and shape-transitions," *FEBS letters*, 346(1), 3-16 (1994).
- [20] Woodle, M. C., "Sterically stabilized liposome therapeutics," *Advanced drug delivery reviews*, 16(2), 249-265 (1995).
- [21] Immordino, M. L., Dosio F., and Cattel L., "Stealth liposomes: review of the basic science, rationale, and clinical applications, existing and potential," *International journal of nanomedicine*, 1(3), 297 (2006).
- [22] Bugna, S., Buscema, M., Matviyukiv, S., Urbanics, R., Weinberger, A., Meszaros, T., Szebeni, J., Zumbuehl, A., Saxer, T., and Müller, B., "Surprising lack of liposome-induced complement activation by artificial 1, 3-diamidophospholipids in vitro," *Nanomedicine: Nanotechnology, Biology and Medicine*, 12(3), 845-849 (2016).

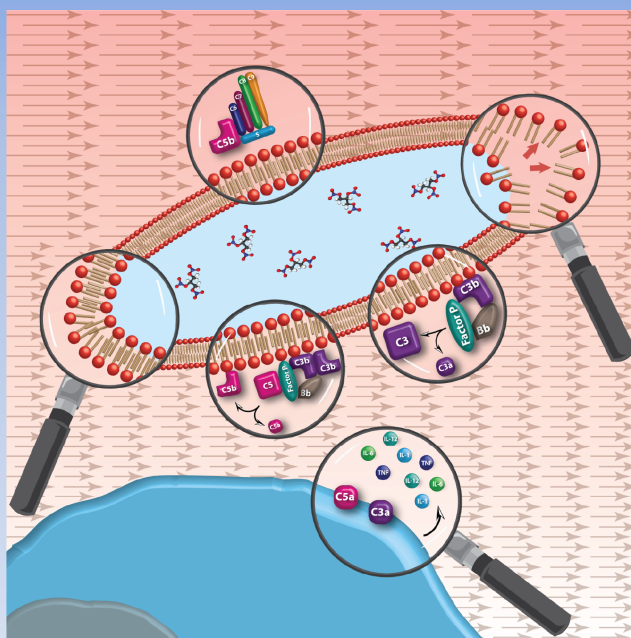
-
- [23] UCB-Pharma AG, "Perlinganit," [package insert], Bulle, Switzerland (2015).
- [24] Wilson, S. S., Kwiatkowski, G. M., Millis, S. R., Purakal, J. D., Mahajan, A. P., and Levy, P. D., "Use of nitroglycerin by bolus prevents intensive care unit admission in patients with acute hypertensive heart failure," *The American Journal of Emergency Medicine*, 35(1), 126-131 (2017).
- [25] Levy, P., Compton, S., Welch, R., Delgado, G., Jennett, A., Penugonda, N., Dunne, R., and Zalenski, R., "Treatment of severe decompensated heart failure with high-dose intravenous nitroglycerin: a feasibility and outcome analysis," *Annals of emergency medicine*, 50(2), 144-152 (2007).
- [26] Szebeni, J., Baranyi, L., Savay, S., Lutz, H. U., Jelezarova, E., Bunger, R., and Alving, C. R., "The role of complement activation in hypersensitivity to pegylated liposomal doxorubicin (Doxil®)," *Journal of Liposome Research*, 10(4), 467-481 (2000).
- [27] Chanan-Khan, A. J., Szebeni, J., Savay, S., Liebes, L., Rafique, N. M., Alving, C. R., and Muggia, F. M., "Complement activation following first exposure to pegylated liposomal doxorubicin (Doxil®): possible role in hypersensitivity reactions," *Annals of Oncology*, 14(9), 1430-1437 (2003).
- [28] Van Den Hoven, J. M., Nemes, R., Metselaar, J. M., Nuijen, B., Beijnen, J. H., Storm, G., and Szebeni, J., "Complement activation by PEGylated liposomes containing prednisolone," *European journal of pharmaceutical sciences*, 49(2), 265-271 (2013).
- [29] Szebeni, J., "Hemocompatibility testing for nanomedicines and biologicals: predictive assays for complement mediated infusion reactions," *European Journal of Nanomedicine*, 4(1), 33-53 (2012).

2.2 Immunocompatibility of Rad-PC-Rad liposomes *in vitro*, based on human complement activation and cytokine release

Published in Precision Nanomedicine

Precision Nanomedicine

The official Journal of CLINAM



Immunocompatibility of Rad-PC-Rad liposomes in vitro, based on human complement activation and cytokine release

Matviykov S, Buscema M, Gerganova G, Mészáros T, Kozma GT, Mettal U,
Neuhaus F, Ishikawa T, Szabeni J, Zumbuehl A, Müller B.

Prec. Nanomed. 2018, Apr;1(1):43-62.



Immunocompatibility of Rad-PC-Rad liposomes *in vitro*, based on human complement activation and cytokine release

Sofiya Matviyiv^a, Marzia Buscema^a, Gabriela Gerganova^a, Tamás Mészáros^{b,c}, Gergely Tibor Kozma^{b,c}, Ute Mettal^d, Frederik Neuhaus^d, Takashi Ishikawa^e, János Szébeni^{b,c,f}, Andreas Zumbuehl^d, and Bert Müller^{a,2}

^aBiomaterials Science Center, Department of Biomedical Engineering, University of Basel, Allschwil, Switzerland

^bNanomedicine Research and Education Center, Institute of Pathophysiology, Semmelweis University, Budapest, Hungary

^cSeroScience Ltd., Budapest, Hungary

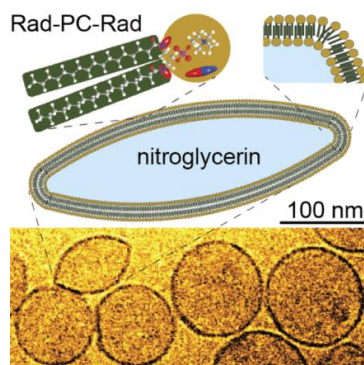
^dDepartment of Chemistry, University of Fribourg, Fribourg, Switzerland

^ePaul Scherrer Institute, Villigen, Switzerland

^fDepartment of Nanobiotechnology and Regenerative Medicine, Miskolc University, Miskolc, Hungary

Submitted: March 26, 2018;

Accepted: April 19, 2018



Graphical Abstract: The mechano-responsive Rad-PC-Rad liposomes, designed to deliver a vasodilator drug to stenosis, are stable even at elevated body temperatures. The question is whether these nano-containers with a specific shape present adverse effects similar to liposomal drugs *in vitro* or they don't.

Abstract

Liposomal drug delivery systems can protect pharmaceutical substances and control their release. Systemic administration of liposomes, however, often activate the innate immune system, resulting in hypersensitivity reactions. These pseudo-allergic reactions can be interpreted as activating the complement system. Complement activation destroys and eliminates foreign substances, either directly through opsonization and the formation of the membrane attack complex (MAC), or by activating leukocytes and initiating inflammatory responses via mediators, such as cytokines. In this study, we investigated the *in vitro* immune toxicity of the recently synthesized Rad-PC-Rad liposomes, analyzing the liposome-induced complement activation. In five human sera, Rad-PC-Rad liposomes did not induce activation, but in one serum high sensitivity via alternative pathway was detected. Such a behavior in adverse phenomena is characteristic for patient-to-patient variation and, thus, the number of donors should be in the order of hundreds rather than tens, hence the present study based on six donors is preliminary. In order to further prove the suitability of mechano-responsive Rad-PC-Rad liposomes for clinical trials, the production of pro-inflammatory cytokines was examined by human white blood cells. The concentrations of the pro-inflammatory cytokines, IL-6, IL-12p70, TNF- α , and IL-1 β , induced by Rad-PC-Rad liposomal formulations, incubated with whole blood samples, were smaller or comparable to PBS (negative control). Because of this favorable *in vitro* hemocompatibility, *in vivo* investigations using these mechano-responsive liposomes should be designed.¹

¹ License: [CC BY-NC-SA 4.0](https://creativecommons.org/licenses/by-nc-sa/4.0/)

² *Corresponding author: phone +41 61 207 5430, bert.mueller@unibas.ch, Biomaterials Science Center, Department of Biomedical Engineering, University of Basel, Gewerbestrasse 14, 4123 Allschwil, Switzerland

Keywords

Nanomedicines, non-spherical liposomes, immune toxicity, complement activation, hypersensitivity reactions, pro-inflammatory cytokines

Purpose and Rationale

The artificial diamidophospholipid Rad-PC-Rad has been synthesized recently [1]. Rad-PC-Rad liposomes aim to preferentially deliver the vasodilator molecules to the stenosed parts of blood vessels. Liposomes, administered intravenously, are immediately exposed to a complex environment of blood cells and proteins. The adsorption of plasma proteins on the surface of liposomes may not only decrease the therapeutic efficiency and biodistribution, but also may result in immunotoxicity. The toxicities which represent the most common safety issues and reasons for nanomedicines failure include complement-mediated reactions and cytokine-mediated inflammation, which can result in anaphylaxis. Therefore, in this study we investigated complement activation and release of pro-inflammatory cytokines, mediated by Rad-PC-Rad liposomes. The immunotoxicity can be also influenced by the therapeutic payload or addition of surface ligands. Therefore, the comparison between nitroglycerin-loaded and drug-free liposomes, as well as PEGylated and non-PEGylated liposomes was evaluated. The physicochemical properties of nanomedicines are crucial to determine their interaction with the immune system. Hence, we characterized the size, zeta potential, and phospholipid concentration of the Rad-PC-Rad liposomes.

Introduction

The latest progress in the nanomedicine field has resulted in the development of smart nanocontainers for drug delivery applications, including liposomes. Liposomes can improve delivery, targeting, and therapeutic efficacy of the drug and, at the same time, increase the half-life of the drug, lower its effective dose, and reduce toxic side effects [2, 3]. Previously, our research team reported on shear stress sensitive Pad-PC-Pad liposomes for targeted delivery of a vasodilator to constricted arteries [4, 5]. A further *in vivo* investigation of Pad-PC-Pad phospholipids was limited owing to their phase transition temperature at 37 °C. Very recently, we have reported on a more thermally stable phospholipid formulation, such as Rad-PC-Rad [1]. This lipid exhibits a bilayer main phase transition temperature of 44.7 °C and preserves the responsiveness for mechanical triggers [1].

The immediate treatment of arterial occlusion generally involves intravenous injection of nitroglycerin (NTG), which acts as a vasodilator. Systemic administration of NTG may cause severe adverse effects including hypotension and diminished blood perfusion to the heart. The targeted delivery of NTG via the incorporation into shear stress sensitive liposomes may reduce these side effects. The direct contact of liposomes with blood carries the risk of immediate activation of the innate immune system [6]. This may result not only in the reduction of the drug's efficacy, but also in the appearance of hypersensitivity reactions (HSRs) [6-8]. The main function of the immune system is to protect the organism from invading pathogens. It can, however, also develop an immune response against non-pathogenic objects, such as nanometer-size liposomes. Therein, the recruitment of the complement system is an important step in the recognition and elimination of foreign materials. The complement system is a group of approximately 30 plasma- and membrane-bound proteins [9]. Their protective function leads to the release of active components, which cause opsonization, inflammation, and the generation of the membrane attack complex (MAC) [10]. According to the current literature, the complement activation occurs via the three established routes: classical, lectin, and alternative pathways [10]. One can discriminate between these pathways by identifying the presence of unique protein fragments: C4d (classical and lectin pathways) and Bb (alternative pathway) [11]. Activation of either pathway results in the turnover of the C3 protein, which is followed by the production of the anaphylatoxins C3a and C5a, and the formation of the MAC (C5b-9). The release of anaphylatoxins causes leukocyte chemotaxis and the production of pro-inflammatory cytokines, which finally induce inflammation (Figure 1). The excessive production of anaphylatoxins can be harmful and may cause anaphylactic shock or even organ failure at relevant concentrations [12]. Binding of the proteins to the liposomes depends also on their composition, size, geometry, surface charge, and hydrophobicity that can act as immunological adjuvant and trigger strong immune response [6, 13]. The undesirable activation of the complement system can be

caused by systemically administered liposomes, such as Doxil[®] (PEGylated liposomal doxorubicin) and AmBisome[®] (liposomal amphotericin B), leading to the development of HSRs, termed complement activation-related pseudoallergy (CARPA) [7, 8]. Approximately 2 - 10% of patients may adversely react to intravenously administered liposomal formulations with mild-to-severe hypersensitivity reactions [8]. CARPA develops at the first exposure and its symptoms involve almost all organ systems [14]. Some of the most important safety concerns for nanoparticle failure are related to the toxicities caused by complement activation-mediated reactions and cytokine-mediated inflammation [15]. Therefore, it is recommended that liposomes intended for intravenous injection are tested *in vitro* and *in vivo* for the potential activation of complement system, as a preclinical immune toxicity test [16]. The assessment of the liposomal physicochemical properties and their impact on complement activation is also an important objective in the development of nanometer-size therapeutics.

The production of pro-inflammatory cytokines *in vitro* is considered a marker of cytokine-associated immunotoxicity *in vivo* [15] and screening for these toxicities early in preclinical characterization will help to avoid potentially toxic candidates in nanomedicine development. Recently, Wolf-Grosse *et al.* reported about cytokine secretion in a complement-dependent manner [17]. They state that cytokine response was generally mostly due to C5a activation, as it is the most potent pro-inflammatory mediator released upon C activation [17]. Therefore, in order to prevent the potential immunotoxicity *in vivo*, we studied the effect of Rad-PC-Rad liposomes on the production of complement proteins and pro-inflammatory cytokines.

Experimental design

In the present article, we address the possibilities that Rad-PC-Rad liposomes,

loaded with NTG solution, would activate the complement system and stimulate the release of pro-inflammatory cytokines, thus raising concern about potential risk for CARPA or cytokine storm. Thus, we have measured *in vitro* complement activation in human sera and the release of the pro-inflammatory cytokines, in human whole blood and isolated leukocytes, upon incubation with Rad-PC-Rad liposomes. The complement pathway activation products C4d and Bb, and terminal complement complex SC5b-9 were measured using an enzyme linked immunosorbent assay (ELISA), and the release of the pro-inflammatory cytokines IL-1 β , IL-6, IL-8, IL-12, TNF- α was measured using a cytometric bead array test. In addition, we analyzed the liposomal physicochemical properties, in terms of liposomes size and zeta potential, using dynamic light scattering (DLS), and estimated membrane thickness from the micrographs, obtained by cryogenic transmission electron microscopy (cryo-TEM).

Materials and Methods

Materials

1,3-Diheptadecanamidopropan-2-yl (2-[trimethylammonio]ethyl) phosphate (Rad-PC-Rad) was synthesized and purified according to the recently reported protocol [1]. Figure 2 shows the structural formula of the Rad-PC-Rad phospholipid. Table S1 lists all the materials used for the experiments.

Human sera from six healthy volunteers and whole blood samples from two healthy donors were obtained through an institutionally approved phlebotomy protocol at Semmelweis University (Budapest, Hungary). Human sera were stored at a temperature of -80°C until usage. Whole blood samples were freshly collected into sterile hirudin-treated tubes and immediately employed for experiment. Freshly drawn blood, used for leukocytes isolation, was provided by the Hungarian National Blood Transfusion Service.

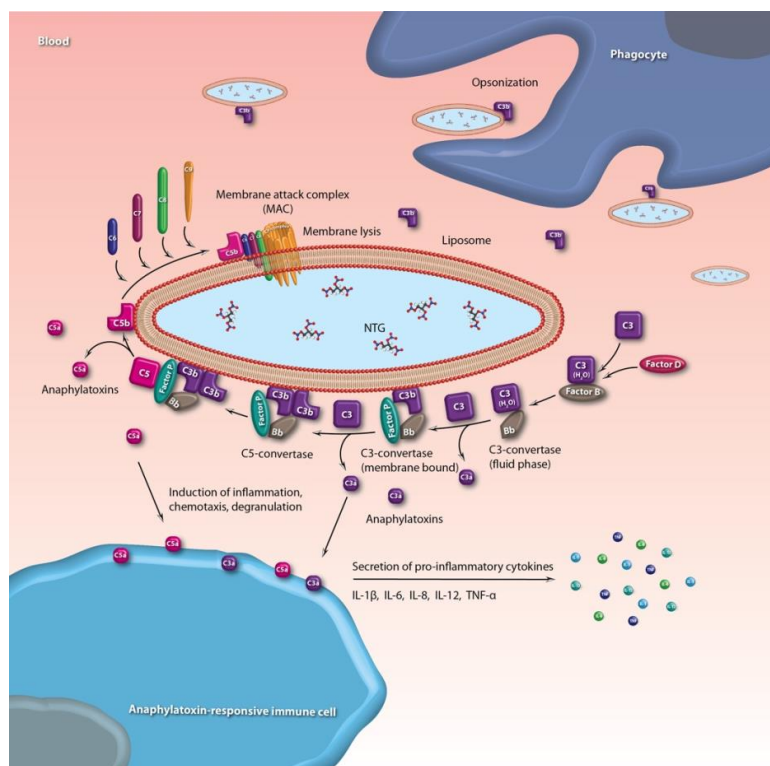


Figure 1. Schematic representation of complement (C) activation triggering pro-inflammatory cytokines due to anaphylatoxin binding to anaphylatoxin-receptor positive cells (e.g., mast cells, basophils, neutrophils, platelets and pulmonary intravascular macrophages). In the case of Rad-PC-Rad liposomes, C activation proceeds through the alternative pathway. On this pathway C3 directly binds to liposomal phospholipid head-groups. Factor B binds to the newly attached C3b, and again becomes susceptible to cleavage by factor D. Membrane-bound C3bBb is unstable until it is bound by properdin protein (factor P). Stabilized C3-convertase rapidly generates large amounts of C3b that bind more factor B, resulting in dramatic amplification of C3b. Membrane-bound C3b serves as an opsonin and a binding tag for phagocytic cells. Addition of C3b to C3-convertase results in the formation of C5-convertase, which cleaves C5 into C5b, and proceeds to form the MAC. Cleavage of C5 also results in the formation of C5a anaphylatoxin. Together with C3a, the C5a fragment binds to the surface C receptors of mentioned allergy mediating cells. C3a and C5a receptors, after binding small anaphylatoxins, mediate the allergic reaction by stimulating the release of vasoactive mediators (e.g., histamine, thromboxanes, leukotrienes, etc.).

Liposome preparation

Four Rad-PC-Rad/DSPE-PEG₂₀₀₀ phospholipid formulations were prepared, namely R1, R2, R3, and R4 (see Table 1). Lipids were dissolved in chloroform in molar ratios as listed in Table 1. The preparation of the liposomal formulations is described in detail in ref. [18]. The samples were purified through sterile filters and stored at a temperature of 4 °C until usage.

Characterization of liposomal formulations

Phospholipid concentration. A colorimetric assay (phosphate test 2.0) [19] was used for the determination of the phospholipid content of the liposomal formulations after extrusion and

purification. Here, the phosphate moiety in the head group of the phospholipids was a measure of the total phospholipid concentration.

Table 1. Composition of Rad-PC-Rad liposomal formulations

Label	Lipid composition (molar %)		Loading buffer
	Rad-PC-Rad	DSPE-PEG ₂₀₀₀	
R1	100	-	saline
R2	95	5	saline
R3	100	-	NTG
R4	95	5	NTG

To exclude the variations in lipid concentration, the concentration of each liposomal formulation (R1, R2, R3, and R4) was diluted with 0.9% sodium chloride solution (saline) to a total lipid concentration of 10 mg/mL. In addition, a set of the diluted formulations (R1d, R2d, R3d, and R4d) with 5 mg/mL of phospholipids were prepared for the *in vitro* immunoassays to examine the impact of the lipid concentration on the complement activation level (see Figures S2 and S3).

Physicochemical characteristics. The liposome average diameter, polydispersity index (PDI) and zeta (ζ) potential were obtained by DLS performed at a temperature of 25 °C using a DelsaMax PRO (Beckman Coulter, USA). The suspensions were diluted 100 times in saline prior to the measurements.

Liposome morphology. The morphology of four Rad-PC-Rad formulations was studied using cryogenic transmission electron microscopy (cryo-TEM) (JEM2200FS, JEOL, Tokyo, Japan). The samples, diluted with saline in the ratio 1:1, were imaged as previously reported [1, 18].

Encapsulation efficiency. The encapsulation efficiency of Rad-PC-Rad liposomes for passive loading with nitroglycerin was determined indirectly by measuring the peak of a glucose-trifluoroacetic acid adduct by electrospray ionization mass spectrometry (ESI-MS) on a Bruker esquire HCT ion trap mass spectrometer (Bruker Corporation, USA) [18].

Liposomal release. Two Rad-PC-Rad liposomal formulations, i.e. with and without DSPE-PEG, were loaded with 5(6)-carboxyfluorescein (CF) buffer, and prepared as described in ref. [1]. Seven aliquots with a volume of 2 mL were separated into 5 mL glass vials and kept for selected periods of time (0, 5, 10, 20, 40 min) at a temperature of 37 °C. The CF release was quantified using a fluorospectrometer (SpectraMax 2, Bucher Biotec AG, Switzerland) with the wavelengths of 485 nm for excitation and 538 nm for emission. Sample fluorescence at a temperature of 20 °C served as a negative control (F_0). As a positive control for the maximum dye release (F_{100}), liposomal samples were heated to a temperature of 65 °C, above the lipids transition temperature of 44.7 °C. The release

fraction at the selected time point x was calculated according to:

$$Release(\%) = \frac{F_x - F_0}{F_{100} - F_0}$$

where F_x is the fluorescence at time x .

Complement immunoassay

Activation of human sera with liposomes. Human sera from six healthy donors were thawed and kept at a temperature of 4 °C during the experiment. Due to the limited amount of serum available, the sera #5 and #6 were prepared as pools from distinctive donors in the ratios 1.5:1 and 7.8:1, respectively. The liposomal suspensions in the two concentrations were added to the sera of each donor in the ratio of 1:3. Saline and nitroglycerin were used as negative controls. FDA-approved liposomal drugs, with recorded cardio-toxicity effects and activation of the complement system in sensitive patients, Doxil® (2 mg/mL doxorubicin, 12.77 mg/mL phospholipids, used as provided) and AmBisome® (17.975 mg/mL amphotericin B, 4.02 mg/mL phospholipids, reconstituted with injection water) were employed as well [7]. Zymosan (1.2 mg/mL), known as activator of the complement system, was used as positive control. Each activation mixture was incubated at a temperature of 37 °C. The concentration of the terminal complement complex SC5b-9 was investigated over time. The incubation was terminated after 5, 10, 20, and 40 minutes by adding 10 mM EDTA.

ELISA immunoassays

The ELISA assays were carried out following the manufacturer's protocol. The optical density was measured with a 96-well plate reader (FLUOstar Omega, BMG Labtech, Germany) at a wavelength of 450 nm for SC5b-9, Bb, C3a and C5a as well as at a wavelength of 405 nm for C4d.

Cytokine immunoassay

Isolation of leukocytes from buffy coat. A volume of 400 mL of buffy coat (BC), a pool of white blood cells (WBCs) concentrates of four healthy volunteers, were obtained from the Hungarian National Blood Transfusion Service within 24 hours of blood withdrawal. Altogether three BC pools were used, each consisting of four donors. Leukocytes were further concentrated two times by mixing with DPBS (w/o CaCl₂, MgCl₂) in 1:1 ratio and

centrifuged for a period of ten minutes at a velocity of 750 G and a temperature of 4 ° C. To lyse the remaining erythrocytes, distilled water at a temperature of 4 ° C was added to the BC (4:1 ratio) for 20 seconds. Lysis was stopped by adding one volume hyperosmotic salt solution (containing 1.8% of NaCl). After washing with ice-cold DPBS (w/o CaCl₂, MgCl₂) for platelets elimination, WBCs were re-suspended in R5 medium.

Qualitative and quantitative analysis of isolated leukocytes. The concentration of WBCs, in three independent blood packages was determined. Viable cells were detected using FITC Annexin V apoptosis detection kit, see Table S4. The staining procedure was performed according to the manufacturer's instructions. Leukocytes were further diluted or concentrated to reach the necessary concentration of ~10⁸ cells/mL. The cell viability was also checked after cell isolation and treatments by test materials and control agents. The viability of cells before and after treatments were always higher than 98%, except for the positive control, Table S5.

Activation of BC leukocytes with liposomes. Freshly isolated leukocytes from three independent blood packages were separately incubated with four Rad-PC-Rad liposomal formulations in the ratio 7:1. Samples, with a concentration of 4 mg/mL, were incubated for four hours at a temperature of 37 ° C on a shaker plate. The incubation was stopped by EDTA (final concentration 10 mM). Cell culture supernatants were further used for mixing with cytokine capture beads. The assay was performed according to the suggested protocol the manufacturer provided with the kit.

Activation of human whole blood with liposomes. Freshly collected whole human blood from two donors was separately incubated with four Rad-PC-Rad liposomal formulations at a concentration of 4 mg/mL, following the same procedure as described in the section above. The distinctive step was the incubation time. Here samples were incubated for a period of six hours. Whole blood samples had no R5 medium, instead they contained their own plasma.

Qualitative and quantitative analysis of leukocytes originated from whole blood samples. An aliquot of human blood from two donors was stained as described in the section

above. Cell viability was determined before and after treatments by test materials and control agents. The percentage of viable cells was more than 97%, except for the positive control, Table S5.

Cytometric bead array test. The human inflammatory cytokines kit was used to quantitatively measure interleukin-1 β (IL- β), interleukin-6 (IL-6), interleukin-8 (IL-8), interleukin-12p70 (IL-12p70), tumor necrosis factor α (TNF- α), and interleukin-10 (IL-10) protein levels in the studied samples. The assay was carried out following the manufacturer's instructions. The beads fluorescence was recorded by flow cytometry using a FACScan instrument (BD Biosciences, USA), and the data were analyzed using the Kaluza Analysis 1.5 software (Beckman Coulter, USA).

Statistical analysis

Statistical analysis was carried out using GraphPad Prism 6 (GraphPad Software Inc., USA). Data from the ELISA samples (Figures 4 and 7), except zymosan, were compared with saline as negative control after 40 minutes of incubation. Significance of differences between the groups was determined by non-parametric Kruskal-Wallis test, followed by Dunn's multiple comparisons test. *P*-values lower than 0.05 were considered as statistically significant.

Results

Characterization of Rad-PC-Rad liposomal formulations

The lipid concentration of Rad-PC-Rad ranged from 10 to 20 mg/mL, and the mean diameter of the liposomes in the suspensions was around 100 nm and varied from 95 to 140 nm (see Table 2). Measurements after 20 days showed that the PEGylated liposomes did not change their size, whereas the non-PEGylated ones displayed an increase from 140 to 270 nm (R1) and from 115 to 200 nm (R3).

Table 2 lists the measured zeta potential values of the Rad-PC-Rad formulations. Pure Rad-PC-Rad samples ζ revealed positive potential values, between +1.3 (R1) to +4.7 mV (R3), while PEGylated samples turned to negative potentials, from -2.0 (R4) to -4.5 mV (R2).

The size and morphology of Rad-PC-Rad liposomes, evaluated using cryo-TEM imaging, is represented in Figure 2. These micrographs show intact spherical, lenticular, and faceted

unilamellar liposomes below their main phase transition temperature. The percentage of faceted liposomes within samples was 46% (R1), 72% (R2), 42% (R3), and 52% (R4).

Table 2. Characteristics of Rad-PC-Rad liposomal formulations.

Label	Lipid composition	Lipid content (mg/mL)	Mean diameter (nm)*	PDI*	Membrane thickness (nm)	ζ potential (mV)*
R1	Rad-PC-Rad (saline)	10.17 \pm 0.02	138.6 \pm 3.5	0.15 \pm 0.03	3.27 \pm 0.14	+1.29 \pm 0.37
R2	Rad-PC-Rad/DSPE-PEG ₂₀₀₀ (saline)	18.39 \pm 0.13	106.5 \pm 1.9	0.14 \pm 0.02	3.60 \pm 0.21	-4.52 \pm 1.05
R3	Rad-PC-Rad (NTG)	13.62 \pm 0.72	114.5 \pm 0.4	0.06 \pm 0.03	3.27 \pm 0.19	+4.65 \pm 0.42
R4	Rad-PC-Rad/DSPE-PEG ₂₀₀₀ (NTG)	21.75 \pm 3.35	97.0 \pm 0.6	0.12 \pm 0.01	3.50 \pm 0.24	-2.08 \pm 0.51

* Data were recorded immediately after sample preparation.

The addition of DSPE-PEG (see Figure 2D and 2F), led to the co-existence of flat circular disks and unilamellar liposomes. Depending on the disk orientation, they appear either as small rods with high contrast (red-colored arrows), or, when seen from the top, as circular structures with low uniform contrast (Figure 2D, right).

The liposome membrane thickness was estimated from the cryo-TEM projections of the appropriately oriented membranes (Figure 2). We have measured the individual thicknesses of 100 membranes and found the mean values of R1 to be (3.27 \pm 0.14) nm and of R3 to be (3.27 \pm 0.19) nm, which indicates the interdigitation of the Rad-PC-Rad leaflets. Interdigitation may be one of the driving forces in the formation of faceted liposomes [1]. Samples loaded with DSPE-PEG, i.e. R2 and R4, tended to result in higher mean values. The values correspond to (3.60 \pm 0.21) nm and (3.50 \pm 0.24) nm, respectively. The mean diameters of the liposomes, derived from cryo-TEM images, were 10 - 15% smaller than those obtained from DLS data.

The encapsulation efficiency of NTG-loaded samples was estimated from the ESI-MS

measurements. The calculation is based on the 100% ESI-MS signal of pure NTG and liposome size. The employed NTG solution contained glucose as an excipient, therefore, the NTG encapsulation was determined indirectly. The integral of the glucose-trifluoroacetic acid adduct was evaluated after NTG incorporation. The ratio between these values determines the percentage of NTG encapsulation efficiency (see Table S2). The values correspond to 38% (R3) and 12% (R4).

In order to measure the membrane permeability, a release test of CF-loaded liposomes at a temperature of 37 ° C was performed under static conditions (Figure 3). Both, Rad-PC-Rad and Rad-PC-Rad/DSPE-PEG samples demonstrated an immediate spontaneous release of 17% and 8% CF, respectively. During another 40 minutes of incubation the release level increased to 36% (Rad-PC-Rad) and 33% (Rad-PC-Rad/DSPE-PEG). The initial CF release trend line of both samples was distinctive, however after 25 minutes the spontaneous release level of the two formulations was comparable and reached about 35%.

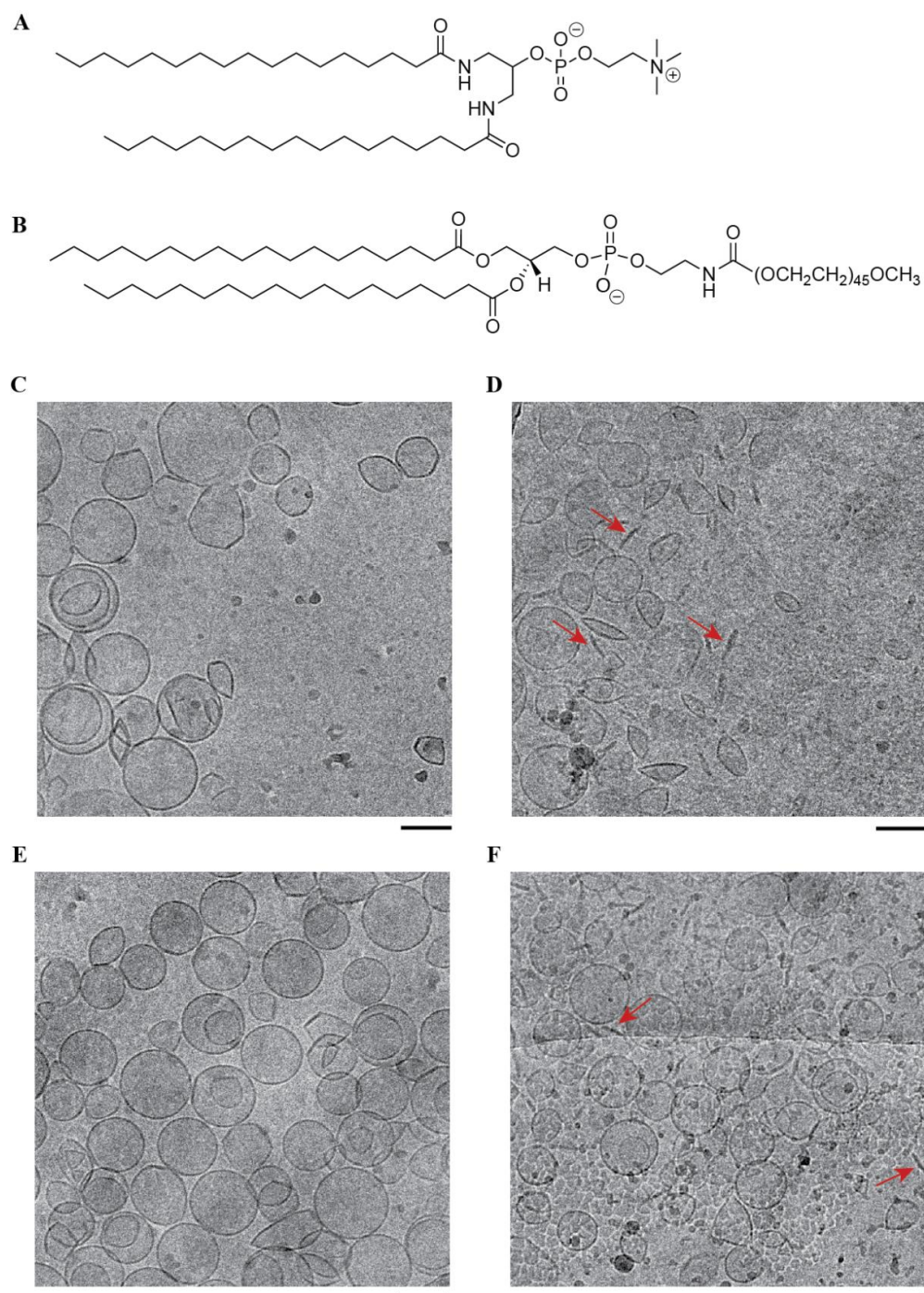


Figure 2. The structure of the two phospholipids used for the liposome preparation: Rad-PC-Rad (A) and DSPE-PEG (B). Cryo-TEM micrographs of the liposomal formulations: R1 (C), R2 (D), R3 (E), R4 (F). Scale bars are 100 nm. The samples contain spherical and faceted liposomes. The incorporation of DSPE-PEG caused the formation of bicelles indicated by the red-colored arrows.

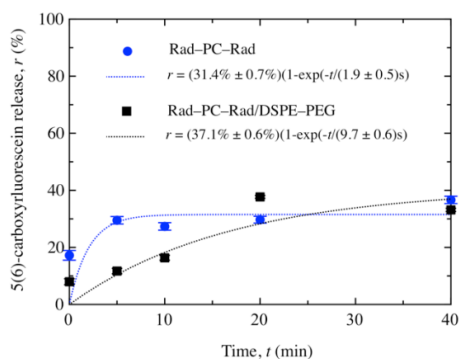


Figure 3. The release of 5(6)-carboxyfluorescein containing liposomes formulated from Rad-PC-Rad and Rad-PC-Rad/DSPE-PEG. The samples were heated to a temperature of 37 ° C and kept at constant temperature for a period of 0, 5, 10, 20, and 40 minutes. The final spontaneous CF release was about 35%. The data are represented as mean values, error bars indicate standard deviation ($n = 5$).

Complement immunoassays

Figure 4A displays the level of SC5b-9 (TCC), which is a marker for the activation of the complement system. The mean values of the six donors demonstrate that the liposomal formulations R1 and R3 have caused an eleven- and 15-fold increase in SC5b-9 concentration in comparison to the negative control (saline), whereas R2 and R4 have raised the SC5b-9 concentration by a factor of eight or nine, respectively. Noticeably, Donor #5 (gray hexagonal) showed a tremendous increase of TCC in the four Rad-PC-Rad liposomal formulations, which largely contributed to the increased mean values of each liposomal sample. The increase of SC5b-9 was at the same level with its positive control, namely about 28-fold compared with saline (Table S3). Certainly, the contribution of Donor #5 into the mean value of all six donors, caused a deviation of mean values up to four times. Doxil® and AmBisome® samples did not reveal a substantial difference in the level of SC5b-9 between the six donors. Doxil® samples showed less than two-fold increase, while AmBisome® demonstrated more than nine-fold elevation of the TCC protein compared to saline. Zymosan caused a considerably high level of

complement activation, namely 55-fold, and was excluded from the diagrams to present the differences between the tested samples in a clearer way. Our findings were statistically confirmed. NTG, which was chosen as another negative control, was compared to saline and no statistical difference was identified. R1 and R3 samples showed very significant to extremely significant differences compared to the negative control. In contrast, the samples R2 and R4 did not reveal a statistically significant difference versus saline. The SC5b-9 level caused by Doxil® among the six sera, showed no statistical difference compared to saline. Certainly, AmBisome® was detected to be extremely significant towards the negative control.

Figure 4B demonstrates the level of C4d protein, which is an experimental marker for the activation of the classical and the lectin pathways. Neither the Rad-PC-Rad liposomes, nor the FDA-approved liposomal formulations revealed a significant increase of C4d protein concentration. The mean values show a less than four-fold increase in comparison to the negative control.

Figure 4C represents the level of Bb fragment as an experimental marker for alternative complement system activation. The serum from Donor #5 towards Rad-PC-Rad liposomal formulation showed four to eight-fold elevation of Bb concentration, whereas the other five donors demonstrated less than three-fold increase compared to saline. All six sera were similarly sensitive to the AmBisome® with an increase of four times above the negative control, revealing a strong statistical significance. A significant serum reactivity towards Doxil® was not observed.

The detection of C3a (Figure 4D) revealed no significant difference between the highly sensitive donor and the others. Most of the values were within the error bars. Rad-PC-Rad liposomes and Doxil® showed values between two- and three-times higher in comparison to saline, while AmBisome® caused an elevation of C3a similar to that one of the positive control – a three- to four-fold increase.

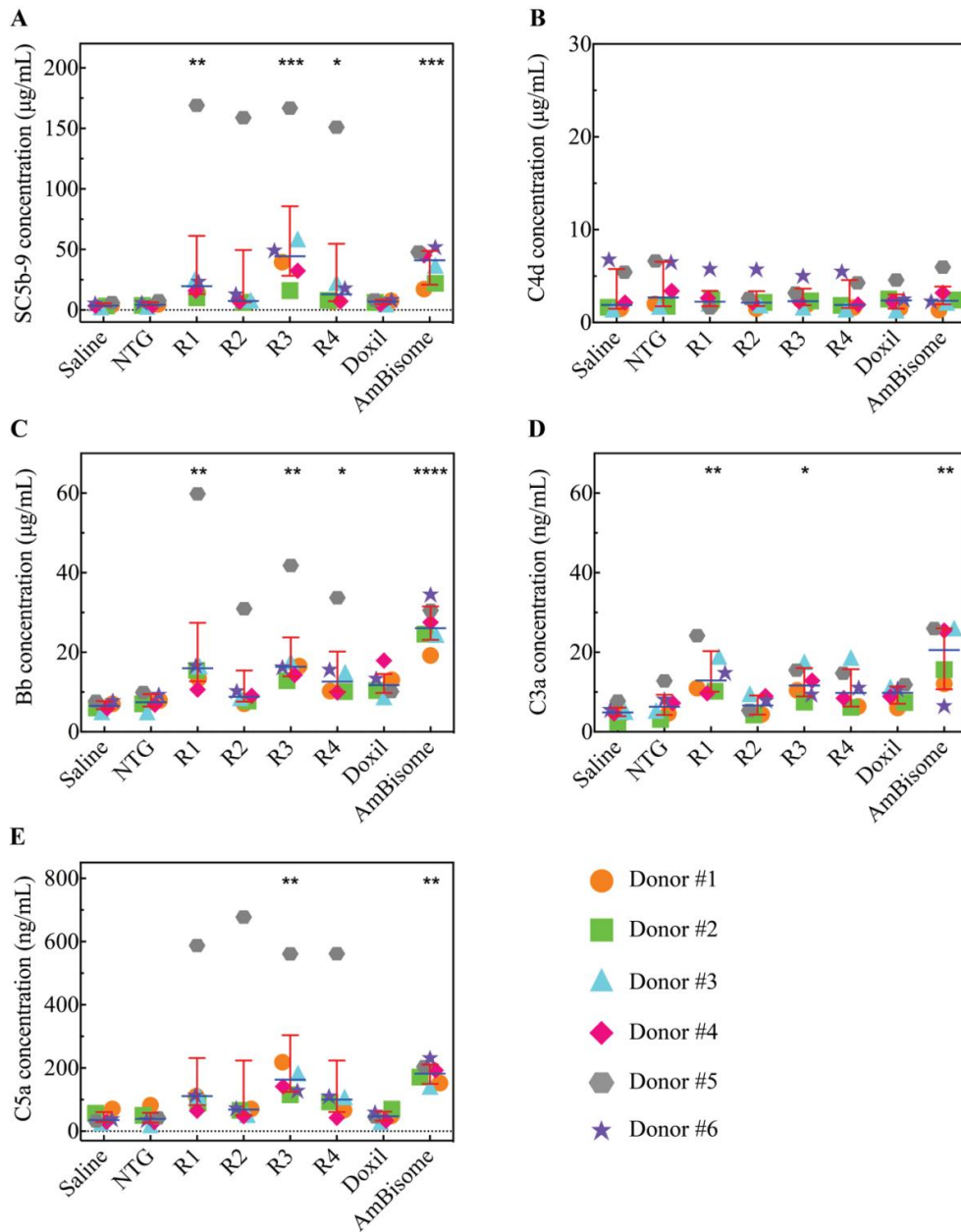


Figure 4. The concentration of SC5b-9 (A), C4d(B), Bb (C), C3a (D), and C5a (E) complement proteins. Human sera from six independent donors were incubated for a period of 40 minutes at a temperature of 37°C with saline, nitroglycerin (NTG), Rad-PC-Rad liposomal suspension of selected composition (R1, R2, R3, R4), Doxil[®] and AmBisome[®]. Saline solution was chosen as negative control. NTG was used as another negative control. Non-PEGylated liposomal formulations caused a higher level of C activation, mainly via the alternative pathway. Highly sensitive serum towards artificial Rad-PC-Rad liposomes was identified. This activation of the C cascade resulted in the increased production of C5a anaphylatoxin. The positive control zymosan caused substantially higher levels of complement activation. The data are represented as median, including error bars derived from the interquartile range among six donors. Each symbol and color represents data from a single donor. Significance of differences among the groups was determined by non-parametric Kruskal-Wallis test, followed by Dunn's multiple comparisons test. P-values lower than 0.05 were considered as statistically significant.

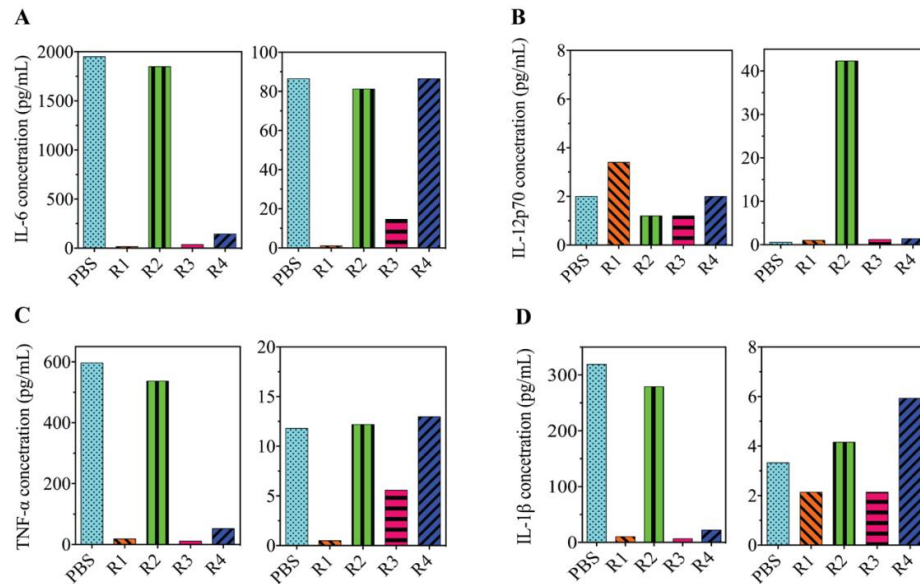


Figure 5. Concentration of pro-inflammatory cytokines IL-6 (A), IL-12p70 (B), TNF- α (C), and IL-1 β (D) induced by Rad-PC-Rad liposomal formulations (R1-R4) incubated with whole blood samples from two donors (first donor: left panels, second donor: right panels) for a period of six hours at a temperature of 37 °C. PBS was chosen as negative control. The effect of Rad-PC-Rad liposomes upon production of cytokines was lower or comparable to the negative control. Less than two-fold increase in the IL-12p70 concentration was observed by R1 treatment (first blood sample). The second blood sample revealed a highly elevated concentration of IL-12p70 induced by R2. IL-1 β concentration of the second donor's blood was close to the detection limit of the kit. The positive control zymosan caused a considerably high level of complement activation, which was mostly above the top standard concentration and was therefore excluded from the graph. The data represent a single value from each donor.

For the activation of SC5b-9, Bb, and C3a, Donor #5 demonstrated a similar trend, where the reactivity towards Rad-PC-Rad samples was higher for the R1 and R3 samples compared to R2 and R4.

Donor #5 showed a significant increase in C5a concentration in comparison to the other five donors (Figure 4E). The values were elevated 17- to 21-fold above the negative control, and the trend was distinctive from the one previously observed (SC5b-9, Bb and C3a). Here, sample R2 revealed the highest C5a level, whereas R1, R3 and R4 were similar. The increase of the C5a concentration detected by the other five donors was below four times the baseline for the Rad-PC-Rad samples and Doxil[®], while AmBisome[®] displayed a four-fold increase

Cytokine immunoassay

The concentration of the inflammatory cytokines is listed in Table S6: IL-6, IL-12p70, TNF- α , IL-1 β , IL-10 and IL-8. Figures 5 and 6 represent the levels of the identified pro-inflammatory cytokines in whole blood and BC

cells, respectively, caused by Rad-PC-Rad liposomal formulations.

The concentration of each cytokine was compared to saline, which served as a negative control. Whole blood samples were collected from two donors and revealed a substantial difference in the sensitivity towards the studied samples. The effect of Rad-PC-Rad liposomal formulations on the production of pro-inflammatory cytokines were lower or comparable to the negative control. Less than a two-fold increase in the cytokine concentration was caused by R1 and R4 samples, in case of IL-12p70 (first blood sample) and IL-1 β (second blood sample), respectively, see diagrams in Figure 5B and 5D. The concentration of IL-1 β (second blood sample) was below the detection limit of the kit (see Table S6). Surprisingly, the second donor showed a large increase in production of IL-12p70 in response to the R2 sample, even higher than the positive control. However, as no additional donor samples were available, we cannot conclude the importance of this increase.

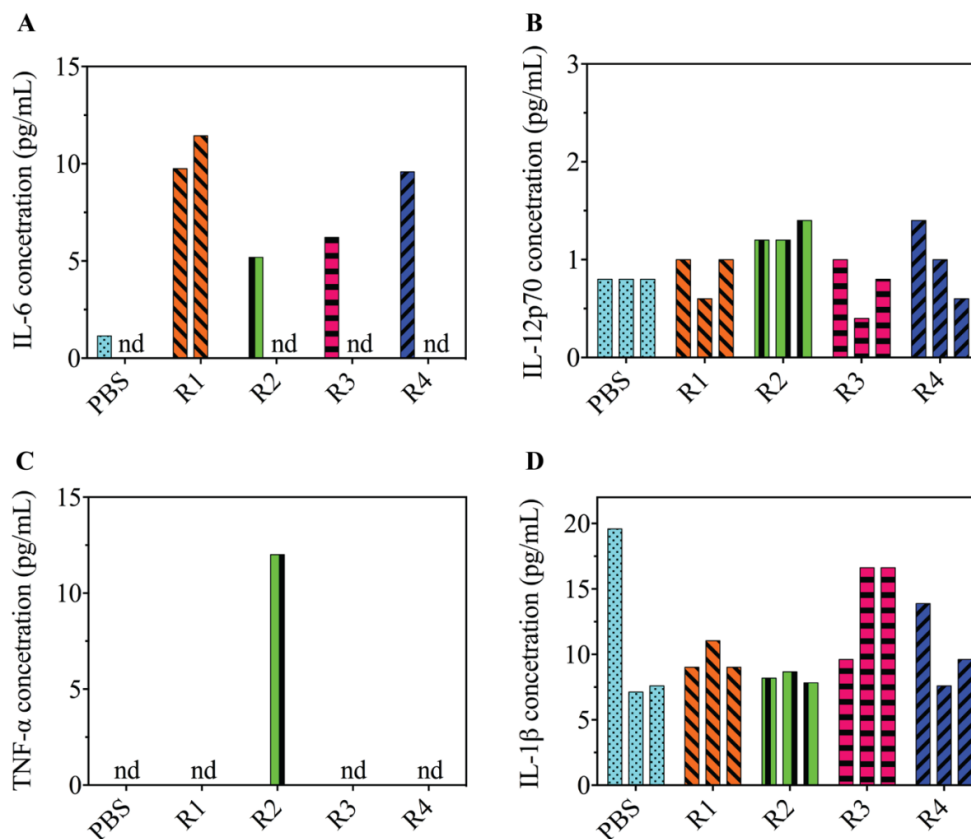


Figure 6. Concentration of pro-inflammatory cytokines induced by Rad-PC-Rad liposomal formulations incubated with isolated leukocytes from three buffy coat pools, each consisting of four donors. Buffy coats were incubated with R1-R4 for a period of four hours at a temperature of 37 ° C. PBS was chosen as negative control. The Rad-PC-Rad formulations caused an elevated level of IL-6 in a part of the buffy coat samples. Insubstantial elevation of IL-12p70 was identified in R2 treated group in each BC. The increase in the level of TNF- α was observed only in one of the buffy coats by R2 sample. The other Rad-PC-Rad liposomal formulations were comparable with PBS. The positive control zymosan caused a considerably higher level of complement activation, which was above the top standard concentration and was therefore excluded from the graph. The data represent a single value from each buffy coat. The label "nd" means not detected.

The concentration of IL-10 was detected only in the samples treated with the positive control. The level of IL-8 gave false positive results and was above the top standard concentration, see Table S6. Therefore, it was excluded from the study.

Rad-PC-Rad formulations caused an elevated level of IL-6, by four- to nine-fold, in one of three BCs compared to PBS (see Figure 6A). The concentration of IL-6 caused by R5 medium, however, was comparable to the one caused by R1 and R4 (see Table S6). Another BC sample demonstrated an increased level of IL-6, caused only by the R1 sample. A raise in the IL-6 concentration caused by the third

tested BC sample was not detected by any of the liposomal formulations (see Figure 6A). In case of IL-12p70, incubation with four Rad-PC-Rad formulations resulted in less than two-fold increase of the cytokine level (see Figure 6B). Moreover, in some of the cases, IL-12p70 levels stimulated by Rad-PC-Rad liposomes were lower than those of the negative control. A surprising increase in the concentration of TNF- α was observed in one of the BC samples by R2 (Figure 6C). None of the other samples elicited an increase in the TNF- α cytokine. In case of IL-1 β , only R3 demonstrated a two-fold increase of the cytokine above the negative control (see Figure 6D) whereas the other Rad-

PC-Rad liposomes revealed an increase of IL-1 β of less than a factor of two. In summary, the cytokines levels caused by Rad-PC-Rad liposomal formulations were comparable with those caused by the negative control.

Discussion

The objective of the study was to investigate the immune response towards the recently developed artificial Rad-PC-Rad liposomes loaded with NTG. For this purpose, we measured the level of C activation markers and pro-inflammatory cytokines *in vitro*. We performed the physicochemical characterization of Rad-PC-Rad liposomes and discussed their potential influence upon the activation of the immune system.

Characterization of Rad-PC-Rad liposomal formulations

The surface charge of Rad-PC-Rad liposomal suspensions was characterized using the ζ -potential, which is one of the principal indicators of the colloid stability. A potential of ± 30 mV has been considered as the limit, above which a colloidal system becomes stable [20]. Rad-PC-Rad liposomes are non-charged nanometer-sized species with relatively low repulsive forces. They tend to aggregate. To improve the stability of the Rad-PC-Rad liposomes, we incorporated DSPE-PEG molecules into the liposomes, which cause a steric repulsion between lipid bilayers [21]. Furthermore, it resulted in the alteration of the ζ -potential to negative values. This alteration is a consequence of the negatively charged DSPE-PEG molecules owing to its phosphodiester moiety [22].

The morphology of Rad-PC-Rad liposomes can deviate from the spherical shape. The liposomes often exhibit irregular facets (Figure 2). The co-existing spherical and faceted liposomes are two forms that may differ in the molecular fraction of the lipid components. Therefore, we have performed differential scanning calorimetry and found that upon repeated heating and cooling additional peaks arose (see Figure S1). This observation clearly indicates that various phases have become coexistent. The occurrence of faceted liposomes is explained by the formation of an intermolecular hydrogen-bonding network at the hydrophobic-hydrophilic interface of the lipids and membrane interdigitation, as recently studied for Rad-PC-Rad in detail [1].

The PEG-containing liposomes, R2 and R4, sometimes appear as flat circular disks (see micrographs D and F in Figure 2). In fact, these features originated from tilted bicelles or micelles [23, 24]. It should be noted that DSPE-PEG is known as a micelle-forming species [25, 26]. The spontaneous formation of bicelles is related to the phase separation between Rad-PC-Rad and DSPE-PEG. The formation of bicelles without an internal cavity led to the decrease of NTG encapsulation by 26%. This shortcoming has to be addressed in future investigations by balancing the PEG-incorporation to optimize the liposomes' stability and minimize bicelles formation.

The cobblestone-like features in the micrograph D of Figure 2 may originate from PEGylated lipids, which failed to form liposomes. The samples have to be frozen for the cryo-TEM data acquisition. The higher viscosity of PEGylated samples results in the formation of thick ice, which impedes the imaging, see micrographs D and F of Figure 2.

Complement immunoassays

We examined the biological effects of Rad-PC-Rad liposomes on C activation. C activation by liposomes depends on several physicochemical factors, including lipid composition, liposome size, morphology, and surface charge [27-29]. Larger liposomes are more prone to activate the complement system than smaller liposomes [30]. This observation explains the increased level of C proteins by the R1 and R3 samples, which diameters were larger and increased with time owing to aggregation. The importance of geometric factors on the assembly of complement convertases [30] or provoking cardiopulmonary distress in pigs [31] can also be a pivotal parameter in combating adverse reactions. The impact of geometry and topology on complement activation was identified by Moghimi *et al.* and Wibroe *et al.* [28, 31]. The cryo-TEM images represented in Figure 2 show Rad-PC-Rad liposomes with faceted and spherical shapes as well as disk-like PEGylated phospholipid-based bicelles. Therefore, the study on adverse reactions of rod- and disk-like particles reported recently [31] is of particular value. Even though this study reports on C-independent adverse injection reactions, it clearly demonstrates the impact of the particle morphology on the immune cells recognition.

The incorporation of PEG into liposomes is

considered to improve C compatibility and prolong liposomes circulation [32]. Their infusion, however, can give rise to HSRs [7, 33, 34]. PEGylated liposomes are able to trigger C activation due to the presence of the anionic phosphate-oxygen moiety of the PEGylated phospholipid [35]. Positive or negative surface charge may also enhance C activation [36], for example by insertion of the negatively charged PEGylated phospholipids. Such negative ζ -potential values were identified in the PEG-containing Rad-PC-Rad liposomal formulations. The C activation-promoting activity of negative surface charges on liposomes was already discussed previously [7]. In our study, only minor differences were observed in PEGylated samples versus negative control.

Another interesting phenomenon was observed, when drug molecules were encapsulated into a liposomal cavity (e.g., Doxil[®], prednisolone). The C activation was considerably higher than for the liposomes of the same size and composition but without the entrapped drug [32, 37]. In case of Doxil[®], this phenomenon was explained by changes in the liposomal morphology arising from the drug loading procedures [28]. Here, we observed that NTG-containing samples (R3 and R4) caused a slightly increased level of C proteins, in comparison to their drug-free counterparts. NTG alone did not have any significant impact on C activation ($P < 0.05$).

The release test showed that 17 - 36% of loaded buffer was spontaneously released during the incubation. These observations suggest that the drug incorporation into the liposomes causes physicochemical changes to the liposomal formulation. Together with a partial release of the drug it may have a synergistic effect on C activation. The frequency of HSRs from FDA-approved liposomal drugs varies, for example ~10% with Doxil[®] and ~30% with AmBisome[®] [7]. AmBisome[®], a highly negatively charged liposome formulation, was found to be a very strong C activator [7]. AmBisome[®] significantly differs from Doxil[®], which causes strong C activation only in certain sensitive sera. This feature was confirmed in our experiment. AmBisome[®] caused the formation of significantly higher ($P < 0.05$) levels of all C proteins (Figure 4).

The increased level of TCC led us to determine

the pathway of C activation. We found that the classical and lectin pathways were not involved in the C activation, but could confirm that the alternative pathway was involved, in agreement with previous results on Pad-PC-Pad liposomes [11].

It has to be noted that one of the six human sera showed an anomaly. This pooled serum, #5, was highly sensitive to the Rad-PC-Rad liposomes. Although the pooling of sera from different donors is common for *in vitro* studies, it should be handled with care and the ratio seems to play an important role: the volumes from each serum should be equal [38]. As this phenomenon has not been considered in the present study, the experimental data were evaluated excluding Donor #5 (see Figure 7).

The differences between the sera provide evidence for the utility of *in vitro* C assays and mimic the clinical situation. HSRs are mostly minor and transient; however, life-threatening reactions can happen occasionally in a hypersensitive individual. It has been suggested that for those donated sera, which cause C activation more than four times the baseline level, the related human being has an elevated risk of HSRs development [33]. The mean level of SC5b-9, within four sera (for R2 and R4) was below four times baseline (saline) (see Figure 4A). Therefore, one could expect that these donors do not carry a risk for developing hypersensitivity reactions *in vivo*. R1 and R3, however, showed a five- and eleven-fold increase in the SC5b-9 concentration, which means that non-PEGylated Rad-PC-Rad liposomes might trigger the development of HSRs *in vivo*. Our previous studies demonstrate that at high phospholipid concentration Pad-PC-Pad liposomes induce weak to none complement activation *in vitro*, but no significant changes in the hemodynamic parameters, nor anaphylactic reactions were observed *in vivo* [18, 39].

The identification of the reactive Donor #5 motivated further studies. Those studies showed that inflammatory mediators, such as C3a and C5a, became activated. The increased level of the anaphylatoxins potentially causes strong pro-inflammatory or anaphylactic responses [6, 10, 40]. Although the C3a concentration caused by Rad-PC-Rad liposomes was below three-fold the baseline level, the non-PEGylated liposomal samples were elevated significantly ($P < 0.05$). In

addition, the Rad-PC-Rad liposomes provoked C activation that resulted in an increased level of C5a anaphylatoxin. It is known that C3a and C5a are major contributors to the release of pro-inflammatory cytokines [6, 9, 40]. These fragments serve as ligands for receptors on leukocytes that trigger inflammation and release of pro-inflammatory cytokines, including IL-1 β , TNF- α , IL-6 and the highly potent chemokine IL-8 [9]. The activation of leukocytes with C3a and C5a is the most relevant property of these proteins for immune compatibility. C5a induces degranulation, chemoattraction and acts with IL-1 β and TNF- α to induce an acute immune response [10]. Recently, a direct link between C activation and the secretion of cytokines, caused by iron nanoparticles was presented [17]. Therefore, to prevent any other potential immunotoxicity *in vivo*, we studied the effect of Rad-PC-Rad liposomes on the production of pro-inflammatory cytokines.

Cytokine immunoassay

The identification of a highly reactive donor to Rad-PC-Rad liposomes, as demonstrated by a consistently and significantly higher level of complement proteins and C5a anaphylatoxin prompted us to investigate the pro-inflammatory response to Rad-PC-Rad. Measuring the cytokine release allows estimating the inflammatory properties of the tested species. To quantify the impact of Rad-PC-Rad liposomes on cytokines' production, we used isolated leukocytes and human whole blood. Our results obtained with whole blood showed differences between the two donors. Multiple factors have impact on the cytokine level, such as intra-individual differences in physical activity and exercising. Chronic exercise training results in decreased levels of many circulating cytokines [41]. One of the donors was physically active, which explains the reduced cytokine level. The samples R1 and R2 were above the negative control owing to the IL-12p70 production. The IL-1 β level was below the detection limit. The results indicate that Rad-PC-Rad liposomes hardly cause the

production of pro-inflammatory cytokines in whole blood. Liposomes induce cytokine production as a result of the physicochemical parameters, i.e. size below 100 nm, surface charge (cationic lipids), and hydrophobicity [13]. We did not observe cytokine production upon the positive charge. Both positively charged Rad-PC-Rad liposomal formulations R1 and R3 showed unrelated variations of the elevated cytokine levels. The results show no indication that the liposomal size plays a role in cytokine production. The PEG-free samples R1 and R3 with higher mean liposome diameters do not lead to elevated cytokines' production. In all cases the response to the liposomes showed levels of pro-inflammatory cytokines comparable to the ones of saline or R5 medium (see Table S6). The main causes of increased cytokine production, however, are unknown, as immunotoxicity mechanisms relate to the composition of nanomaterials, the cell type and cycle, the animal model, and the disease status. The biological variability may have more impact on the immune reaction than expected. The possibility that certain results are attributable to endotoxin contamination [42] are valid, even though the samples were passed through a sterilized filter, and experiments were conducted under a sterilized hood.

IL-8 is an essential chemokine involved in the recruitment of neutrophils to the site of inflammation. More than 50% of the tested nanomaterials, which induce the activation of pro-inflammatory cytokines, caused exclusive production of IL-8, without inducing TNF- α and IL-1 β . Besides, more than 50% of such inducers were liposomes and emulsions [15]. This phenomenon is not fully understood; however, a study suggests the involvement of oxidative stress [43].

Within the present study, the cytometric bead array test gave false positive results of IL-8. This means that the concentration of IL-8 in the negative and positive controls was above the standard concentration of the kit (see Table S6). Thus, we cannot conclude whether Rad-PC-Rad liposomes induce the production of IL-8 or not.

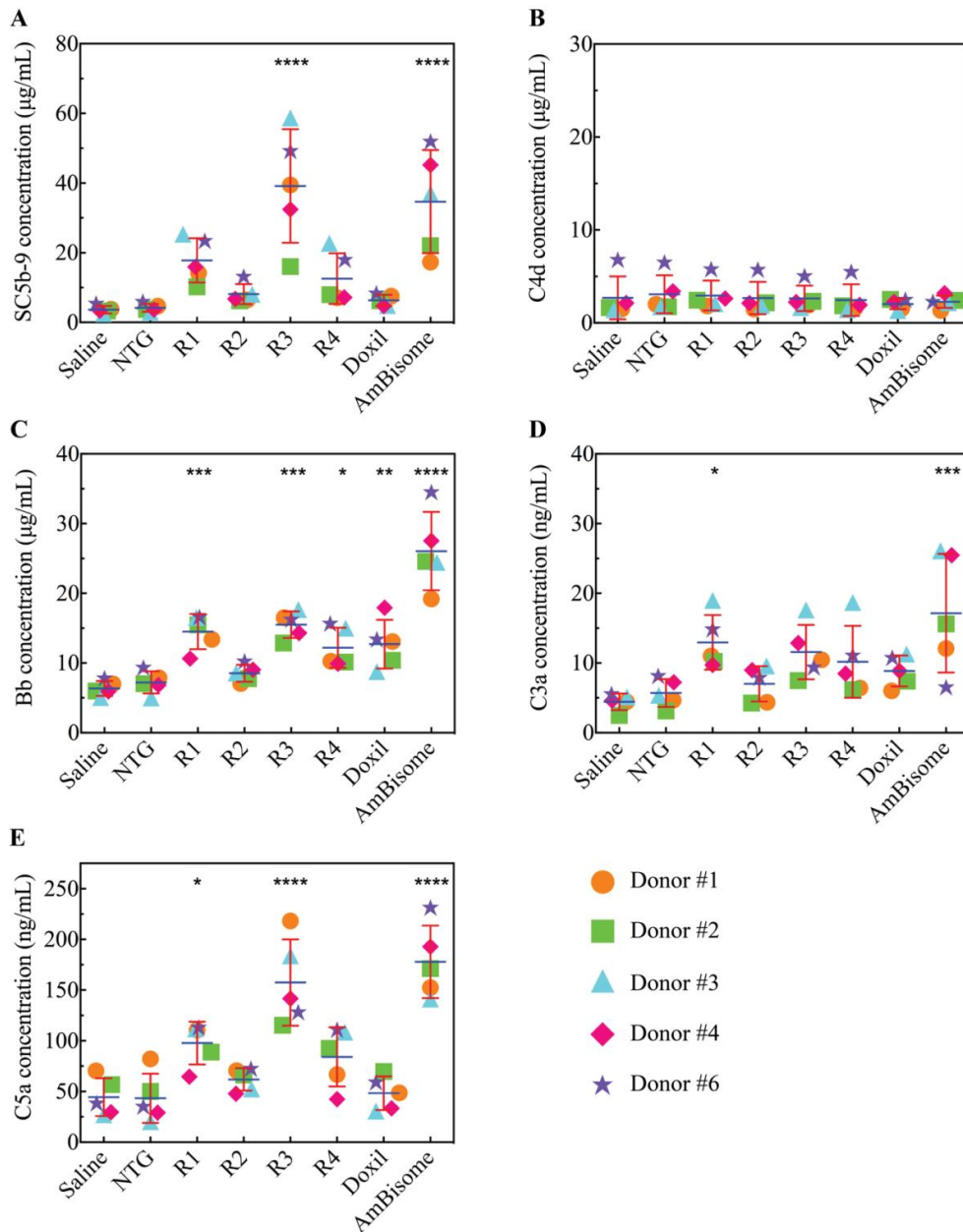


Figure 7. The levels of SC5b-9 (A), C4d (B), Bb (C), C3a (D), and C5a (E) complement proteins. Human sera from five independent donors were incubated for a period of 40 minutes at a temperature of 37°C with saline, nitroglycerin (NTG), Rad-PC-Rad liposomal suspensions of selected composition (R1, R2, R3, R4), Doxil[®] and Ambisome[®]. Saline solution was chosen as negative control. NTG was used as another negative control. Non-PEGylated liposomal formulations caused a higher level of C activation, mainly via the alternative pathway. The activation of the C cascade resulted in the increased production of C5a anaphylatoxin. The positive control zymosan caused substantially higher levels of complement activation. The data are represented as mean, including error bars derived from the standard deviation among the five donors. Each symbol and color represent data from a single donor. Significance of differences among the groups was determined by ordinary one-way ANOVA, followed by Dunnett's multiple comparisons test. P-values lower than 0.05 were considered as statistically significant.

Limitations of the study

Several studies on adverse reactions, which were very recently published, are based on six or less donors [17, 31, 44]. Thus, the choice of six donors in the present study seems to be reasonable. One out of the six donors showed a specific behavior, which is similar to reactions of some individuals to liposomal drugs. Therefore, a substantially higher number of donors should be incorporated into future studies and the presented results have a preliminary character. The present results, however, could support the selection of the number of donors. In literature, one usually finds numbers of ten and above [32, 34, 45].

We hypothesize that the false positive results, as observed in IL-8 production originate from the limitations of the multiplex array system, which necessitates the testing of the samples at multiple dilutions to detect lower and higher abundance cytokines. Another challenge in cytokine detection is their short half-life, such as six to seven minutes for TNF- α [46].

Furthermore, the prepared liposomes exhibited a wide variety of shapes and have to be regarded as a mixture of spherical and non-spherical species. Additional efforts have to be invested to obtain a homogeneous and uniform size and shape distribution.

Conclusions

The extensive research interest of nanomedicines, whether biologically derived or synthetically created, draws attention to their immunotoxicity. Nanometer-sized species interact with the immune system according to their morphology and composition. C activation and cytokine response can induce immune-stimulation and potentially life-threatening conditions, including anaphylaxis and cytokine storm. Therefore, we have carefully studied the interactions of the artificially synthesized Rad-PC-Rad liposomes with cellular and humoral components of the innate immune system in human blood and obtained promising results. In summary, the experimental results indicate that Rad-PC-Rad liposomes are promising shear-responsive nano-containers and related *in vivo* experiments could be foreseen in near future.

Acknowledgments

S.M. acknowledges the financial support of the Swiss Government via the Excellence Scholarship Program for Foreign Scholars and Artists (2015-2018 a.y.). A.Z and F.N. acknowledge funding by the Swiss National Centre of Competence in Research in Chemical Biology. T.M., G.T.K. and J.S. acknowledge the supports by the European Union Seventh Framework Program grants NMP-2012-309820 (NanoAthero) and NMP-2013-602923 (TheraGlio) and the Applied Materials and Nanotechnology Center of Excellence at Miskolc University, Hungary. We thank PSI EM Facility for the cryo-TEM support.

References:

1. Neuhaus, F., et al., *Synthesis and biophysical characterization of an odd-numbered 1,3-diamidophospholipid*. Langmuir 2018, **34**(10): p. 3215-3220, DOI: 10.1021/acs.langmuir.7b04227.
2. Farokhzad, O.C. and R. Langer, *Impact of nanotechnology on drug delivery*. ACS Nano, 2009, **3**(1): p. 16-20, DOI: 10.1021/nn900002m.
3. Shi, J., et al., *Nanotechnology in drug delivery and tissue engineering: from discovery to applications*. Nano Letters, 2010, **10**(9): p. 3223-3230, DOI: 10.1021/nl102184c.
4. Holme, M.N., et al., *Shear-stress sensitive lenticular vesicles for targeted drug delivery*. Nature Nanotechnology, 2012, **7**(8): p. 536-543, DOI: 10.1038/nnano.2012.84.
5. Saxer, T., A. Zumbuehl, and B. Müller, *The use of shear stress for targeted drug delivery*. Cardiovascular Research, 2013, **99**(2): p. 328-333, DOI: 10.1093/cvr/cvt102.
6. Szebeni, J. and S.M. Moghimi, *Liposome triggering of innate immune responses: a perspective on benefits and adverse reactions: biological recognition and interactions of liposomes*. Journal of Liposome Research, 2009, **19**(2): p. 85-90, DOI: 10.1080/08982100902792855.
7. Szebeni, J., et al., *Liposome-induced complement activation and related cardiopulmonary distress in pigs: factors promoting reactogenicity of Doxil and AmBisome*. Nanomedicine:

- Nanotechnology, Biology and Medicine, 2012, **8**(2): p. 176-184, DOI: 10.1016/j.nano.2011.06.003.
8. Szebeni, J., *Complement activation-related pseudoallergy: a stress reaction in blood triggered by nanomedicines and biologicals*. Molecular Immunology, 2014, **61**(2): p. 163-173, DOI: 10.1016/j.molimm.2014.06.038.
 9. Nilsson, B., et al., *The role of complement in biomaterial-induced inflammation*. Molecular Immunology, 2007, **44**(1): p. 82-94, DOI: 10.1016/j.molimm.2006.06.020.
 10. Owen, J.A., J. Punt, and S.A. Stranford, *Kuby immunology*. 2013: WH Freeman New York, ISBN: 1464137846.
 11. Matviyukiv, S., et al., *Liposomes: bio-inspired nano-containers for physically triggered targeted drug delivery*. Proceedings of SPIE 10162, 2017, **10162**: p. 101620A, DOI: 10.1117/12.2258378.
 12. Szebeni, J., et al., *Complement activation-related cardiac anaphylaxis in pigs: role of C5a anaphylatoxin and adenosine in liposome-induced abnormalities in ECG and heart function*. American Journal of Physiology-Heart and Circulatory Physiology, 2006, **290**(3): p. H1050-H1058, DOI: 10.1152/ajpheart.00622.2005.
 13. Landesman-Milo, D. and D. Peer, *Altering the immune response with lipid-based nanoparticles*. Journal of Controlled Release, 2012, **161**(2): p. 600-608, DOI: 10.1016/j.jconrel.2011.12.034.
 14. Szebeni, J., *Hemocompatibility testing for nanomedicines and biologicals: predictive assays for complement mediated infusion reactions*. European Journal of Nanomedicine, 2012, **4**(1): p. 33-53, DOI: 10.1515/ejnm-2012-0002.
 15. Dobrovol'skaia, M.A., *Pre-clinical immunotoxicity studies of nanotechnology-formulated drugs: challenges, considerations and strategy*. Journal of Controlled Release, 2015, **220**: p. 571-583, DOI: 10.1016/j.jconrel.2015.08.056.
 16. European Medicine Agency. *Reflection paper on the data requirements for intravenous products developed with reference to an innovator liposomal product*. EMA/CHMP/806058/2009/Rev. 02, 2013,
 17. Wolf-Grosse, S., et al., *Iron oxide nanoparticles induce cytokine secretion in a complement-dependent manner in a human whole blood model*. International Journal of Nanomedicine, 2017, **12**: p. 3927, DOI: 10.2147/IJN.S136453.
 18. Buscema, M., et al., *Immunological response to nitroglycerin-loaded shear-responsive liposomes in vitro and in vivo*. Journal of Controlled Release, 2017, **264**: p. 14-23, DOI: 10.1016/j.jconrel.2017.08.010.
 19. Stalder, E. and A. Zumbuehl, *Phosphate test 2.0*. CHIMIA International Journal for Chemistry, 2013, **67**(11): p. 819-821, DOI: 10.2533/chimia.2013.819.
 20. Uskoković, V., *Dynamic light scattering based microelectrophoresis: main prospects and limitations*. Journal of Dispersion Science and Technology, 2012, **33**(12): p. 1762-1786, DOI: 10.1080/01932691.2011.625523.
 21. Silvander, M., *Steric stabilization of liposomes—a review*. Lipid and Polymer-Lipid Systems, 2002: p. 35-40, DOI: 10.1007/3-540-45291-5_5.
 22. Garbuzenko, O., et al., *Electrostatics of PEGylated micelles and liposomes containing charged and neutral lipopolymers*. Langmuir, 2005, **21**(6): p. 2560-2568, DOI: 10.1021/la0479105.
 23. Liebi, M., et al., *Magnetically enhanced bicelles delivering switchable anisotropy in optical gels*. ACS Applied Materials & Interfaces, 2014, **6**(2): p. 1100-1105, DOI: 10.1021/am4046469.
 24. Kuntsche, J., J.C. Horst, and H. Bunjes, *Cryogenic transmission electron microscopy (cryo-TEM) for studying the morphology of colloidal drug delivery systems*. International Journal of Pharmaceutics, 2011, **417**(1): p. 120-137, DOI: 10.1016/j.ijpharm.2011.02.001.
 25. Johnsson, M. and K. Edwards, *Liposomes, disks, and spherical micelles: aggregate structure in mixtures of gel phase phosphatidylcholines and poly(ethylene glycol)-phospholipids*. Biophysical Journal, 2003, **85**(6): p. 3839-3847, DOI: 10.1016/S0006-3495(03)74798-5.
 26. Almgren, M., K. Edwards, and G. Karlsson, *Cryo transmission electron microscopy of liposomes and related structures*. Colloids and Surfaces A: Physicochemical and Engineering Aspects, 2000, **174**(1): p. 3-21, DOI: 10.1016/S0927-7757(00)00516-1.

27. Moghimi, S.M. and I. Hamad, *Liposome-mediated triggering of complement cascade*. Journal of Liposome Research, 2008, **18**(3): p. 195-209, DOI: 10.1080/08982100802309552.
28. Moghimi, S.M., et al., *Material properties in complement activation*. Advanced Drug Delivery Reviews, 2011, **63**(12): p. 1000-1007, DOI: 10.1016/j.addr.2011.06.002.
29. Szebeni, J. and Y. Barenholz, *Complement activation, immunogenicity, and immune suppression as potential side effects of liposomes*. Handbook of Harnessing Biomaterials in Nanomedicine: Preparation, Toxicity, and Applications, Pan Stanford Publishing Pte. Ltd., Singapore, 2012: p. 309-334, DOI: 10.4032/9789814364270.
30. Devine, D.V., et al., *Liposome—complement interactions in rat serum: implications for liposome survival studies*. Biochimica et Biophysica Acta, 1994, **1191**(1): p. 43-51, DOI: 10.1016/0005-2736(94)90231-3.
31. Wibroe, P.P., et al., *Bypassing adverse injection reactions to nanoparticles through shape modification and attachment to erythrocytes*. Nature Nanotechnology, 2017, **12**(6): p. 589-594, DOI: 10.1038/nnano.2017.47.
32. Van Den Hoven, J.M., et al., *Complement activation by PEGylated liposomes containing prednisolone*. European Journal of Pharmaceutical Sciences, 2013, **49**(2): p. 265-271, DOI: 10.1016/j.ejps.2013.03.007.
33. Chanan-Khan A J, S.J., Savay S, Liebes L, Rafique N M, Alving C R, Muggia F M., *Complement activation following first exposure to pegylated liposomal doxorubicin (Doxil®): possible role in hypersensitivity reactions*. Annals of Oncology, 2003, **14**(9): p. 1430-1437, DOI: 10.1093/annonc/mdg374.
34. Szebeni, J., et al., *Role of complement activation in hypersensitivity reactions to doxil and hynic PEG liposomes: experimental and clinical studies*. Journal of Liposome Research, 2002, **12**(1-2): p. 165-172, DOI: 10.1081/LPR-120004790.
35. Moghimi, S.M., et al., *Methylation of the phosphate oxygen moiety of phospholipid-methoxy (polyethylene glycol) conjugate prevents PEGylated liposome-mediated complement activation and anaphylatoxin production*. The FASEB Journal, 2006, **20**(14): p. 2591-2593, DOI: 10.1096/fj.06-6186fje.
36. Szebeni, J., et al., *Activation of complement by therapeutic liposomes and other lipid excipient-based therapeutic products: prediction and prevention*. Advanced Drug Delivery Reviews, 2011, **63**(12): p. 1020-1030, DOI: 10.1016/j.addr.2011.06.017.
37. Szebeni, J., et al., *The role of complement activation in hypersensitivity to pegylated liposomal doxorubicin (Doxil®)*. Journal of Liposome Research, 2000, **10**(4): p. 467-481, DOI: 10.3109/08982100009031112.
38. COMPATH. *Serum preparation information sheet*. Available from: http://compath.com.au/user_assets/17dbd37927d046b9835ed2a829f9709e1c22f7d9/serum_preparation_may2015.pdf.
39. Bugna, S., et al., *Surprising lack of liposome-induced complement activation by artificial 1, 3-diamidophospholipids in vitro*. Nanomedicine: Nanotechnology, Biology and Medicine, 2016, **12**(3): p. 845-849, DOI: 10.1016/j.nano.2015.12.364.
40. Andersen, A.J., et al., *Complement: alive and kicking nanomedicines*. Journal of Biomedical Nanotechnology, 2009, **5**(4): p. 364-372, DOI: 10.1166/jbn.2009.1045.
41. Zhou, X., et al., *Conceptual and methodological issues relevant to cytokine and inflammatory marker measurements in clinical research*. Current Opinion in Clinical Nutrition and Metabolic Care, 2010, **13**(5): p. 541, DOI: 10.1097/MCO.0b013e32833cf3bc.
42. Jones, C.F. and D.W. Grainger, *In vitro assessments of nanomaterial toxicity*. Advanced Drug Delivery reviews, 2009, **61**(6): p. 438-456, DOI: 10.1016/j.addr.2009.03.005.
43. Ilinskaya, A.N., et al., *Induction of oxidative stress by Taxol® vehicle Cremophor-EL triggers production of interleukin-8 by peripheral blood mononuclear cells through the mechanism not requiring de novo synthesis of mRNA*. Nanomedicine: Nanotechnology, Biology and Medicine, 2015, **11**(8): p. 1925-1938, DOI: 10.1016/j.nano.2015.07.012.
44. Wibroe, P.P., et al., *An integrated assessment of morphology, size, and complement activation of the PEGylated liposomal doxorubicin products Doxil®, Caelyx®, DOXOrubicin, and*

-
- SinaDoxosome*. Journal of Controlled Release, 2016, **221**: p. 1-8, DOI: 10.1016/j.jconrel.2015.11.021.
45. Benasutti, H., et al., *Variability of Complement Response toward Preclinical and Clinical Nanocarriers in the General Population*. Bioconjugate chemistry, 2017, **28**(11): p. 2747-2755, DOI: 10.1021/acs.bioconjchem.7b00496.
46. Beutler, B.A., I.W. Milsark, and A. Cerami, *Cachectin/tumor necrosis factor: production, distribution, and metabolic fate in vivo*. The Journal of Immunology, 1985, **135**(6): p. 3972-3977, OSTI: 5529162.

ⁱ **Quote as:** Matviykv S, Buscema M, Gerganova G, Mészáros T, Kozma GT, Mettal U, Neuhaus F, Ishikawa T, Szebeni J, Zumbuehl A, Müller B. Immunocompatibility of Rad-PC-Rad liposomes in vitro, based on human complement activation and cytokine release. *Prec. Nanomed.* 2018 Apr;1(1):43-62. DOI: [10.29016/180419.2](https://doi.org/10.29016/180419.2)

SUPPORTING INFORMATION**Immunocompatibility of Rad-PC-Rad liposomes *in vitro*, based on human complement activation and cytokine release**

Sofiya Matviyukiv^a, Marzia Buscema^a, Gabriela Gerganova^a, Tamás Mészáros^{b,c}, Gergely Tibor Kozma^{b,c}, Ute Mettal^d,
Frederik Neuhaus^d, Takashi Ishikawa^e, János Szebeni^{b,c,f}, Andreas Zumbuehl^d, and Bert Müller*^a

^a*Biomaterials Science Center, Department of Biomedical Engineering, University of Basel, Allschwil, Switzerland*

^b*Nanomedicine Research and Education Center, Institute of Pathophysiology, Semmelweis University, Budapest, Hungary*

^c*SeroScience Ltd., Budapest, Hungary*

^d*Department of Chemistry, University of Fribourg, Fribourg, Switzerland*

^e*Paul Scherrer Institute (PSI), OFLB/010, 5232 Villigen PSI, Switzerland*

^f*Department of Nanobiotechnology and Regenerative Medicine, Miskolc University, Miskolc, Hungary*

*corresponding author: phone +41 61 207 5430, bert.mueller@unibas.ch, Biomaterials Science Center, Department of Biomedical Engineering, University of Basel, Gewerbestrasse 14, 4123 Allschwil, Switzerland

1. Materials used for the experiments

The purchased chemical compounds were used without further purification.

Table S1. List of materials used in the experiments.

Name	Company	City, country
DSPE-PEG ₂₀₀₀	Lipoid AG	Steinhausen, Switzerland
Doxil [®]	Janssen Cilag Ltd.	Beerse, Belgium
AmBisome [®]	Gilead Sciences Ltd.	Foster City, CA, USA
Nitroglycerin Bioren 0.1% solution	Sintetica SA	Mendrisio, Switzerland
0.9 % saline solution	Bichsel AG	Interlaken, Switzerland
ELISA MicroVue kits (SC5b-9 Plus, C4d, Bb, C3a, C5a)	Quidel Corp.	San Diego, CA, USA
FITC Annexin V Apoptosis Detection Kit	BioLegend Ltd.	Budapest, Hungary
Cytometric Bead Array (Human inflammatory cytokine kit)	BD Biosciences	Budapest, Hungary
Dulbecco's phosphate buffered saline (DPBS) with and without CaCl ₂ , MgCl ₂	Sigma-Aldrich Co.	Budapest, Hungary
R5 cell medium consisting of Roswell Park Memorial Institute (RPMI) medium with Glutamine		
10 % Fetal Bovine Serum (FBS)		
0.1 mM non-essential amino acids (NEAAs)		
1 % penicillin-streptomycin solution		
50 μM β-mercaptoethanol		
1 mM pyruvate		
Ethylenediaminetetraacetic acid (EDTA)		
Zymosan		
Millex-GV 0.22 μm syringe filter		
Whatman Nuclepore Track-Etched Membranes	Sigma-Aldrich	Buchs, Switzerland
PD-10 desalting columns	GE Healthcare Bio-Sciences AB	Uppsala, Sweden
Hirudin-treated tubes	Roche Kft.	Budapest, Hungary
50 mM 5(6)-carboxyfluorescein, powder	Sigma-Aldrich	Buchs, Switzerland
10 mM HEPES buffer, powder		

2. Calculation of NTG encapsulation efficiency

Table S2. NTG encapsulation efficiency.

Formula	R3	R4
Averaged [Mw] molecular weight (g/mol)	760.00	862.2748
[C] measured conc. (g/L)	13.6	21.8
[M] molarity (mol/L) = [C]/[Mw]	0.00132	0.00116
Number of lipid molecules [No _{lipid mol}] = [M] * Avogadro No	7.92368×10^{20}	6.98385×10^{20}
[D] liposome diameter (nm)	114.5	97
[R1] liposome outer radius (nm) *	57.25	48.5
Liposome outer area (nm ²) [OA] = $4 * 3.14 * R1^2$	41187.06438	29559.24477
[R2] liposome inner radius (nm) **	53.25	44.5
Liposome inner area (nm ²) [IA] = $4 * 3.14 * R2^2$	35632.72867	24884.55498
Total area per liposome (nm ²) [TA] = [OA] + [IA]	76819.79305	54443.79976
[A] Area per lipid (nm ²)***	0.474	0.474
Number of lipids per liposome [No _{lipids}] = [TA]/[A]	162067.074	114860.337
Number of vesicles per 1L [N] = [No _{lipid mol}] / [No _{lipids}]	4.88914×10^{15}	6.0803×10^{15}
Volume of liposome (nm ³) [V] = $(4/3) * 3.14 * R2^3$	632480.9338	369120.8989
Entrapped volume per 1L (nm ³) [EV] = [N]*[V]	3.09229×10^{21}	2.24437×10^{21}
[EV] conversion nm ³ into L per 1L; mL/mL	0.003092287	0.002244365
Area under curve [AUC] of NTG 100% signal in 1 mL	501428.6667	501428.6667
Theoretical value of 100% signal in liposomes [EA]*[AUC]	1550.561388	1125.389191
Measured value of % signal in liposomes	590.157	132.237
Encapsulation efficiency of NTG (%) [EE] = [measured]/[theoretical]*100	38.06	11.75

* mean diameter from DLS measurement

** R2 = R1 - 4 nm (thickness of bilayer)

*** X-ray data, converted from Å² to nm²

3. Differential scanning calorimetry (DSC)

DSC were directly measured from the prepared Rad-PC-Rad and Rad-PC-Rad/DSPE-PEG vesicle suspensions. Liposomal suspensions were degassed for 30 minutes using a TA degassing station. The alternative heating-cooling scans were recorded on a TA Nano DSC (TA Instruments, USA) from 5 °C to 90 °C with a scanning speed of 0.5 K/min. The experiment was performed twice, starting with new suspensions, in order to ensure reproducibility. The scans of the second heating-cooling scans are reported in Figure S1. Raw data was baseline corrected and converted to molar heat capacity (MHC) using the NanoAnalyze software (TA Instruments, USA).

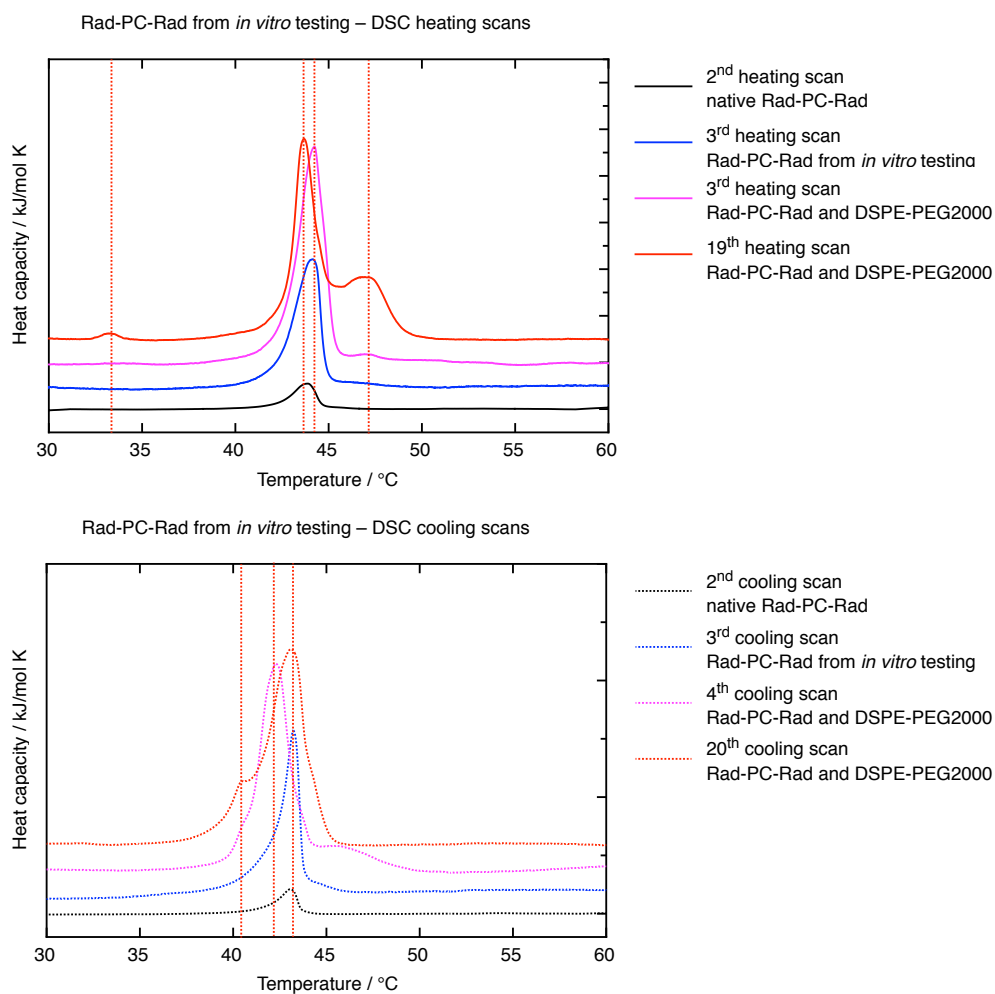


Figure S1. DSC heating and cooling curves measured for Rad-PC-Rad and Rad-PC-Rad/DSPE-PEG vesicles.

4. Complement immunoassay

The activation of the complement system is concentration- and time-dependent. Therefore, identification of the proper lipid concentration would help to avoid the appearance of unexpected side reactions. However, the applied concentration should be still therapeutically relevant. Therefore, before the conduction of the complement assay, we had to perform preliminary tests in order to find the appropriate lipid concentration for further studies. We tested two lipid formulations – R3 and R4. We started from the maximum concentration that we obtained after liposome preparation, which was 10 mg/mL. Those samples were diluted two, four and eight times. The observed results are presented in Figure S2. PEG-free sample R3 demonstrated an increase in complement activation, with increasing the lipid concentration. While PEG-containing sample R4 has shown slight decrease of SC5b-9 level with increasing the lipid concentration. Based on this preliminary result, we have decided to test Rad-PC-Rad liposomal formulations at two concentrations: 10 and 5 mg/mL.

Figure S3 demonstrates the level of complement fragments, induced by incubation with Rad-PC-Rad liposomes at higher and lower concentrations ('d' indicates 'diluted' samples). As it was initially observed by a preliminary test, PEG-free liposomal formulations, R1 and R3, show a statistical significance in the complement activation between concentrated and diluted samples (Figure 3B, D); while PEG-containing formulations, R2 and R4, show no statistical difference. This phenomenon was partially true in case of C3a and C5a, because the observed differences were too small to be detected statistically. No differences were observed in the concentration of C4d fragment, as the lectin pathway is not involved in the activation of the complement system.

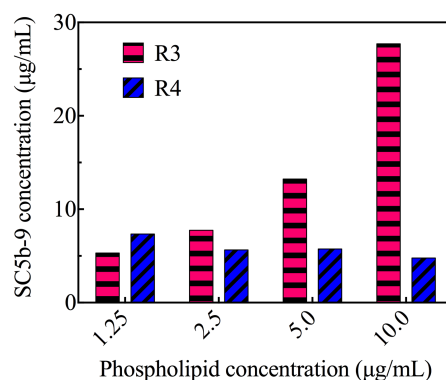


Figure S2. The level of SC5b-9 protein complex after incubation of one human sera with R3 and R4 liposomal suspensions at four phospholipid concentrations: 1.25, 2.5, 5.0 and 10 µg/mL. Incubation was performed for a period of 40 min at 37 °C.

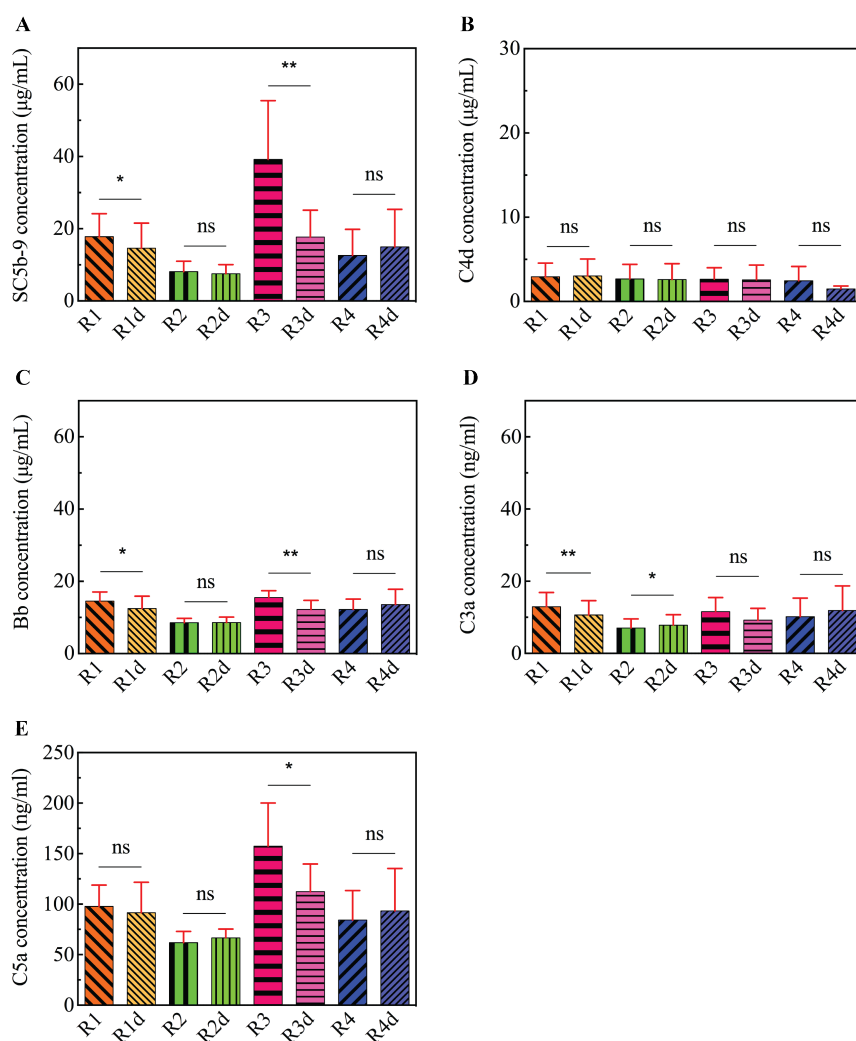


Figure S3. The level of SC5b-9 (A), C4d (B), Bb (C), C3a (D) and C5a (E) complement proteins after incubation of Rad-PC-Rad samples at two phospholipid concentrations: 10 µg/mL (R1, R2, R3, R4) and 5 µg/mL (R1d, R2d, R3d, R4d). Incubation was performed for a period of 40 min at 37 °C for all samples. Sera of donor #5 was excluded from the graph to better distinguish the contrast in complement activation between Rad-PC-Rad liposomal samples with and without DSPE-PEG. The data are represented as mean values with error bars derived from the standard deviation among six donors. The significance of differences among the corresponding groups was determined by paired T-test. *P*-values lower than 0.05 were considered as statistically significant.

To further proceed with the analysis, we examined the level of complement activation over time.

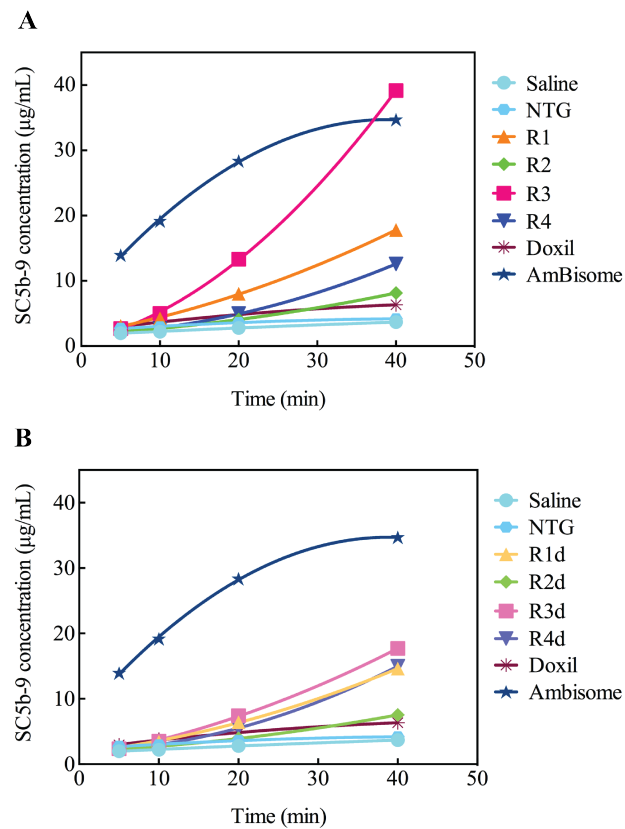


Figure S4. The level of TCC at various time points. SC5b-9 concentration from six human sera incubated at 37 °C with the negative controls, Rad-PC-Rad liposomes at (A) higher lipid content (10 mg/mL) and at (B) lower lipid content (5 mg/mL), Doxil and AmBisome. The reaction was terminated after 5, 10, 20, and 40 minutes. The data are shown as the mean value among the five donors. The serum of donor #5 was omitted for clarity.

Table S3 provides the concentration values of complement proteins. Human sera from six independent donors were incubated for a period of 40 minutes at a temperature of 37 °C with saline, nitroglycerin (NTG), Rad-PC-Rad liposomal suspensions of selected composition (R1, R2, R3, R4), Doxil® and AmBisome®.

Table S3. The concentration of SC5b-9, C4d, Bb, C3a and C5a complement proteins.

Complement protein	Donors	Treatment samples								
		Saline	NTG	R1	R2	R3	R4	Doxil®	AmBisome®	Zymosan
SC5b-9 (µg/mL)	#1	3.81	4.69	14.16	6.53	39.48	7.11	7.52	17.30	199.52
	#2	3.33	3.74	10.19	6.22	16.04	7.98	6.27	22.02	198.94
	#3	2.50	2.96	25.30	8.06	58.67	22.68	4.86	36.95	177.28
	#4	3.35	3.67	15.94	6.74	32.43	7.17	4.73	45.19	182.59
	#5	5.99	7.66	169.08	158.85	166.79	150.99	8.30	47.91	171.66
	#6	5.40	5.92	23.39	13.12	49.23	17.97	8.36	51.90	252.54
C4d (µg/mL)	#1	1.49	2.01	1.83	1.49	1.93	1.61	1.55	1.35	1.78
	#2	1.64	1.75	2.44	2.16	2.33	1.85	2.52	2.42	3.00
	#3	1.42	1.72	2.06	1.88	1.65	1.42	1.33	2.16	2.25
	#4	2.15	3.39	2.63	2.12	2.25	1.92	2.26	3.19	3.42
	#5	5.42	6.63	1.58	2.59	3.18	4.28	4.57	5.96	7.04
	#6	6.80	6.52	5.77	5.73	5.03	5.49	2.50	2.27	3.88
Bb (µg/mL)	#1	7.02	7.89	13.39	7.07	16.50	10.27	13.08	19.20	40.39
	#2	6.00	7.04	15.48	7.77	12.87	10.15	10.39	24.58	44.80
	#3	5.03	5.00	16.50	8.56	17.67	15.00	8.77	24.44	29.00
	#4	5.92	6.83	10.63	9.03	14.31	9.91	17.93	27.53	33.76
	#5	7.69	9.91	59.83	30.94	41.79	33.71	10.15	30.56	36.87
	#6	7.82	9.35	16.59	10.25	16.23	15.67	13.39	34.53	51.03
C3a (ng/mL)	#1	4.43	4.66	11.01	4.37	10.46	6.42	6.01	12.08	18.51
	#2	2.48	3.12	10.23	4.25	7.49	6.16	7.39	15.63	18.80
	#3	5.12	5.38	18.98	9.58	17.62	18.69	11.28	26.09	21.27
	#4	4.62	7.23	9.72	8.97	12.87	8.48	8.89	25.46	20.98
	#5	7.74	12.81	24.20	5.39	15.51	14.74	11.86	25.98	14.60
	#6	5.55	8.14	14.84	7.88	9.38	11.09	10.76	6.53	20.61
C5a (ng/mL)	#1	70.36	82.12	110.56	70.54	218.23	66.71	48.75	152.44	1471.22
	#2	56.86	50.12	88.96	66.26	115.40	92.51	69.72	171.31	1488.54
	#3	26.96	20.22	111.75	52.49	183.86	108.38	30.61	141.23	748.25
	#4	29.61	29.06	64.52	47.75	141.65	42.46	33.43	192.78	759.19
	#5	32.51	42.00	587.64	677.53	561.06	561.41	45.10	204.00	791.10
	#6	38.27	35.08	113.02	72.45	128.16	110.84	59.05	231.35	1344.49

5. Qualitative and quantitative analysis of WBCs

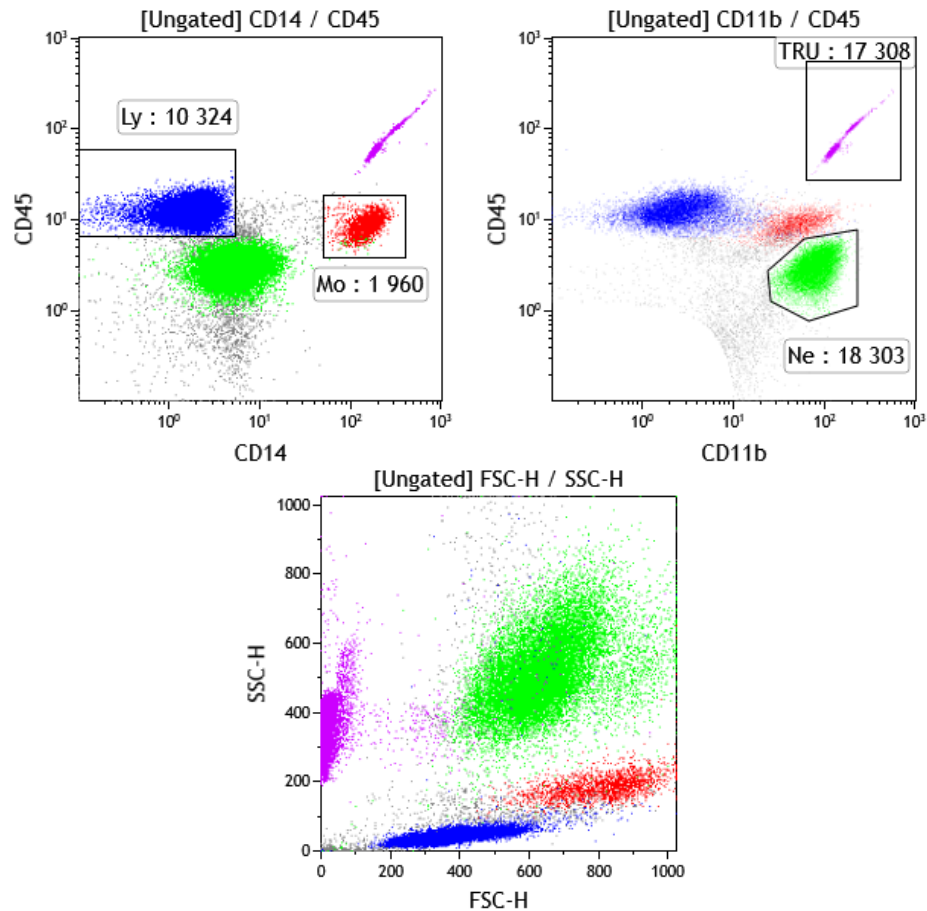


Figure S5. Gating strategy (upper panels) to identify the absolute cell concentration of samples' cells by flow cytometry. Scatter plot (lower panel, SSC/SSC) of gated cells is presented by the same color.

The cell content of samples was analyzed by flow cytometry using a FACScan instrument (BD Biosciences, USA). Before the actual tests, 50 μL of the cells were stained by antibody mixture containing fluorescein isothiocyanate (FITC) labeled anti-CD14, phycoerythrin (PE) labeled anti-CD11b and PerCP-Cy5.5 labeled anti-CD45 in TRUCount tubes (BD, cat.: 340334) for 15 min in the dark. Thereafter, WBC were resuspended in 450 μL of lysing solution (BD, cat.: 349202) for 15 min. As the employed TRUCount tubes contained a known number (48 100) of beads (gating name: TRU) measured together with cells, the exact cell concentrations of the original samples could be identified, since no centrifuge step was applied during the sample staining process. After gating, which strategy is summarized in Figure S5, the concentration and total cell number of monocytes (Mo), neutrophil granulocytes (Ne) and lymphocytes (Ly) was quantitatively determined as it is presented in Table S4. The number of WBCs was determined prior to the incubation with tested material. In case of buffy coat samples, the number of cells was determined twice: before (original) and after isolation of leukocytes. Cells were stained according to the procedure described above.

Table S4. Concentration of WBCs in the buffy coat (BC), before and after leukocytes isolation, and in whole blood (WB) samples.

	Cell concentration (cell/mL)			
	Monocytes	Neutrophils	Lymphocytes	Total cells
BC1 original	2'364'360	17'869'287	15'101'890	35'335'536
BC1 isolated cells	4'059'419	15'811'548	16'888'079	36'759'046
BC2 original	1'915'442	12'791'686	11'303'143	26'010'271
BC2 isolated cells	19'003'419	100'469'999	67'771'808	187'245'226
BC3 original	2'105'082	18'639'499	11'822'281	32'566'862
BC3 isolated cells	25'539'472	171'957'831	67'099'037	264'596'339
WB1	310'963	2'223'685	2'014'609	4'549'258
WB2	372'776	2'214'462	2'596'503	5'183'741

The viability of the cells after activation with test material and control agents was quantified by FITC labeled AnnexinV (Table S5) among (PerCP-Cy5.5 labeled) CD45 positive leukocytes. The percentage of dead cells were less than 3% after each treatment with the exception of zymosan, confirming that the observed phenomena in cytokine productions are not a consequence of different cell mortality after treatments.

Table S5. Cell viability assay of isolated leukocytes and whole blood after activation with liposomal formulations and corresponding control agents.

Sample	Viable cells (%)						
	PBS	MR5	R1	R2	R3	R4	Zymosan
BC2	98.4	98.18	98.06	98.12	98.34	98.37	64.32
WB2	97.57	98.43	97.49	97.75	97.53	97.95	60.52

6. Concentration of inflammatory cytokines

Table S6 provides the concentration values of inflammatory cytokines. WB and BC samples were incubated with R5 medium, PBS, Rad-PC-Rad liposomal suspension of selected composition (R1, R2, R3, R4) and zymozan at a temperature of 37 °C.

Table S6. The concentration of IL-6, IL-12p70, TNF- α , IL-1 β , IL-8 and IL-10 inflammatory cytokines.

Cytokines	Donors	Samples						
		MR5	PBS	R1	R2	R3	R4	Zymosan
IL-6 (pg/mL)	WB1	1086.69	1950.84	15.83	1848.47	36.11	144.90	>5000.00
	WB2	98.70	86.46	0.98	81.19	14.65	86.46	>5000.00
	BC1	9.24	1.15	9.75	5.19	6.21	9.58	na
	BC2	1.32	nd	11.44	nd	nd	nd	>5000.00
	BC3	nd	nd	nd	nd	nd	nd	>5000.00
IL-12p70 (pg/mL)	WB1	1.80	2.00	3.40	1.20	1.20	2.00	20.51
	WB2	0.00	0.60	1.00	42.28	1.20	1.40	2.20
	BC1	1.20	0.80	1.00	1.20	1.00	1.40	na
	BC2	0.80	0.80	0.60	1.20	0.40	1.00	8.03
	BC3	1.00	0.80	1.00	1.40	0.80	0.60	4.20
TNF- α (pg/mL)	WB1	230.91	596.55	18.63	536.73	11.41	52.42	>5000.00
	WB2	10.83	11.80	0.50	12.19	5.57	12.97	>5000.00
	BC1	nd	nd	nd	nd	nd	nd	na
	BC2	nd	nd	nd	12.00	nd	nd	4519.33
	BC3	nd	nd	nd	nd	nd	nd	1656.93
IL-1 β (pg/mL)	WB1	212.39	319.06	10.44	279.20	6.53	22.32	>5000.00
	WB2	7.24	3.33	2.14	4.16	2.14	5.93	>5000.00
	BC1	28.62	19.59	9.02	8.19	9.61	13.89	na
	BC2	7.24	7.12	11.04	8.66	16.62	7.60	>5000.00
	BC3	9.37	7.60	9.02	7.83	16.62	9.61	>5000.00
IL-8 (pg/mL)	WB1	>5000.00	>5000.00	4033.03	>5000.00	4747.50	>5000.00	>5000.00
	WB2	>5000.00	>5000.00	1497.28	>5000.00	2835.68	4565.74	>5000.00
	BC1	>5000.00	>5000.00	>5000.00	>5000.00	>5000.00	>5000.00	na
	BC2	>5000.00	>5000.00	>5000.00	>5000.00	>5000.00	>5000.00	>5000.00
	BC3	>5000.00	>5000.00	>5000.00	>5000.00	>5000.00	>5000.00	>5000.00
IL-10 (pg/mL)	WB1	nd	nd	nd	0.69	nd	nd	151.91
	WB2	nd	nd	nd	nd	nd	nd	148.40
	BC1	nd	nd	nd	nd	nd	nd	na
	BC2	nd	nd	nd	nd	nd	nd	314.32
	BC3	nd	nd	nd	nd	nd	nd	196.37

Cytokines detection limit (pg/mL): IL-6 – 2.5, IL-12p70 – 1.9, TNF- α – 3.7, IL-1 β – 7.2, IL-8 – 3.6, IL-10 – 3.3. nd – not detected, na – not available.

2.3 Small-angle neutron scattering study of temperature-induced structural changes in liposomes

Published in Langmuir

Small-Angle Neutron Scattering Study of Temperature-Induced Structural Changes in Liposomes

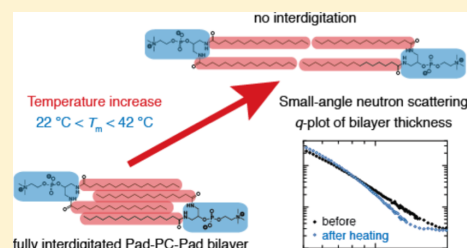
Sofiya Matviyukiv,[†] Hans Deyhle,^{†,||} Joachim Kohlbrecher,[‡] Frederik Neuhaus,[§] Andreas Zumbuehl,[§] and Bert Müller^{*,†,Ⓜ}

[†]Biomaterials Science Center, Department of Biomedical Engineering, University of Basel, Allschwil 4123, Switzerland

[‡]Laboratory for Neutron Scattering and Imaging, Paul Scherrer Institute, Villigen PSI 5232, Switzerland

[§]National Center of Competence in Research in Chemical Biology, Geneva 1211, Switzerland

ABSTRACT: Liposomes of specific artificial phospholipids, such as Pad-PC-Pad and Rad-PC-Rad, are mechanically responsive. They can release encapsulated therapeutics via physical stimuli, as naturally present in blood flow of constricted vessel segments. The question is how these synthetic liposomes change their structure in the medically relevant temperature range from 22 to 42 °C. In the present study, small-angle neutron scattering (SANS) was employed to evaluate the temperature-induced structural changes of selected artificial liposomes. For Rad-PC-Rad, Pad-PC-Pad, Sur-PC-Sur, and Sad-PC-Sad liposomes, the SANS data have remained constant because the phase transition temperatures are above 42 °C. For Pad-PC-Pad and Pes-PC-Pes liposomes, whose phase transitions are below 42 °C, the *q*-plots have revealed temperature-dependent structural changes. The average diameter of Pad-PC-Pad liposomes remained almost constant, whereas the eccentricity decreased by an order of magnitude. Related measurements using transmission electron microscopy at cryogenic temperatures, as well as dynamic light scattering before and after the heating cycles, underpin the fact that the non-spherical liposomes flatten out. The SANS data further indicated that, as a consequence of the thermal loop, the mean bilayer thickness increased by 20%, associated with the loss of lipid membrane interdigitation. Therefore, Pad-PC-Pad liposomes are unsuitable for local drug delivery in the atherosclerotic human blood vessel system. In contrast, Rad-PC-Rad liposomes are thermally stable for applications within the human body.



INTRODUCTION

Liposomes are composed of lipid bilayers and usually have a spherical shape.¹ Using artificial phospholipids with a dedicated backbone chemistry and tail length that form interdigitated bilayers, faceted liposomes have been discovered.² These liposomes are beneficial in medical therapies because they possess distinctive characteristics. As conventional liposomes, they can encapsulate therapeutic molecules and transport them to the desired location, preventing direct contact between drug and blood. Upon mechanical stimuli, however, these liposomes can undergo structural changes to release the cargo.³ In this manner, the totally administered dose and the related objectionable side effects along the patient's 60 000-miles-long blood vessel system being currently flooded with the drug can be kept extremely low, whereas the purely physical trigger renders possible an unrivaled local dose to pathological constrictions.

The thermal stability of these faceted liposomes within the physiologically relevant temperature range, however, has hardly been studied yet. It is well known that the body temperature is generally close to 37 °C. On grounds of ill health, the body temperatures can raise to above 40 °C, but at a temperature of 42 °C the circulation fails. Hypothermia, as, for example, intentionally induced during heart surgery, gives rise to body

temperatures close to 20 °C.⁴ Therefore, the present study covers the temperature range between 22 and 42 °C.

The size and shape of liposomes including their distributions can be assessed by employing dynamic light scattering (DLS) and cryogenic transmission electron microscopy (cryo-TEM). For the structural characterization of the lipid bilayer thickness, however, a technique with better resolving power is needed. Therefore, we applied small-angle neutron scattering (SANS) as a tool to obtain quantitative information about the structural parameters of liposomes as the function of temperature. SANS allows for the investigation of fully hydrated systems, offering the additional feature of contrast variation via solvent exchange. More importantly, our setup was equipped with a heating stage to conveniently control the temperature of the liposomal suspensions within the medically relevant range.

Liposomes from DPPC exhibit a spherical shape. Non-spherical shapes can be obtained replacing the 1,2- by the 1,3-arrangement of the fatty acyl chains in the backbone as found in Pad-PC-Pad, Rad-PC-Rad, Pes-PC-Pes, Sur-PC-Sur, and Sad-PC-Sad, see Figures 1 and 2 below. This arrangement increases the spacing between the chains and leads to

Received: May 28, 2019

Revised: July 19, 2019

Published: July 25, 2019



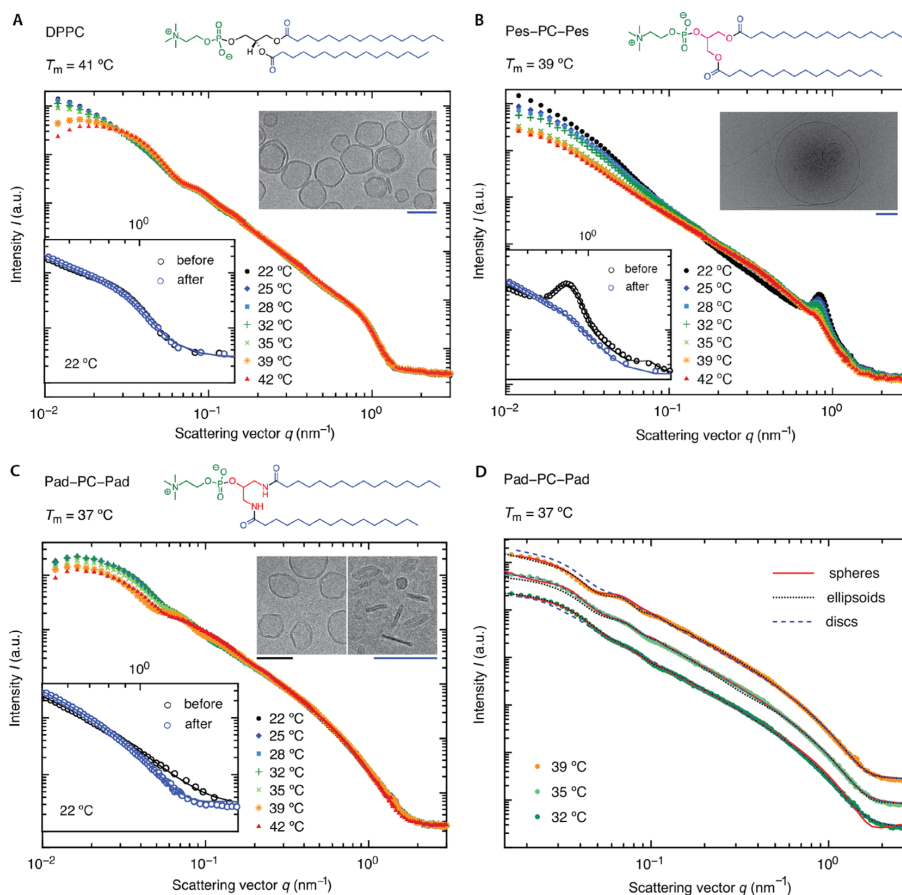


Figure 1. SANS data and related cryo-TEM images of liposomal suspensions reveal temperature-induced structural changes close to their transition temperatures T_m . The structural representations of the phospholipids show color-coded chemical motives. The inset diagrams display the scattering signal for higher q -values, before (black circles) and after (blue circles) heating and the related fits using the generalized Guinier law. The scale bars of the TEM micrographs correspond to 100 nm, where black and blue indicate imaging was recorded before and after the heating cycle, respectively. Diagram (D) provides the reader an idea how far the liposomes can be approximated by spheres, ellipsoids, or discs. The goodness of fit, described by reduced chi-square, is for the spheres 91.2, 30.1, 51.0, for the ellipsoids 21.7, 178.7, 17.6, and for the discs 65.4, 18.3, 237.0 at the temperatures 32, 35 and 39 °C, respectively. To suitably visualize the differences, the values for 35 and 39 °C were shifted with respect to those for 32 °C along the ordinate by a factor of three and 10, respectively.

interdigitated lipids in the membrane. Longer carbon chains improve the thermal stability by increasing the hydrophobic forces between the chains, revealed by an increase in the transition temperature. Because this class of liposomes has substantially stiffer lipid bilayers than the established natural membranes, faceted liposomes with specific defects and related mechanical features can be tailored. Pad-PC-Pad and Rad-PC-Rad as well as the less reported Pes-PC-Pes, Pad-Pad-PC, Sur-PC-Sur, and Sad-PC-Sad lipids belong to a family that forms metastable non-spherical liposomes. Their interdigitated lipid bilayers are thinner and more rigid than the conventional ones such as the well-established DPPC liposomes. They exhibit a distinct curvature in only one direction associated with defect lines. Therefore, these non-spherical liposomes represent a metastable state, and the application of mechanical or thermal energy can result in structural changes. The mechanical stimulation was already studied in some detail,⁵ whereas the thermal characterization was mainly restricted to

the measurement of the main membrane phase transition temperature from a gel to the liquid crystalline phase.^{3,6}

In this study, we detect temperature-dependent changes in the size, shape, and bilayer properties of liposomal formulations, composed of the family of selected artificial phospholipids, and, in this regard, the structural changes at medically relevant body temperatures are of particular interest.

MATERIALS AND METHODS

Liposome Preparation. The lipids were synthesized as reported.^{3,6–9} The liposomes were formulated following the standard extrusion protocol.¹⁰ Briefly, 10 mg of lipids were dissolved in CH_2Cl_2 . After evaporating the organic solvent, the thin film was dried further under vacuum conditions with a pressure of 40 mbar overnight. The film was hydrated with D_2O for a period of 30 min. Five freeze–thaw cycles from liquid nitrogen temperature to 65 °C were carried out and followed by eleven extrusion cycles, using a Mini Extruder (Avanti Polar Lipids, USA) and track-edged filters with

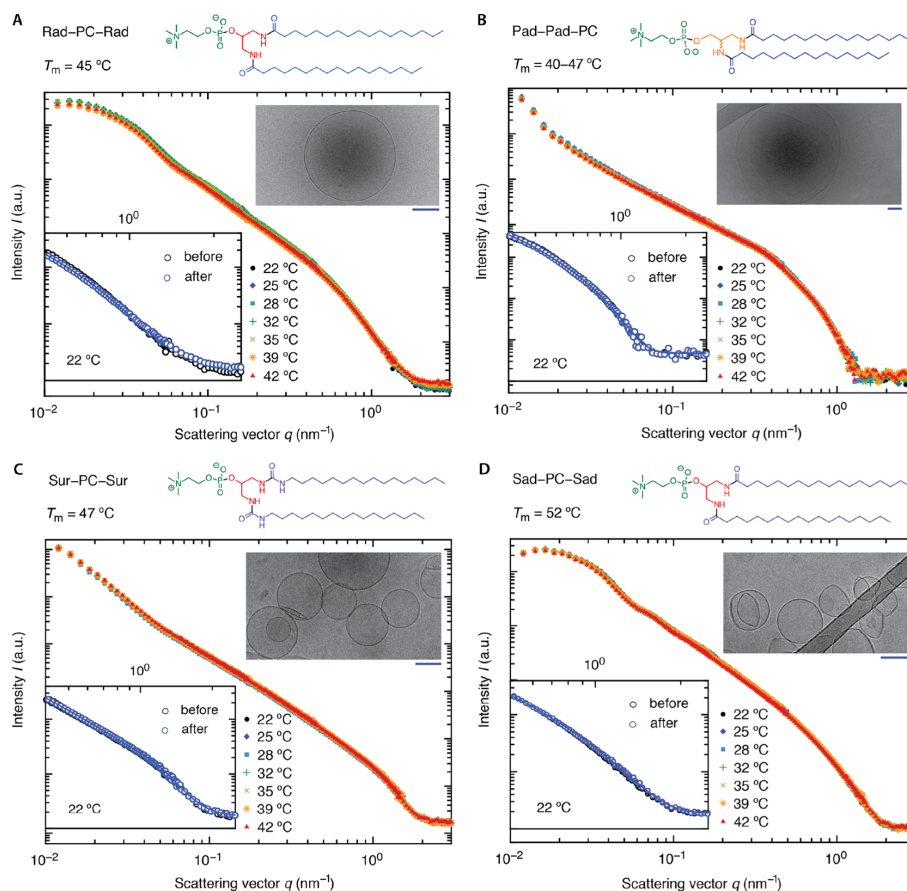


Figure 2. SANS data and cryo-TEM images of Rad-PC-Rad, Pad-Pad-PC, Sur-PC-Sur, and Sad-PC-Sad liposomes hardly show any thermal effect, because the transition temperatures T_m are above the medically relevant range. The structural representations of the phospholipids show color-coded chemical motives, i.e. the C16 chain—dark blue, the C17 chain—light blue, and the C18 chain—purple. The inset diagrams display the scattering signal for higher q -values, before (black circles) and after (blue circles) heating and the related fits using the generalized Guinier law. The scale bars of the micrographs correspond to 100 nm.

100 nm pore size (Whatman, USA). The obtained liposomal formulations exhibited a lipid concentration of about 10 mg/mL.

Dynamic Light Scattering. The DLS traces were measured using the DelsaMax PRO apparatus (Beckman Coulter, USA). Here, the photodiode is positioned at 168° backscatter angle and detector position at 163.5° associated with scattering angles ranging from 4 to 15° . The measurements were carried out at room temperature and at a lipid concentration of 0.3 mg/mL in D_2O . The data were averaged among five independent measurements before heating cycles and three measurements eight months after applying the heating cycles. The data were treated with the cumulant analysis method.

cryo-Transmission Electron Microscopy. The liposomal suspensions were diluted at a ratio of 1:2 with D_2O and thus to a concentration of 5 mg/mL. Next, $4 \mu L$ aliquots of each suspension were adsorbed onto a holey carbon-coated grid (Lacey, Ted Pella, USA), blotted with Whatman 1 filter paper and vitrified into liquid ethane at a temperature of $-178^\circ C$, using a Leica GP plunger (Leica, Austria). Frozen grids were transferred onto a Talos electron microscope (Thermo Fisher, USA), using a Gatan 626 cryo-holder. Electron micrographs were recorded at an accelerating voltage of 200 kV and a nominal magnification of 45 000 \times , using a low-dose system ($0.20 e^-/nm^2$) and keeping the sample at liquid nitrogen temperature. Micrographs were recorded on the CETA camera. Pixel size at the sample level was $(0.326 \text{ nm})^2$. Because some of the cryo-

TEM micrographs exhibited slowly varying brightness variations, we compensated for such artefacts using a modified fuzzy C-means algorithm.^{11,12}

Small-Angle Neutron Scattering. The SANS measurements were performed at the SANS-I facility, Swiss Spallation Neutron Source SINQ, Paul Scherrer Institute, Switzerland. Neutrons with an energy of 400 meV, which corresponds to a wavelength λ of 0.045 nm, were used at sample-to-detector distances of 1.6, 6.0, and 18.0 m and exposure times of 190 and 564 s. In addition, neutrons with an energy of 60 meV ($\lambda = 0.12 \text{ nm}$) at a sample-to-detector distance of 18.0 m and an exposure time of 950 s were employed. The wavelength's spread was about 10%. This choice of parameters allowed for the data collection over the range of scattering vectors q between 0.01 and 10 nm^{-1} , required to observe both the global size and shape of liposomes as well as their membrane thickness. The samples were loaded into 2 mm-path length boron-free quartz glass cells and mounted in the temperature-controlled holder. This system allows for controlling the temperature of the specimen with an accuracy better than 1 K. The liposomal suspensions were measured between 22 and $42^\circ C$ in 3–4 K steps. Subsequently, the suspensions were cooled down to $22^\circ C$ (room temperature) and measured again. The scattering data were collected with a two-dimensional ^3He -detector using an array of 128×128 pixels. They were radially averaged to obtain the one-dimensional $I(q)$ signals using the scattering angle θ

C

Table 1. Results of the Dynamic Light Scattering from the Liposomes Used^a

lipid	T_m , °C	before heating		after heating	
		size, nm	PDI	size, nm	PDI
DPPC	41	120 ± 2	0.01 ± 0.01	600 ± 40	0.33 ± 0.02
Pad-PC-Pad	37	126 ± 4	0.19 ± 0.04	53 ± 4	0.33 ± 0.04
Rad-PC-Rad	45	150 ± 3	0.57 ± 0.01	700 ± 100	0.32 ± 0.03
Pes-PC-Pes	39	170 ± 20	0.57 ± 0.01	3100 ± 200	0.92 ± 0.08
Pad-Pad-PC	40–47	1500 ± 30	0.57 ± 0.01	n.a. ^b	n.a.
Sur-PC-Sur	47	400 ± 100	0.57 ± 0.01	n.a.	n.a.
Sad-PC-Sad	52	160 ± 3	0.23 ± 0.01	220 ± 10	0.20 ± 0.02

^aThe errors originate from the standard deviations of independent measurements. ^bHere, n.a. means the data could not be extracted because of aggregate size.

$$q = \frac{4\pi}{\lambda} \sin\left(\frac{\theta}{2}\right) \quad (1)$$

The data were corrected for transmission, background scattering, and detector efficiency according to a standard procedure using the BerSANS software package.^{13,14}

Models Used for SANS Data Analysis. The SANS data were analyzed using the SASfit software¹⁵ and the implemented models. The datasets of Pad-PC-Pad and Rad-PC-Rad liposome suspensions were fitted over the entire q -range measured. Here, we used the spherical, ellipsoidal shell and discs models with a homogeneous cross-section¹⁶ and size distributions in terms of both thickness and radius. The elliptical shell model is defined by three orthogonal axes with lengths $a = b = R$ and $c = \varepsilon R$, along with eccentricity $\varepsilon > 0$, ($\varepsilon < 1$: oblate, $\varepsilon = 1$: spherical, and $\varepsilon > 1$: prolate). For Pad-PC-Pad, we also included the sticky hard sphere model^{17,18} to account for interparticle interactions, as it defines the stickiness parameter, which characterizes the adhesive strength and helps to describe liposome aggregation. The fits of the other liposomal suspensions were restricted to the q -range related to the lipid bilayer thickness. Here, we used a generalized Guinier approximation^{19,20} to extract the bilayer thickness. This approximation is extended to planar objects and based on local planes with a homogeneous cross section. It does not include any assumption of the overall shape of the liposomes and is given by

$$I(q) = \frac{2\pi}{q^2} A \exp(-R_\alpha^2 q^2) \quad (2)$$

where A is the constant pre-factor, see for example ref 20.

The bilayer thickness t was calculated according to

$$t = \sqrt{12} R_\alpha \quad (3)$$

The bilayer thickness is orders of magnitude smaller than the diameter of the liposomes. In such case, the form factor can be factorized.²¹ Therefore, the extraction of the bilayer thickness is allowed without loss of quality.

Multi-lamellar contributions for DPPC, Pad-Pad-PC, Pes-PC-Pes, and Sur-PC-Sur were integrated using the para-crystalline theory.^{22,23}

RESULTS

Liposome Characterization by Dynamic Light Scattering. Table 1 lists the hydrodynamic diameter and polydispersity of the liposomes before ($n = 5$) and after ($n = 3$) the thermal cycles performed for the temperature-dependent SANS measurements. The main phase transition temperatures T_m are known.^{3,6,8,9,24} In the course of the SANS experiments, the liposomes underwent heating to 42 °C and back to room temperature, which resulted in substantial changes of hydrodynamic sizes and the polydispersity indices. In general, the liposomes showed an increase in size, which could be understood by aggregation owing to the low repulsive forces between the basically neutral liposomes. The exception

was found for Pad-PC-Pad liposomes, which exhibited a decrease by a factor of two. This result for the DLS measurements was confirmed using cryo-TEM.

Small-Angle Neutron Scattering Measurements. Figures 1 and 2 summarize the temperature-dependent neutron scattering experiments for the liposomes with T_m below and above 42 °C, respectively. The SANS experiment almost covers the entire nanometer range because the q -range from 0.01 to 3 nm⁻¹ corresponds to real-space periodicities between 2 and 600 nm. Liposomes, however, have aperiodic spacing and, thus, the maximum liposome diameter, that can be determined, is given by $\pi/q_{\min} \approx 300$ nm. Therefore, only some of the liposomal suspensions can be characterized with respect to the liposome size, but the SANS data allow measuring the lipid bilayer thickness for all of them.

The bilayer thickness of the selected liposomes for the medically relevant temperature range is compiled in Tables 2 and 3. As expected, the liposomes with a transition temperature above 42 °C do not exhibit any change in bilayer thickness. Pes-PC-Pes and Pad-PC-Pad liposomes, however, show the tendency for losing interdigitation of the lipid bilayers already well below T_m .

Table 2. Most Probable¹⁵ Bilayer Thickness (nm) of the Selected Liposomes as a Function of Temperature^a

phospholipid	temperature, °C							
	22	25	28	32	35	39	42	22
DPPC	4.6	4.6	4.6	4.6	4.6	4.7	4.7	4.7
Rad-PC-Rad	4.6	4.6	4.6	4.5	4.5	4.4	4.4	4.5
Pad-Pad-PC	5.6	5.6	5.6	5.5	5.5	5.6	5.6	5.7
Pes-PC-Pes	3.9	4.2	4.5	4.4	4.6	4.7	4.6	4.8
Sur-PC-Sur	3.1	3.1	3.1	3.1	3.1	3.1	3.1	3.1
Sad-PC-Sad	3.2	3.5	3.5	3.5	3.5	3.4	3.3	3.0

^aThe goodness of the fit, described by reduced chi-square, varies between 3 and 15.

The well-established DPPC liposomes were incorporated into the study for comparison. The decrease of forward scattered intensity for DPPC with increasing temperature is likely caused by increasing repulsive interactions associated with the pre-transition temperature of DPPC, which varies between 33.5 and 35.8 °C, and is even 37.4 °C in case of the use of D₂O.²⁵ This hypothesis has to be verified by a future study. The mean size of the DPPC liposomes, as derived from cryo-TEM images and represented exemplarily in Figure 1A, was (87 ± 20) nm, and about 16% of them were multi-lamellar. The SANS data of Pes-PC-Pes liposomes, see Figure

Table 3. Structural Data Derived from SANS Demonstrate the Pad-PC-Pad Liposome Shape Changes Close to T_m^a

temperature, °C	radius, nm	eccentricity	bilayer thickness, nm	reduced chi-square
22	70 ± 19	0.35	3.5 ± 1.1	18.9
25	66 ± 21	0.35	3.4 ± 0.9	18.1
28	70 ± 16	0.32	3.3 ± 0.9	22.4
32	70 ± 16	0.31	3.4 ± 0.9	21.7
35	70 ± 7 (65)	0.1 (0.88)	3.3 ± 0.7 (3.4 ± 0.9)	178.7 (19.2)
39	72 ± 5	0.04	3.4 ± 0.8	17.5
42	71 ± 5	0.05	3.6 ± 0.7	107.1
22	70 ± 32	0.04	4.2 ± 0.7	9.4

^aAt a temperature of 35 °C, the contribution for discs with homogeneous cross-section was accounted for—values in brackets.

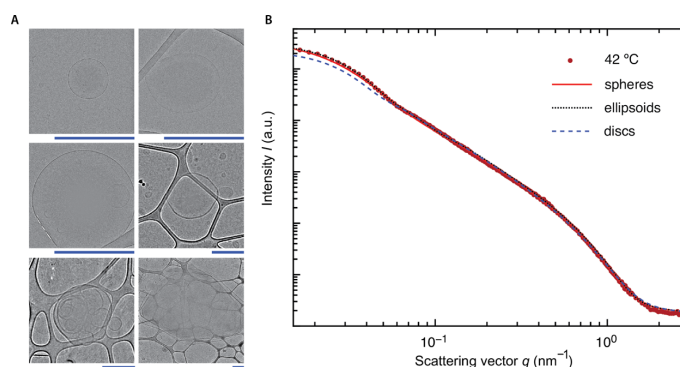


Figure 3. (A) Exemplified cryo-TEM images verify the manifold shapes and sizes of the Rad-PC-Rad liposomes used. The scale bars correspond to a length of 500 nm. (B) Discs less suitably describe the SANS data of Rad-PC-Rad liposomes than the ellipsoidal and spherical models.

1B, indicate the presence of two liposome populations with sizes of about 100 and 1000 nm—no plateau at low q -values and of stacked lipid bilayers—prominent BRAGG peak at $q = 0.83 \text{ nm}^{-1}$. Increasing the temperature, the peak gradually diminishes associated with the disintegration of the stacked lipid bilayers.

The fitting of the SANS data for Pad-PC-Pad liposomes was especially challenging. Therefore, not only the bilayer thickness was determined but also their radius and eccentricity. The radius was not affected by the temperature cycle, whereas the eccentricity abruptly changed already well below the transition temperature, i.e. between 32 and 35 °C. This change in shape, however, is not linked with the increase of the bilayer thickness, which has been observed after cooling-down to room temperature. The shape change of Pad-PC-Pad liposomes from ellipsoidal or better faceted entities to discs as the result of the heating was validated by the cryo-TEM images, exemplarily displayed in Figure 1C.

For Rad-PC-Rad, Pad-Pad-PC, Sur-PC-Sur, and Sad-PC-Sad liposomes, the q -plots derived coincide, which proves their thermal stability within the medically relevant temperature range. The fitting of SANS data for Rad-PC-Rad liposomal suspensions was challenging, easily explained by the presence of their size and shape distributions indicated in the micrographs of Figure 3A. Figure 3B exemplarily summarizes the fitting of the data obtained at a temperature of 42 °C. Ignoring the inter-particle interactions and considering ellipsoid shape, one can find a better approximation than for the discoid model. The goodness of fit, described by reduced chi-square, is for spheres 11.4, for ellipsoids 30.3, and for discs 47.8. The thermal stability of the Rad-PC-Rad liposomes with their wide-spread size and shape distribution within the

medically relevant temperature range, however, is the key observation and more essential than the selection of the most appropriate model.

DISCUSSION AND CONCLUSIONS

The bilayer thickness of the DPPC liposomes derived in this study perfectly agrees with the values reported,^{26,27} which indicates an appropriate fitting procedure. The liposomes of Pes-PC-Pes, also known as β -DPPC, exhibit interdigitated lipid bilayer in the gel phase but not in the liquid crystalline phase.²⁸ Therefore, the phase transition results in a bilayer thickness increase by 20%²⁸—a value consistent with the present study. The study also shows that the changes in the tail-to-tail van der Waals forces and inter-head-group hydrogen bonding in the series from Pad-Pad-PC via Sur-PC-Sur to Sad-PC-Sad do hardly affect the overall properties of the liposomes. Likewise, Pad-PC-Pad lipids are interdigitated below T_m and lose this structural property at higher temperatures.^{3,8m} In agreement with the present study, recent SAXS data have indicated that the head-to-head distance of Pad-PC-Pad bilayer increases as the result of mechanical stimuli.⁵ The observed 20% increase in bilayer thickness after heating above T_m denotes thermally induced structural changes. These structural changes of Pad-PC-Pad liposomes within the physiologically relevant temperature range is counter-indicative of its use as a carrier for targeted drug delivery in humans.

The C17 homologue of Pad-PC-Pad, that is, Rad-PC-Rad, which features a higher transition temperature,⁶ should allow for mechanically responsive drug delivery within the human body. Although the used Rad-PC-Rad liposomes possess a wide variety of sizes and shapes, they show the structural stability at the level of the bilayer membrane in the

physiologically relevant temperature range between 22 and 42 °C.

AUTHOR INFORMATION

Corresponding Author

*E-mail: bert.mueller@unibas.ch.

ORCID

Bert Müller: 0000-0003-4078-9109

Present Address

^{||}Institute of Sound and Vibration Research (ISVR), University of Southampton, Highfield, Southampton, SO17 1BJ, UK.

Author Contributions

The study was designed by A.Z. The samples were prepared by F.N. The SANS experiments were carried out by J.K., A.Z., F.N., and S.M. The data analysis and interpretation were mainly performed by J.K., H.D., and S.M. with the active support of B.M. The manuscript including the figures and tables were compiled by S.M. and B.M. All authors have given approval to the final version of the manuscript.

Funding

S.M. obtained financial support from the Swiss Government Excellence Scholarship Program for a period of 36 months. The study is partially based on the funding by the Swiss National Science Foundation (SNSF) via the National Research Program (NRP) 62 “Smart Materials”. A.Z. was financially supported by the Swiss National Science Foundation through a Professorial Fellowship.

Notes

The authors declare no competing financial interest.

ACKNOWLEDGMENTS

S.M. acknowledges the financial support of the Swiss Government via the Excellence Scholarship Program for Foreign Scholars and Artists (2015-2018). The authors are grateful to the funding provided by the Swiss National Science Foundation (SNSF) within project #126090. The authors thank the Paul Scherrer Institute, Villigen (Switzerland) for beamtime and the Bio-EM Lab (Biozentrum, University of Basel, Switzerland) for the cryo-TEM support as well as Takashi Ishikawa, Villigen, Switzerland for the early discussion of cryo-TEM results. The support of Georg Schulz, Basel, Switzerland for the background correction of the micrographs in Figure 3 is gratefully acknowledged.

ABBREVIATIONS

cryo-TEM, cryogenic transmission electron microscopy; DLS, dynamic light scattering; DPPC, 1,2-dipalmitoyl-*sn*-glycero-phosphocholine; Pad-Pad-PC, 1,2-dipalmityl-amido-*glycero*-3-phosphocholine; Pad-PC-Pad, 1,3-dipalmityl-amido-*glycero*-2-phosphocholine; PDI, polydispersity index; Rad-PC-Rad, 1,3-diheptadecyl-amido-*glycero*-phosphocholine; SANS, small-angle neutron scattering; SAXS, small-angle X-ray scattering; Sad-PC-Sad, 1,3-distearoyl-amido-*glycero*-phosphocholine; Sur-PC-Sur, 1,3-dihexadecyl-urea-*glycero*-2-phosphocholine

REFERENCES

- (1) Allen, T. M.; Cullis, P. R. Liposomal Drug Delivery Systems: From Concept to Clinical Applications. *Adv. Drug Delivery Rev.* **2013**, *65*, 36–48.
- (2) Zumbuehl, A. Artificial Phospholipids and Their Vesicles. *Langmuir* **2018**, DOI: 10.1021/acs.langmuir.8b02601.

- (3) Holme, M. N.; Fedotenko, I. A.; Abegg, D.; Althaus, J.; Babel, L.; Favarger, F.; Reiter, R.; Tanasescu, R.; Zaffalon, P.-L.; Ziegler, A.; Müller, B.; Saxer, T.; Zumbuehl, A. Shear-Stress Sensitive Lenticular Vesicles for Targeted Drug Delivery. *Nat. Nanotechnol.* **2012**, *7*, 536–543.
- (4) American Heart Association, Guidelines for Cardiopulmonary Resuscitation and Emergency Cardiovascular Care. *Circulation* **2005**, *112*, IV1-IV205.
- (5) Buscema, M.; Deyhle, H.; Pfohl, T.; Zumbuehl, A.; Müller, B. Spatially resolved small-angle X-ray scattering for characterizing mechanoresponsive liposomes using microfluidics. *Mater. Today Bio* **2019**, *1*, 100003.
- (6) Neuhaus, F.; Mueller, D.; Tanasescu, R.; Balog, S.; Ishikawa, T.; Brezesinski, G.; Zumbuehl, A. Synthesis and Biophysical Characterization of an Odd-Numbered 1,3-Diamidophospholipid. *Langmuir* **2018**, *34*, 3215–3220.
- (7) Neuhaus, F.; Mueller, D.; Tanasescu, R.; Stefaniu, C.; Zaffalon, P.-L.; Balog, S.; Ishikawa, T.; Reiter, R.; Brezesinski, G.; Zumbuehl, A. Against the Rules: Pressure Induced Transition from High to Reduced Order. *Soft Matter* **2018**, *14*, 3978–3986.
- (8) Weinberger, A.; Tanasescu, R.; Stefaniu, C.; Fedotenko, I. A.; Favarger, F.; Ishikawa, T.; Brezesinski, G.; Marques, C. M.; Zumbuehl, A. Bilayer Properties of 1,3-Diamidophospholipids. *Langmuir* **2015**, *31*, 1879–1884.
- (9) Neuhaus, F.; Mueller, D.; Tanasescu, R.; Balog, S.; Ishikawa, T.; Brezesinski, G.; Zumbuehl, A. Vesicle Origami: Cuboid Phospholipid Vesicles Formed by Template-Free Self-Assembly. *Angew. Chem.* **2017**, *129*, 6615–6618.
- (10) Walde, P. Preparation of Vesicles (Liposomes). *Encyclopedia of Nanoscience and Nanotechnology*; American Scientific Publishers, 2004; Vol. 8, pp 43–79.
- (11) Schulz, G.; Waschkes, C.; Pfeiffer, F.; Zanette, I.; Weitkamp, T.; David, C.; Müller, B. Multimodal Imaging of Human Cerebellum—Merging X-Ray Phase Microtomography, Magnetic Resonance Microscopy and Histology. *Sci. Rep.* **2012**, *2*, 826.
- (12) Ahmed, M. N.; Yamany, S. M.; Mohamed, N.; Farag, A. A.; Moriarty, T. A Modified Fuzzy C-Means Algorithm for Bias Field Estimation and Segmentation of MRI Data. *IEEE Trans. Med. Imaging* **2002**, *21*, 193–199.
- (13) Keiderling, U. The New “BerSANS-PC” Software for Reduction and Treatment of Small Angle Neutron Scattering Data. *Appl. Phys. A: Mater. Sci. Process.* **2002**, *74*, s1455–s1457.
- (14) Strunz, P.; Šaroun, J.; Keiderling, U.; Wiedenmann, A.; Przenioslo, R. General Formula for Determination of Cross-Section from Measured SANS Intensities. *J. Appl. Crystallogr.* **2000**, *33*, 829–833.
- (15) Breßler, I.; Kohlbrecher, J.; Thünemann, A. F. SASfit: a tool for small-angle scattering data analysis using a library of analytical expressions. *J. Appl. Crystallogr.* **2015**, *48*, 1587–1598.
- (16) Guiner, A.; Fournet, G.; Walker, C. *Small Angle Scattering of X-Rays*; Jahn Willey-Champan: New York, 1955.
- (17) Baxter, R. J. Percus-Yevick Equation for Hard Spheres with Surface Adhesion. *J. Chem. Phys.* **1968**, *49*, 2770–2774.
- (18) De Kruijff, C. G. Adhesive Hard-Sphere Colloidal Dispersions. A Small-Angle Neutron-Scattering Study of Stickiness and the Structure Factor. *Langmuir* **1989**, *5*, 422–428.
- (19) Hjelm, R. P.; Schteingart, C. D.; Hofmann, A. F.; Thiyagarajan, P. Structure of Conjugated Bile Salt–Fatty Acid–Monoglyceride Mixed Colloids: Studies by Small-Angle Neutron Scattering. *J. Phys. Chem. B* **2000**, *104*, 197–211.
- (20) Fratzl, P. Statistical Model of the Habit and Arrangement of Mineral Crystals in the Collagen of Bone. *J. Stat. Phys.* **1994**, *77*, 125–143.
- (21) Pedersen, J. S. Modelling of Small-Angle Scattering Data from Colloids and Polymer Systems. *Neutrons, X-rays and Light*; Elsevier, 2002; pp 391–420.
- (22) Schwartz, S.; Cain, J. E.; Dratz, E. A.; Blasie, J. K. An Analysis of Lamellar X-Ray Diffraction from Disordered Membrane Multilayers

with Application to Data from Retinal Rod Outer Segments. *Biophys. J.* **1975**, *15*, 1201–1233.

(23) Frühwirth, T.; Fritz, G.; Freiburger, N.; Glatter, O. Structure and Order in Lamellar Phases Determined by Small-Angle Scattering. *J. Appl. Crystallogr.* **2004**, *37*, 703–710.

(24) Tanasescu, R.; Lanz, M. A.; Mueller, D.; Tassler, S.; Ishikawa, T.; Reiter, R.; Brezesinski, G.; Zumbuehl, A. Vesicle Origami and the Influence of Cholesterol on Lipid Packing. *Langmuir* **2016**, *32*, 4896–4903.

(25) Matsuki, H.; Okuno, H.; Sakano, F.; Kusube, M.; Kaneshina, S. Effect of Deuterium Oxide on the Thermodynamic Quantities Associated with Phase Transitions of Phosphatidylcholine Bilayer Membranes. *Biochim. Biophys. Acta, Biomembr.* **2005**, *1712*, 92–100.

(26) Nele, V.; Holme, M. N.; Kauscher, U.; Thomas, M. R.; Douth, J. J.; Stevens, M. M. Effect of Formulation Method, Lipid Composition, and PEGylation on Vesicle Lamellarity: A Small-Angle Neutron Scattering Study. *Langmuir* **2019**, *35*, 6064–6074.

(27) Nagle, J. F.; Tristram-Nagle, S. Structure of Lipid Bilayers. *Biochim. Biophys. Acta, Rev. Biomembr.* **2000**, *1469*, 159–195.

(28) Serrallach, E. N.; Dijkman, R.; De Haas, G. H.; Shipley, G. G. Structure and thermotropic properties of 1,3-dipalmitoyl-glycero-2-phosphocholine. *J. Mol. Biol.* **1983**, *170*, 155–174.

3 Conclusions and Outlook

In the framework of the current thesis project, mechano-responsive liposomes of nanometer size, designed for physically-triggered drug delivery within the diseased human blood vessel system, were carefully prepared and in-depth characterized. The structural characterization of the Pad-PC-Pad liposomes as a function of the physiologically relevant temperatures by means of SANS has revealed that these liposomes are thermally not stable enough for the application beyond mucosa. Rad-PC-Rad liposomes with diameters of around 100 nm — even with a wide variety of shape — however, they exhibit the necessary thermal stability to be used for the dilation of atherosclerotic human arteries. In order to obtain homogeneous liposomal suspensions, future work should focus on the improvement of the preparation protocol. The clustering of the liposomes, as the consequence of the low zeta potential, can be prevented by PEGylation, so that these liposomes are promising nanocontainers for the envisioned targeted treatment of atherosclerosis.

The nitroglycerin-loaded Rad-PC-Rad liposomes, formulated from artificial phospholipids, should be parenterally administered. The related safety concerns can be, *inter alia*, addressed detecting the complement activation to quantify the immune-mediated adverse effects. Herein, the ELISA assay has been performed to determine the level of complement proteins activated in serum upon incubation with liposomes. The experiments with Rad-PC-Rad liposomes have verified a level of complement proteins low-to-moderate relative to the currently available FDA-approved liposomal drugs. The activation of the complement cascade was initiated via the alternative pathway, as found for both Pad-PC-Pad and Rad-PC-Rad liposomes. The results are, however, preliminary, since the number of donors for complement activation has to be increased to the order of one hundred. Future studies should not only focus on complement activation, but include preclinical evaluations, comprising the detection of hemolysis, platelet aggregation, oxidative stress, cell viability, phagocytosis, contamination, *etc.*

Additional investigations must be conducted before human trials can start. The structural changes of the nanometer-size, nitroglycerin-loaded Rad-PC-Rad liposomes under physiological flow conditions, mimicking the shear stress of constricted arteries, at temperatures up to 42 °C have to be identified. Future studies should include the pharmacokinetic and pharmacodynamic efficacy of nitroglycerin-loaded liposomes in comparison to the current systemic use of nitroglycerin. Finally, *in vivo* studies should yield the desired dosage in a patient-specific manner.

Bibliography

- [1] World Health Organization. “Cardiovascular diseases.” (2018).
- [2] V. Nossaman, B. Nossaman, and P. Kadowitz. “Nitrates and nitrites in the treatment of ischemic cardiac disease.” *Cardiology in Review* **18** (2010)(4), 190.
- [3] UCB-Pharma AG. “Perlinganit, *package insert*.” UCB-Pharma AG: Bulle, Switzerland (2015).
- [4] S. Piper and T. McDonagh. “The role of intravenous vasodilators in acute heart failure management.” *European Journal of Heart Failure* **16** (2014)(8), 827–34.
- [5] M. A. Hlatky, H. Cotugno, C. O’Connor, D. B. Mark, D. B. Pryor, and R. M. Califf. “Adoption of thrombolytic therapy in the management of acute myocardial infarction.” *American Journal of Cardiology* **61** (1988)(8), 510–4.
- [6] K. Huber, M. S. Runge, C. Bode, and D. Gulba. “Thrombolytic therapy in acute myocardial infarction - update 1996.” *Annals of Hematology* **73 Suppl 1** (1996), S29–38.
- [7] C. K. W. Chan, L. Zhang, C. K. Cheng, H. Yang, Y. Huang, X. Y. Tian, and C. H. J. Choi. “Recent advances in managing atherosclerosis via nanomedicine.” *Small* **14** (2018)(4).
- [8] M. Zamanlu, M. Farhoudi, M. Eskandani, J. Mahmoudi, J. Barar, M. Rafi, and Y. Omid. “Recent advances in targeted delivery of tissue plasminogen activator for enhanced thrombolysis in ischaemic stroke.” *Journal of Drug Targeting* **26** (2018)(2), 95–109.
- [9] W. J. Geldenhuys, M. T. Khayat, J. Yun, and M. A. Nayeem. “Drug delivery and nanoformulations for the cardiovascular system.” *Research & Reviews: Drug Delivery* **1** (2017)(1), 32–40.
- [10] B. S. Pattni, V. V. Chupin, and V. P. Torchilin. “New developments in liposomal drug delivery.” *Chemical Reviews* **115** (2015)(19), 10938–10966.
- [11] D. Mellal and A. Zumbuehl. “Exit-strategies – smart ways to release phospholipid vesicle cargo.” *Journal of Materials Chemistry B* **2** (2014)(3), 247–252.
- [12] C. Cheng, F. Helderma, D. Tempel, D. Segers, B. Hierck, R. Poelmann, A. van Tol, D. J. Duncker, D. Robbers-Visser, N. T. Ursem, R. van Haperen, J. J. Wentzel, F. Gijzen, A. F. van der Steen, R. de Crom, and R. Krams. “Large variations in absolute wall shear stress levels within one species and between species.” *Atherosclerosis* **195** (2007)(2), 225–35.
- [13] W. Yin, S. K. Shanmugavelayudam, and D. A. Rubenstein. “3d numerical simulation of coronary blood flow and its effect on endothelial cell activation.” *Conference proceedings IEEE Engineering in Medicine and Biology Society* **2009** (2009), 4003–6.

- [14] N. Korin, M. Kanapathipillai, B. D. Matthews, M. Crescente, A. Brill, T. Mamamoto, K. Ghosh, S. Jurek, S. A. Bencherif, D. Bhatta, A. U. Coskun, C. L. Feldman, D. D. Wagner, and D. E. Ingber. “Shear-activated nanotherapeutics for drug targeting to obstructed blood vessels.” *Science* **337** (2012)(6095), 738–42.
- [15] M. N. Holme, I. A. Fedotenko, D. Abegg, J. Althaus, L. Babel, F. Favarger, R. Reiter, R. Tanasescu, P.-L. Zaffalon, and A. Ziegler. “Shear-stress sensitive lenticular vesicles for targeted drug delivery.” *Nature Nanotechnology* **7** (2012)(8), 536–543.
- [16] T. Saxer, A. Zumbuehl, and B. Müller. “The use of shear stress for targeted drug delivery.” *Cardiovascular Research* **99** (2013)(2), 328–333.
- [17] M. N. Holme, G. Schulz, H. Deyhle, T. Weitkamp, F. Beckmann, J. A. Lobrinus, F. Rikhtegar, V. Kurtcuoglu, I. Zanette, and T. Saxer. “Complementary x-ray tomography techniques for histology-validated 3d imaging of soft and hard tissues using plaque-containing blood vessels as examples.” *Nature Protocols* **9** (2014)(6), 1401–1415.
- [18] M. Buscema, G. Schulz, H. Deyhle, A. Khimchenko, S. Matviyiv, M. N. Holme, A. Hipp, F. Beckmann, T. Saxer, and K. Michaud. “Histology-validated x-ray tomography for imaging human coronary arteries.” In “Developments in X-Ray Tomography X,” volume 9967, page 99670O. International Society for Optics and Photonics (2016).
- [19] M. Buscema. “Evaluation of 100-nm-size mechano-responsive liposomes for targeted delivery at constricted arteries.” Thesis, University of Basel (2018).
- [20] S. Matviyiv, M. Buscema, H. Deyhle, T. Pfohl, A. Zumbuehl, T. Saxer, and B. Müller. “X-ray micro computed tomography for the visualization of an atherosclerotic human coronary artery.” In “Journal of Physics: Conference Series,” volume 849, page 012002. IOP Publishing (2017). ISBN 1742-6596.
- [21] J. Szebeni and S. M. Moghimi. “Liposome triggering of innate immune responses: A perspective on benefits and adverse reactions: Biological recognition and interactions of liposomes.” *Journal of Liposome Research* **19** (2009)(2), 85–90.
- [22] J. Szebeni and G. Storm. “Complement activation as a bioequivalence issue relevant to the development of generic liposomes and other nanoparticulate drugs.” *Biochemical and Biophysical Research Communications* **468** (2015)(3), 490–497.
- [23] D. Bobo, K. J. Robinson, J. Islam, K. J. Thurecht, and S. R. Corrie. “Nanoparticle-based medicines: A review of fda-approved materials and clinical trials to date.” *Pharmaceutical Research* **33** (2016)(10), 2373–2387.
- [24] C. L. Ventola. “Progress in nanomedicine: Approved and investigational nanodrugs.” *Pharmacy and Therapeutics* **42** (2017)(12), 742.
- [25] B. Halamoda-Kenzaoui and S. Bremer-Hoffmann. “Main trends of immune effects triggered by nanomedicines in preclinical studies.” *International Journal of Nanomedicine* **13** (2018), 5419.

-
- [26] J. Szebeni, D. Simberg, A. Gonzalez-Fernandez, Y. Barenholz, and M. A. Dobrovolskaia. “Roadmap and strategy for overcoming infusion reactions to nanomedicines.” *Nature Nanotechnology* (2018).
- [27] J. Szebeni. “Complement activation-related pseudoallergy: A new class of drug-induced acute immune toxicity.” *Toxicology* **216** (2005)(2-3), 106–121.
- [28] L. Sercombe, T. Veerati, F. Moheimani, S. Y. Wu, A. K. Sood, and S. Hua. “Advances and challenges of liposome assisted drug delivery.” *Frontiers in Pharmacology* **6** (2015), 286.
- [29] S. Siegrist, E. Cörek, P. Detampel, J. Sandström, P. Wick, and J. Huwyler. “Preclinical hazard evaluation strategy for nanomedicines.” *Nanotoxicology* (2018), 1–27.
- [30] European Medicine Agency. “Reflection paper on the data requirements for intravenous products developed with reference to an innovator liposomal product.” (2013).
- [31] S. Wolf-Grosse, A. M. Rokstad, S. Ali, J. D. Lambris, T. E. Mollnes, A. M. Nilsen, and J. Stenvik. “Iron oxide nanoparticles induce cytokine secretion in a complement-dependent manner in a human whole blood model.” *International Journal of Nanomedicine* **12** (2017), 3927.
- [32] M. A. Dobrovolskaia. “Pre-clinical immunotoxicity studies of nanotechnology-formulated drugs: Challenges, considerations and strategy.” *Journal of Controlled Release* **220** (2015), 571–583.
- [33] American Heart Association. “American heart association guidelines for cardiopulmonary resuscitation and emergency cardiovascular care.” *Circulation* **112** (2005), IV1–IV205.
- [34] Hypothermia after Cardiac Arrest Study Group. “Mild therapeutic hypothermia to improve the neurologic outcome after cardiac arrest.” *New England Journal of Medicine* **346** (2002)(8), 549–556.
- [35] S. A. Bernard, T. W. Gray, M. D. Buist, B. M. Jones, W. Silvester, G. Gutteridge, and K. Smith. “Treatment of comatose survivors of out-of-hospital cardiac arrest with induced hypothermia.” *New England Journal of Medicine* **346** (2002)(8), 557–563.
- [36] H. S. Sharma. *Neurobiology of Hyperthermia*, volume 162. Elsevier (2011). ISBN 0080549993.
- [37] A. Bouchama and J. P. Knochel. “Heat stroke.” *New England Journal of Medicine* **346** (2002)(25), 1978–1988.
- [38] G. D. Bynum, K. B. Pandolf, W. H. Schuette, R. F. Goldman, D. E. Lees, J. Whang-Peng, E. R. Atkinson, and J. M. Bull. “Induced hyperthermia in sedated humans and the concept of critical thermal maximum.” *American Journal of Physiology-Regulatory, Integrative and Comparative Physiology* **235** (1978)(5), R228–R236.

- [39] M. Buscema, S. Matviykov, T. Mészáros, G. Gerganova, A. Weinberger, U. Mettetal, D. Mueller, F. Neuhaus, E. Stalder, T. Ishikawa, R. Urbanics, T. Saxer, T. Pfohl, J. Szebeni, A. Zumbuehl, and B. Müller. “Immunological response to nitroglycerin-loaded shear-responsive liposomes in vitro and in vivo.” *Journal of Controlled Release* **264** (2017), 14–23.
- [40] S. Bugna, M. Buscema, S. Matviykov, R. Urbanics, A. Weinberger, T. Meszaros, J. Szebeni, A. Zumbuehl, T. Saxer, and B. Müller. “Surprising lack of liposome-induced complement activation by artificial 1, 3-diamidophospholipids in vitro.” *Nanomedicine: Nanotechnology, Biology and Medicine* **12** (2016)(3), 845–849.
- [41] F. Neuhaus, D. Mueller, R. Tanasescu, S. Balog, T. Ishikawa, G. Brezesinski, and A. Zumbuehl. “Synthesis and biophysical characterization of an odd-numbered 1, 3-diamidophospholipid.” *Langmuir* **34** (2018)(10), 3215–3220.
- [42] S. Matviykov, M. Buscema, G. Gerganova, T. Mészáros, G. Tibor Kozma, U. Mettetal, F. Neuhaus, T. Ishikawa, J. Szebeni, A. Zumbuehl, and B. Müller. “Immunocompatibility of rad-pc-rad liposomes in vitro, based on human complement activation and cytokine release.” *Precision Nanomedicine* **1** (2018)(1), 43–62.
- [43] A. Weinberger, R. Tanasescu, C. Stefaniu, I. A. Fedotenko, F. Favarger, T. Ishikawa, G. Brezesinski, C. M. Marques, and A. Zumbuehl. “Bilayer properties of 1, 3-diamidophospholipids.” *Langmuir* **31** (2015)(6), 1879–1884.
- [44] I. A. Fedotenko, P.-L. Zaffalon, F. Favarger, and A. Zumbuehl. “The synthesis of 1, 3-diamidophospholipids.” *Tetrahedron Letters* **51** (2010)(41), 5382–5384.
- [45] E. Di Cola, I. Grillo, and S. Ristori. “Small angle x-ray and neutron scattering: Powerful tools for studying the structure of drug-loaded liposomes.” *Pharmaceutics* **8** (2016)(2), 10.

Acknowledgments

This work was only possible due to the contribution and cooperation of a number of people. I would like to take this opportunity to thank all of them.

First and foremost, I would like to express my sincere gratitude to my thesis advisor Prof. Dr. Bert Müller for the opportunity to work in this multidisciplinary project at the Biomaterials Science Center. Prof. Dr. Bert Müller was always very supportive, starting from the day of my application for a Ph.D. scholarship until the last day of the thesis submission. Prof. Dr. Bert Müller has guided me during these years, always providing his precious scientific advice. His motivation and optimism were very inspiring and helped me to deal with scientific challenges along my doctoral studies. I am very grateful for that.

Also, I would like to thank Prof. Dr. Jörg Huwyler for kindly acting as the second advisor of my thesis and for giving the access to the laboratory at the Pharmazentrum. Samples preparation and basic characterization was partially conducted at his lab.

I would like to thank Prof. Dr. Regine Willumeit-Römer for kindly being the external reviewer and for the evaluation of my doctoral thesis.

Great thanks go to Dr. Andreas Zumbühl and his former research team (Dr. Fredrik Neuhaus, Dr. Ute Mettal, Dr. Radu Tanasescu, Dr. Dennis Müller, Etienne Stalder) at the University of Fribourg, who were very supportive in providing “precious” lipids for all of my experiments and helping with liposome preparation and characterization, even on the weekends. I specially thank Dr. Andreas Zumbühl for numerous scientific discussions, valuable feedback to all my publications, and for being ready to answer any chemistry-related question.

I would like to thank Dr. Joachim Kohlbrecher at the Paul Scherrer Institute for his assistance during the beamtime, the extensive explanations of neutron scattering and help with data analysis and interpretation.

I am very grateful to Dr. Hans Deyhle for his unique support with SANS data analysis and productive discussions. And thank you for kindly agreeing to be a part of the doctoral committee.

Big thanks go to Prof. Dr. János Szebeni and his research team (Tamás Mészáros, Dr. Gergely Kozma) at the Semmelweis University for their rewarding support in conducting *in vitro* experiments and help with data analysis and results discussion. Our experiments were always tight on time, and even sometimes until midnight, but their availability and dedication helped to obtain promising results.

I would like to thank Dr. Thomas Pfohl for his optimistic ideas and our fruitful scientific discussions. And thank you for kindly agreeing to be a part of the doctoral committee.

I am thankful to Prof. Dr. Thomas Jung, who kindly agreed to chair my Ph.D. defense.

Special thanks go to Dr. Marzia Buscema and Gabriela Gerganova who worked with me as part of the NO-stress project. Thank you for your immense support during *in*

vitro experiments in Budapest and for creative discussions during manuscript writing. Our “NanoStressGirls” group helped me to stay positive and motivated, even when results were not very promising. Apart from long and stressful experiments, we also had many enjoyable moments like discovering Budapest, cooking pasta and shopping together. I really enjoyed working hand-in-hand with you.

I would like to thank Dr. Georg Schulz for his help with discussion of XRM article, Dr. Bekim Osmani for introducing me to the AFM instrument, Dr. Tino Töpper for perfect organization of summer school, all social events and Christmas dinners. I am very thankful to Griffin Rodgers for his great support in proof-reading and formatting this thesis. I am also thankful to Dr. Till Saxer and Dr. Jeannette von Jackowski for the last minute proof-read of thesis summary from a medical perspective.

I am thankful to all present and former members of the Biomaterials Science Center, in particular Dr. Simone Hieber, Dr. Anna Khimchenko, Dr. Florian Weiss, Dr. Marco Dominietto, Dr. Christos Bikis, Dr. Natalia Chicherova, Dr. Peter Thalmann, Dr. Vanessa Leung, Verena Grötzinger, Matej Siketanc, Sebastian Buchmann, Willy Kuo, and Maria Karapetkova. All of these people, as well as many of those mentioned before, contributed to interesting discussions during lunch and coffee breaks, conferences, and social events. Thank you for a pleasant atmosphere in our group. It was great to meet you all!

Special thanks is addressed to Bruno Aor. Thank you for your endless help with figures preparation, for teaching me graphical, presentation and all the Mac software, and for your 24/7 availability.

I gratefully acknowledge The Swiss State Secretariat for Education, Research and Innovation for providing the Excellence Scholarship funding sources that made my Ph.D. work possible.

I would like sincerely thank the most important people in my life who have always supported me and who had a tremendous influence on what I achieved to this point: my family. Limitless thanks to my parents Oleh and Svitlana, my brother Danylo, my grandparents, uncle and aunts and their families.

Curriculum Vitae



I am a Ph.D. researcher in Nanosciences, with expertise in liposomal drug delivery. Based on my international research experience in multi-disciplinary projects, I acquired broad scientific knowledge in the field of biomaterials. As an organized and persistent individual, I take ownership of project management and strive to achieve excellent results in my work. Passionate about science contributing to a better world.

PERSONAL INFORMATION

 **Nationality**
Ukraine

 **Address**
4153 Reinach, Basel Country
Switzerland

 **Phone**
+41 61 207 54 31

 **E-mail**
sofiya.matviyiv@gmail.com

SOCIAL MEDIA

 **LinkedIn**
www.linkedin.com/in/sofiya_matviyiv/

 **ResearchGate**
www.researchgate.net/profile/Sofia_Matviyiv2

Sofiya Matviyiv



RESEARCH EXPERIENCE

September 2015 - August 2019

Ph.D. researcher, Biomaterials Science Center, University of Basel (Switzerland)

- *Research and collaboration in multi-disciplinary project focused on drug delivery.*
- *Characterized physico-chemical properties and immunocompatibility of liposomes.*
- *Good Clinical Practice certification, Swiss TPH (2019).*

June 2015 - July 2015

Research fellowship, Functional materials, University of Würzburg (Germany)

- *Own initiative research project focused on development and characterization of a composite biomaterial (silk fibroin/magnesium phosphate) for bone tissue engineering.*

July 2014 - September 2014

Master thesis internship, BioTech Research Center, University of Trento (Italy)

- *Investigated stabilization of silk fibroin based biomaterial for tissue regeneration.*

November 2012 - May 2013

Bachelor thesis internship, Lviv Polytechnic National University (Ukraine)

- *Identified optimal conditions for in vitro cultivation of protected rare medicinal plant.*



EDUCATION

September 2015 - January 2019

Dr. phil. des. in Nanosciences, Department of Biomedical Engineering, University of Basel (Switzerland)

- *Thesis title: "Preparation and characterization of nanometer-sized mechano-responsive liposomes for physically-triggered drug delivery"*

September 2013 - November 2014

Master of Sciences in Pharmaceutical Biotechnology, Department of Biotechnology, Lviv Polytechnic National University (Ukraine)

- *Thesis title: "Fabrication and characterization of a regenerative scaffold"*

Master courses in Cellular and Molecular Biotechnology, University of Trento (Italy)

September 2009 - August 2013

Bachelor of Sciences in Biotechnology, Department of Biotechnology, Lviv Polytechnic National University (Ukraine)

- *Thesis title: "Cultivation of *Carlina acaulis* L. in vitro"*

LANGUAGE PROFICIENCY

C1

English
(professional
knowledge)

B1

German

B2

Italian

A2

Polish

C2

Ukrainian
(native speaker)

C1

Russian

* A1 - beginner A2 - lower intermediate
B1 - intermediate B2 - upper intermediate
C1 - advanced C2 - proficient

PERSONAL SKILLS

- Project organization & management
- Written & oral communication
- Analytical thinking
- Problem solving
- Proactiveness
- Team oriented
- Flexibility

REFERENCES



Prof. Dr. Bert Müller
University of Basel
Phone: +41 61 207 54 31
E-mail: bert.mueller@unibas.ch



TECHNICAL SKILLS

Laboratory experience

- Liposomes preparation
- Mammalian cell isolation & culture

Analytical methods

- Dynamic light scattering
- Enzyme-linked immunosorbent assay
- Atomic force microscopy
- Size-exclusion chromatography
- Mass spectrometry
- Fluorescence-activated cell sorting
- Gel electrophoresis
- Transmission electron microscopy
- Small-angle neutron scattering
- X-ray micro computed tomography

IT competence

- Microsoft Office Suite
- Document preparation (LaTeX)
- Statistical software (Prism)
- Data analysis, plotting, fitting (pro Fit)
- Imaging software (Image J)
- Graphical & web design (Adobe Ai, Ps, Dwg)



AWARDS & CERTIFICATES

- Event manager of Pint of Science festival, Basel, Switzerland (2019).
- Antelope @ Novartis career development program, Switzerland (2018).
- Best oral presentation award at 28th Biomaterials Annual Conference of the European Society, Greece (2017).
- Best student paper award (2nd place) at SPIE: Smart Structures NDE, in Bioinspiration, Biomimetics, and Bioreplication VII conference, USA (2017).
- Swiss Government Excellence Ph.D. Scholarship awarded on a competitive basis by Swiss Confederation (2015-2018).



SELECTED PUBLICATIONS

- [S. Matviykov](#), et al. "Small-Angle Neutron Scattering Study of Temperature-Induced Structural Changes in Liposomes", *Langmuir* (2019), *in press*.
- [S. Matviykov](#), et al. "Immunocompatibility of Rad-PC-Rad liposomes in vitro, based on human complement activation and cytokine release", *Precision Nanomedicine* 1 (2018) 45-67.
- [S. Matviykov](#), et al. "Liposomes - bio-inspired nano-containers for physically triggered targeted drug delivery", *Proceedings of SPIE* 10162, 101620A (2017).
- M. Buscema, [S. Matviykov](#), et al. "Immunological response to nitroglycerin-loaded shear-responsive liposomes in vitro and in vivo", *Journal of Controlled Release* 264 (2017) 14-23.
- [S. Matviykov](#) et al. "X-ray micro computed tomography for the visualization of an atherosclerotic human coronary artery", *Journal of Physics* 849 (2017) 012002.

List of Posters and Presentations

S. Matviykov, H. Deyhle, J. Kohlbrecher, F. Neuhaus, A. Zumbuehl, B. Müller “Temperature-dependent small-angle neutron scattering of mechano-responsive liposomes”; Annual Meeting of Swiss Society for Biomedical Engineering, 28 August 2018, Biel, Switzerland - POSTER PRESENTATION

S. Matviykov, M. Buscema, G. Gerganova, T. Mészáros, G.T. Kozma, F. Neuhaus, J. Szebeni, A. Zumbuehl, B. Müller “Immunocompatibility of Rad-PC-Rad liposomal nano-containers *in vitro*”; 11th European and Global Summit for Clinical Nanomedicine, 2-5 September, 2018, Basel, Switzerland - POSTER PRESENTATION

S. Matviykov, M. Buscema, G. Gerganova, T. Mészáros, J. Szebeni, A. Zumbuehl, B. Müller “Smart liposomes for targeted vasodilation”; 28th Annual Conference of the European Society for Biomaterials, 4-8 September, 2017, Athens, Greece - ORAL PRESENTATION

S. Matviykov, M. Buscema, G. Gerganova, T. Mészáros, T. Pfohl, J. Szebeni, A. Zumbuehl, B. Müller “Adverse immune effects to artificial, shear-responsive liposomes”; Annual Meeting of Swiss Society for Biomedical Engineering, 30 August 2017, Winterthur, Switzerland - POSTER PRESENTATION + “SMALL TALK”

S. Matviykov, M. Buscema, T. Mészáros, G. Gerganova, T. Pfohl, J. Szebeni, A. Zumbuehl, B. Müller “Immunotoxicity studies of liposomal nano-containers for targeted drug delivery”; 10th European and Global Summit for Clinical Nanomedicine, 7-10 May 2017, Basel, Switzerland - POSTER PRESENTATION

S. Matviykov, M. Buscema, T. Mészáros, T. Pfohl, A. Zumbuehl, J. Szebeni, B. Müller “Liposomes – bio-inspired nano-containers for physically triggered drug delivery”; SPIE Conference: Smart Structures + Nondestructive Evaluation (Bioinspiration, Biomimetics, and Bioreplication section), 25-29 March 2017, Portland, OR, USA - ORAL PRESENTATION

S. Matviykov, M. Buscema, S. Bugna, T. Mészáros, J. Szebeni, A. Zumbuehl, B. Müller “Complement activation of artificial, non-spherical liposomes”; 9th European Conference for Clinical Nanomedicine, 26-29 June 2016, Basel, Switzerland - POSTER PRESENTATION

S. Matviykov, M. Buscema, S. Bugna, T. Mészáros, J. Szebeni, A. Zumbuehl, B. Müller “Complement activation of artificial liposomes about 100 nm in diameter”; 22nd Swiss Conference on Biomaterials and Regenerative Medicine, Schulthess Klinik, Zürich, Switzerland, 9 - 10 June 2016 - POSTER PRESENTATION

List of Awards

Best oral presentation award at 28th Annual Conference of the European Society for Biomaterials, Greece (2017)

H. Don Wolpert award for the 2nd place best student paper at the Bioinspiration, Biomimetics, and Bioreplication section of SPIE conference: Smart Structures + Nondestructive Evaluation, sponsored by the Optical Society of Southern California, USA, 2017

Student Travel Award from the Swiss Society for Biomaterials and Regenerative Medicine, Switzerland, 2017

Awarded with Swiss Government Excellence Scholarship (2015-2018) for the conduction of Ph.D. thesis.